Subsurface Characterization of the Massachusetts Military Reservation Main Base Landfill Superfund Site

by

Dan S. Alden

B.S., Electrical Engineering
University of Alaska, Fairbanks, 1987

Submitted to the Department of Civil and Environmental Engineering in Partial Fulfillment of the Requirements for the Degree of

Master of Engineering in Civil and Environmental Engineering

at the

Massachusetts Institute Of Technology

June 1996

Signature of Author_____
Department of Civil and Environmental Engineering
May 10, 1996

Certified by_____
John T. Germaine
Principal Research Associate
Thesis Supervisor

Accepted by_____
Joseph M. Sussman, Chairman
Departmental Committee on Graduate Studies

Subsurface Characterization of the Massachusetts Military Reservation Main Base Landfill Superfund Site

by

Dan S. Alden

Submitted to the Department of Civil and Environmental Engineering on May 10, 1996 in partial fulfillment of the requirements for the degree of
Master of Engineering in Civil and Environmental Engineering

ABSTRACT

This study characterizes the extent of halogenated volatile organic compounds contained in the groundwater emanating from the Massachusetts Military Reservation Main Base Landfill on Cape Cod. Water sample data was used from seventy-three well locations spread over approximately 4 square miles. The data came from an investigation performed by CDM Federal from 1993 to 1994. Dynplot software developed by Camp, Dresser, McKee, Inc. was used to plot contamination concentration contours. The total area where contamination levels exceeded US Environmental Protection Agency (EPA) drinking water standards was about 2 square miles. The shallowest depth of contaminated water exceeding the EPA drinking water standard was about 10 feet below the water table.

In addition, different methods for determining hydraulic conductivity were compared at 23 locations. This included three methods which use grain size distributions and one method which measures the recovery of well levels to head disturbances (slug test). The data for this part of the study also came from the CDM Federal investigation. The values for hydraulic conductivity determined by slug tests were put through a gauss filter algorithm. The results were contoured and used to evaluate the aquifer hydrogeology for the purpose of establishing model parameters for predicting future plume movement.

This study was done in conjunction with the work of a project team formed under the Master of Engineering program in Civil and Environmental Engineering at the Massachusetts Institute of Technology. The purpose of the team project was to characterize, model, ascertain risk, and propose remedial action for the LF-1 plume.

Thesis Supervisor: Dr. John T. Germaine
Title: Principal Research Associate

Acknowledgments

I would like to thank my thesis advisor, Dr. John T. Germaine, for all his guidance and help with this project. I would also like to thank Professor Lynn W. Gelhar for his helpful direction and instruction. I am very grateful to Bruce L. Jacobs for all his help, especially with the computer program Dynplot.

I am very indebted to my advisor, Professor David H. Marks, and Shawn P. Morrissey for their great assistance in guiding me through the Master of Engineering program.

My thanks go to the other members of the Master of Engineering project team who contributed to this document, Kishan Amarasekera, Michael Collins, Karl G. Elias, Jim Hines, Benjamin R. Jordan, and Robert F. Lee.

Last but foremost, I would like to thank my wife, Cate MacKinnon, for all her support and encouragement, and her parents, Bob and Dorothy MacKinnon.

A very special acknowledgment belongs to my parents, Dr. Gayle S. Alden and June L. Kopecky (1927 - 1995). I am eternally grateful for all the love they have shown me. May their rewards be great.

Table of Contents

List of Figures

List of Tables

Chapter I. Introduction

The purpose of this work is to characterize the groundwater contamination plume and hydrogeology associated with the Massachusetts Military Reservation Main Base Landfill (LF-1) on western Cape Cod. This study was done in conjunction with the work of a project team formed under the Master of Engineering program in Civil and Environmental Engineering at the Massachusetts Institute of Technology. The purpose of the team project was to characterize, model, ascertain risk, and propose remedial action for the LF-1 plume. The research team included Dan Alden, Kishan Amarasekera, Michael Collins, Karl G. Elias, Jim Hines, Benjamin R. Jordan, and Robert F. Lee.

Objectives and Scope of this Study

This study focused on characterizing the type and extent of halogenated volatile organic compounds contained in the groundwater emanating from LF-1, in terms of Environmental Protection Agency drinking water standards and total mass. Water sample data were used from seventy-three well locations spread out over approximately 4 square miles. The data came from an investigation performed by CDM Federal from 1993 to 1994. These sparse data (an average of 1.5 million square feet per well) were used to create a number of two-dimensional concentration contours of different contaminant aggregations. Dynplot software developed by Camp, Dresser, McKee, Inc. was used to interpret the point data and plot these contours.

In addition, different methods for determining hydraulic conductivity were compared. This included three methods which use subsurface grain size distributions and one method which measures the recovery of well water levels to head disturbances (slug test). The values for hydraulic conductivity determined by slug tests were put through a gauss filter algorithm. The resultant contours were used to evalutate the aquifer hydrogeology for the purpose of establishing model parameters for predicting future plume movement.

Team Project Report

An extensive amount of data on contamination at the MMR has been collected and is maintained by the MMR Installation Restoration Program (IRP) office. The IRP acts as principal agent for the U.S. government on behalf of the MMR. These reports are available for public review and are the principal source of information used for analysis in this study and the team project report.

The project report examines potential impacts of LF-1 on public health and welfare and how these effects might be mitigated. The scope of the research project includes: site characterization and groundwater modeling, risk assessment, management of public interaction, study of source containment, and bioremediation technology. The specific underlying objectives of the project report are as follows:

- Characterization of the site through evaluation of subsurface hydraulic conductivity,
- Characterization of the landfill plume constituents, dimensions, and movement through use of existing data and groundwater modelling,

- Evaluation of the potential cancer risk which materials identified in the groundwater present to people located near the landfill plume, as well as risks associated with ingestion of potentially contaminated shellfish,
- Characterization of the management of public interaction surrounding base cleanup activities,
- Protection of the Cape Cod groundwater aquifer from further contamination by source containment through the design of a landfill cover system,
- Design of a bioremediation scheme to remediate contaminated groundwater.

Each individual on the project team researched a specific topic associated with the site. Individual findings were compiled as individual thesis reports in partial fulfillment of the Master of Engineering Degree. Chapter II in this work, Project Background and Site Description, is taken from the team project report. A description of project results can be found in Appendix F.

Chapter II. Background and Site Description

Upper Cape Geography and Land Use

The Massachusetts Military Reservation (MMR) is located in the northwestern portion of Cape Cod, Massachusetts, covering an area of approximately 30 square miles (ABB, 1992). Figure 2.1 is a regional map of western Cape Cod. Military operations on the MMR began in the early 1900's. It has been used by several branches of the armed services, including the United States Air Force, Army, Navy, Coast Guard, and the Massachusetts Air National Guard. Operations by the Air National Guard and Coast Guard are ongoing.

The area of present study is the Main Base Landfill site, termed LF-1 by the MMR Installation Restoration Program. The landfill is about 10,000 feet from the western and southern MMR boundaries and occupies approximately 100 acres. The landfill has operated since the early 1940's as the primary waste disposal facility at the MMR (CDM Federal, 1995). Unregulated disposal of waste at LF-1 continued until 1984, at which time disposal began to be regulated by the Air National Guard.

Waste disposal operations at LF-1 took place in five distinct disposal cells and a natural kettle hole, as shown in Figure 2.2. These are termed the 1947, 1951, 1957, 1970, post-1970, and kettle hole cells. The date designations indicate the year in which disposal operations ceased at that particular cell. Accurate documentation of the wastes deposited at LF-1 does not exist. The wastes may include any or all of the following: general refuse, fuel tank sludge,

herbicides, solvents, transformer oils, fire extinguisher fluids, blank small arms ammunition, paints, paint thinners, batteries, DDT powder, hospital wastes, municipal sewage sludge, coal ash, and possibly live ordnance (ABB, 1992). Wastes were deposited in linear trenches, and covered with approximately 2 feet of native soil. Waste depth is uncertain, but estimated to be approximately 20 feet below the ground surface on average. Waste disposal at the landfill ceased in 1990. A plume of dissolved chlorinated volatile organic compounds, primarily tetrachloroethylene (PCE) and trichloroethylene (TCE), has developed in the aquifer to the west of the landfill.

The four towns of interest on the western Cape are Bourne, Sandwich, Mashpee, and Falmouth. The total population of this area, according to a 1994 census, is 67,400. The area is mostly residential, with some small industry. A significant amount of economic activity is associated with restaurants, shops, and other tourist-type industry. The total population of Cape Cod is estimated to triple in summer, when summer residents and tourists make up most of the population. The total Cape population has doubled in the last twenty years. It has been one of the fastest growing areas in New England. In 1986, 27% of economic activity was attributed to retirees; tourism accounted for 26%; seasonal residents, 22%; manufacturing, 10%; and business services (fishing, agriculture, and other), 15%. The economy is currently experiencing a shift from seasonal to year-round jobs. (Cape Cod Commission, 1996).

Climate

The Cape Cod climate is categorized as a humid, continental climate. Average wind speeds range from 9 mph from July through September to 12 mph from October through

March. Precipitation is fairly evenly distributed, with an average of approximately 4 inches per month. Annual precipitation is approximately 47 inches. There is very little surface runoff. Approximately 40% of the precipitation infiltrates the ground and enters the groundwater system (CDM Federal, 1995). The remainder goes back into the atmosphere either directly through evaporation or indirectly through plant transpiration.

Groundwater System

Cape Cod is underlain by a large, unconfined groundwater flow system. This phreatic aquifer has been designated a sole source aquifer by the Federal Environmental Protection Agency. The aquifer is divided into six flow cells according to the hydraulic boundaries of the flow system. The Massachusetts Military Reservation and LF-1 plume are located in the west Cape flow cell, the largest of the six flow cells. The west Cape aquifer system and water table contours are depicted in Figure 2.3.

The water table in this region generally occurs at a depth of 40-80 feet below the ground surface. Surface water is also present in the study area as intermittent streams in drainage swales and more importantly as ponds in kettle holes. However, there are no large kettle ponds that can signficantly influence the flow regime in the vicinity of the LF-1 plume. It is thought that the cranberry bogs west of the LF-1 site are underlain by localized perched water tables, and thus hydrologically disconnected from the larger aquifer system (CDM Federal, 1995).

Vertical Hydraulic Gradients

Vertical gradients that have been calculated for the MMR are very small. However, significant upward gradients exist where groundwater discharges into large ponds and near coastal areas where the aquifer discharges into the ocean. Small downward gradients of about 10^{-3} to 10^{-4} are observed throughout the rest of the study area (CDM Federal, 1995). The general pattern is best characterized as upward flow near the shoreline and large surface water bodies and downward flow elsewhere.

Horizontal Hydraulic Gradients

Groundwater flow in the region is driven mostly by horizontal gradients. These can be measured by dividing a groundwater elevation contour interval by the horizontal distance between the contours. The latter value can be estimated from a contour map similar to Figure 2.3. Horizontal gradients calculated for the LF-1 study area using February 1994 water levels range from 1.3×10^{-3} to 6.8×10^{-3} (CDM Federal, 1995). These gradients are observed to steepen from the LF-1 source area westwards.

Seepage Velocity

Calculated seepage velocities in the LF-1 study area indicate that advective contaminant transport takes place at velocities ranging from 0.10 ft/day to over 3 ft/day. Since seepage velocity is a function of hydraulic conductivity, estimates for the different conductivities of the various sediment types will strongly influence calculated seepage velocities. An estimate of contaminant seepage velocity made using observed LF-1 plume migration distance and time yielded an average seepage velocity of 0.9 ft/day (CDM Federal, 1995).

MMR's Listing on the National Priorities List

The MMR is one of 1,236 sites that have been placed on the National Priority List (NPL) by the U.S. Environmental Protection Agency (EPA). NPL sites are those to which the EPA has given particularly high human health and environmental risk ranking. Rankings are determined from an evaluation of the relative risk to public health and the environment from hazardous substances identified in the air, water and geologic surroundings local to a site. Once placed on the NPL, sites are targeted for remedial clean-up financed by the Superfund, which is the federal government's fiduciary and political device for remediating hazardous waste sites. Additional funding for cleanup is provided by potentially responsible parties (PRPs), those individuals and organizations whose activities have resulted in contamination.

Present Activity

Due to the health and environmental risks which have been attributed to activities at the MMR, federal activity is underway to further quantify and reduce, to the extent required, the risk imposed upon human health and the environment. As part of remediation operations at MMR, several of the landfill cells have recently been secured (1994) with a final cover system. These cells include the 1970 cell, the post-1970 cell, and the kettle hole. The remaining cells (1947, 1951, and 1957) have collectively been termed the Northwest Operable Unit (NOU). Remedial investigations as to the necessity of a final closure system for these

cells is ongoing. Other IRP activities associated with the LF-1 site include design of a plume containment system and further plume delineation and groundwater modelling.

Figure 2.1: Site Location Map (ABB, 1992)

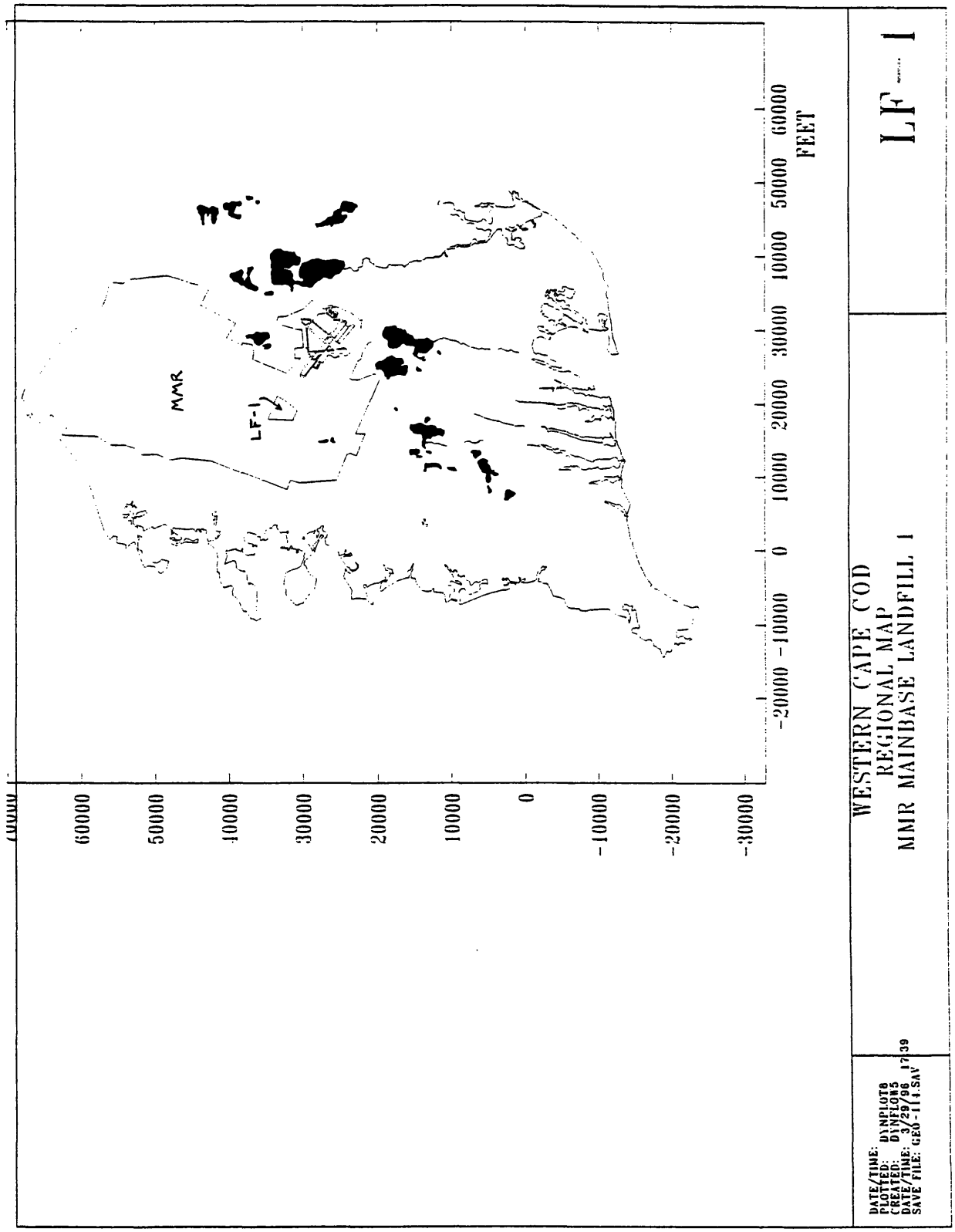

Figure 2.2: Photogrammetric Map of Landfill Layout (ABB, 1992)

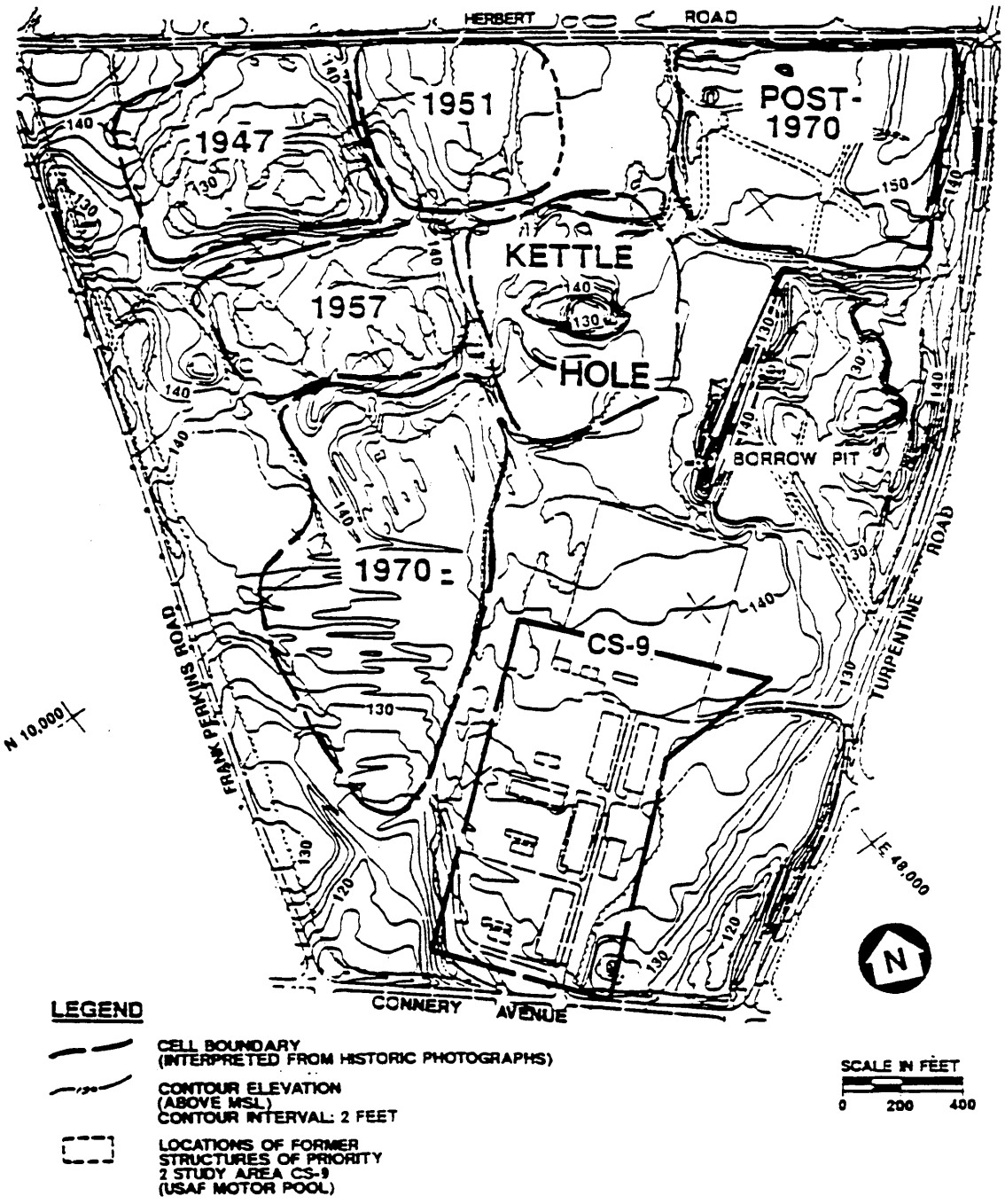

Figure 2.3: West Cape Cod Aquifer System
Groundwater Contour Map (Automated Sciences, 1994)

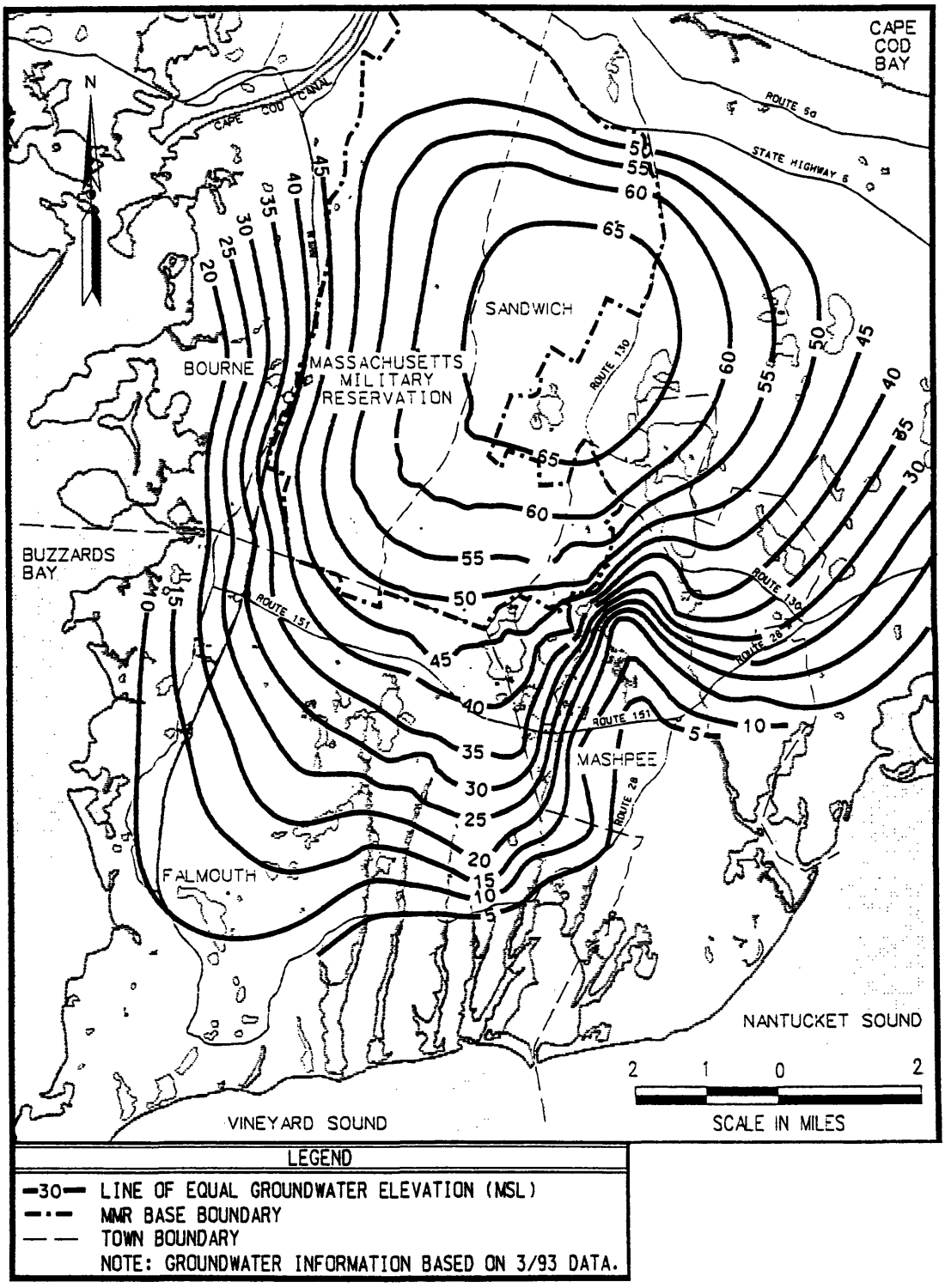

Chapter III. Literature Review

Geology

The Cape Cod Basin consists of material deposited as a result of glacial action during the Wisconsinian stage of the Pleistocene Epoch, between 7000 and 80,000 years ago. Advancing glaciers from the north transported rock debris gouged from the underlying crystalline bedrock until reaching the southernmost point of advance at Martha's Vineyard and Nantucket Island (Oldale, 1984). Subsequent periods of glacial retreat, melting, and erosion created three distinct geologic regions. These are called the Mashpee Pitted Plain (MPP), Buzzards Bay Moraine (BBM), and Buzzards Bay Outwash (BBO) (see Figure 3.1). The Main Base Landfill lies within the Mashpee Pitted Plain. The plume has migrated westward through the Buzzards Bay Moraine and into the Buzzards Bay Outwash region.

As the glaciers retreated from their farthest advance at Martha's Vineyard, they left behind a relatively thin layer of pulverized material called basal glacial till. This material is composed of very dense, poorly sorted, fine to coarse sand, gravel, silt and clay. The retreating glaciers stopped for a period of time near the western and northern shores of Cape Cod. During this stagnation period, a great deal of sediment was washed out of the glaciers in a southeast direction, forming a broad alluvial plain on top of the basal glacial till. This area is called the Mashpee Pitted Plain (CDM Federal, 1995.).

The braided streams flowing from the glaciers tended to sort the sediments by grain size. In general, stream velocities and land-surface slopes decrease as the distance from the source

increases. As a result, dense material is carried by the more energetic portion of the stream and then falls out as the stream energy declines. Increasingly finer material is carried a farther distance. Consequently, in the Mashpee Pitted Plain, the coarse sand and gravel sediments are about 300 feet thick near the moraines and 50 feet thick near Nantucket Sound. Conversely, medium to fine sand and silt deposits range from 0 feet thick near the moraines to 200 feet thick near Nantucket Sound (Thompson, 1994).

The Buzzard's Bay Moraine resulted from the melting of the stagnated Buzzards Bay glacier. As a result, this ridge does not display the same trends in stratified drift as does the Mashpee deltaic deposits. Since the sediments dropped directly from the glacial ice, they are not as well-sorted as outwash deposits. In general, they exhibit a wider range and finer average size (E.C. Jordan, 1989). Another theory states that the BBM is the result of a re-advance of the glacier after retreating farther to the west (Oldale, 1984). This theory is supported by bore hole samples showing a discontinuous layer of what could be fine basal till within the moraine, deposited when the re-advancing glacier partially overrode existing alluvial deposits. As a result, these deeper outwash deposits have been compacted by the weight of the ice. Material deposited above the till layer is typical of deposits left behind by a melting glacier (CDM Federal, 1995).

The Buzzards Bay Outwash was deposited as a result of sedimentation between the retreating glacier and the newly deposited Buzzards Bay Moraine. BBO sediments are generally sand and gravel, and are considered to be stratified in the same manner as the MPP outwash, with a general trend of fining downwards. This trend may be explained by the same outwash dynamics explained previously. At any particular location, the grain size will

increase with elevation if the source of outwash material (the glacier) is advancing and streams are progressively laying down coarser material (Thompson, 1994). A discontinuous layer of basal till, similar to that found in the BBM, has been found at mid-elevations within the BBO, once again suggesting a glacial re-advancement (CDM Federal, 1995).

Hydrogeology

Porosity measurements over the entire western cape vary from 0.20 to 0.40. Hydraulic conductivity (K) measurements range from a maximum of 800 feet/day to a minimum of 0.4 feet/day. The outwash sediments exhibit the highest K values (15 to 800 feet/day). The moraine materials show intermediate K values (11 to 48 feet/day) and the basal till sediments have the lowest K values (0.4 to 28 feet/day) (E.C. Jordan, 1989).

Jordan reports that the large variability in the outwash K values is due to anticipated spatial variability (due to the fluvial nature of sediment deposition) and also to the application of different interpretive methods. Data were collected by the United States Geological Survey and Jordan. Because the data were collected by several investigators at different times, using different sampling, measuring, or analytical techniques, Jordan estimates that the variability due to analytical methods may be as great as one order of magnitude (E.C. Jordan, 1989).

Anisotropy measurements (the ratio of horizontal K to vertical K) in the outwash regions range from 2:1 to 5:1 on a regional basis. Given that the outwash areas consist of stratified sediments, these are relatively low ratios. This is primarily due to the small percentage of fine-grained sediments (E.C. Jordan, 1989).

The western Cape Cod region, as shown in Figure 2.3, contains an isolated, unconfined aquifer bounded on the north by the Cape Cod Canal and Cape Cod Bay, on the east by a drainage between Barnstable and Hyannis, on the south by Nantucket Sound, and on the west by Buzzard's Bay. It is dependent upon local rainfall for recharge. Recharge is estimated to be 17 - 23 inches per year. The hydraulic head contours are concentric, following the general shape of the western Cape, and centered on the northern portion of the MMR. The hydraulic gradient on the MMR towards the south is between $1.4x10^{-3}$ and $1.8x10^{-3}$. It is somewhat steeper to the west with an average between $1.7x10^{-3}$ and $2.0x10^{-3}$. These numbers are similar to those found by CDM Federal (1995). Flow through the southern portion of the MMR is estimated to be about 1.7 feet/day. The horizontal flow through the BBM is estimated to vary from 0.07 to 0.6 feet/day (E.C. Jordan, 1989).

Hydraulic Conductivity Slug Tests

Springer

Springer (1991) characterized the large-scale heterogeneity of the hydraulic conductivity of a study site south of the MMR in the MPP operated by the United States Geological Survey (USGS). Slug tests were made in 335 observation wells covering an area of 30 km^2. Springer reviewed the previous work of Hvorslev, Bouwer and Rice, Dagan, Cooper, Van Der Kamp, Molz, and others regarding the determination of K from raw slug test data. He concludes that the analysis of Molz et al (1990) provides the most realistic representation of flow in a slug test. Springer developed an analytic technique for obtaining K values based on the finite element model of Molz et al (1990). He states that the Bouwer and Rice (1976) formulation

both underestimates and overestimates the hydraulic conductivity, depending on the anisotropy, aspect ratio of the well, and distance from the well screen to aquifer boundaries (packing thickness). He believes the Hvorslev partially penetrating formulation overestimates conductivity by 10 percent or more (Springer, 1991).

One third of the slug tests perfomed by Springer exhibited an oscillatory (underdamped) response. Springer observes that Van Der Kamp's (1976) treatment of underdamped response does not present any definitive conclusions regarding frictional effects. Springer proceeds to analyze the effects of water column inertia and wall friction in the well pipe. He concludes that in areas where K values are greater than 32 feet/day, the conductivity may be overestimated by a factor of 2 if inertial effects are neglected. In tests displaying oscillatory response, the conductivity may be underestimated by a factor of 2 if frictional effects are ignored (Springer, 1991).

The geometric mean of the K values calculated by Springer was 171 feet/day and the arithmetic mean was 410 feet/day. The variance of lnK was 2.25. A Gaussian filter with length scales of 1000 meters in the horizontal direction and 5 meters in the vertical was used to identify smoothed large-scale trends in the lnK data. These lengths represent approximately 1/8 of the longest dimension and depth of the study region (approximately 8000 meters by 40 meters deep). This analysis showed substantial vertical layering. Conductivity at the water table was 66 - 164 feet/day, then increased from 328 - 984 feet/day in the elevation range 49 - 82 feet below the water table, and fell to less than 66 feet/day a few meters further down (Springer, 1991).

Van Der Kamp

The data used in this study was taken from the "Remedial Investigation Report," prepared by CDM Federal Programs Corporation for the IRP at MMR as part of the remedial investigation (RI) phase of the Superfund process. Hydraulic conductivity estimates were calculated by CDM using analysis techniques developed by Bouwer and Rice (1976) for the overdamped cases and Van Der Kamp (1976) for the underdamped situation (CDM, 1995).

The Van Der Kamp technique was implemented using the computer program "Harmonic (Smith, 1992)" (CDM, 1995). The following equations outline the method. The water level fluctuation is assumed to be given by

$$w(t) = w_o e^{-\lambda t} \cos\omega t$$

where λ and ω are the damping and angular frequency of the oscillation, respectively. These values are determined from a plot of the water level vs. time. The following parameters, L and d, are calculated from λ and ω .

$$L = g/(\omega^2 + \lambda^2) \quad \text{and} \quad d = \lambda/(g/L)^{1/2}$$

Next, $$a = r_c^2 (g/L)^{1/2}/8d \quad \text{and} \quad b = -a\ln[0.79 r_f^2 S(g/L)^{1/2}]$$

where g is the acceleration due to gravity, r_c is the inside well radius, r_f is the filter radius of the well, and S is the storage coefficient. Finally,

$$T = b + a\ln T$$

where T is the aquifer transmissivity. K, hydraulic conductivity, is found by dividing transmissivity by the depth of the aquifer.

An iterative process is used with T_o = b as a first approximation.

$$T_n = b + a \ln T_{n-1} \quad n \geq 1$$

Large variations in the values of r_f and S result in only small variations in the value of b, and therefore a reasonably good estimate of r_f and S is sufficient for most practical purposes (Van Der Kamp, 1976).

Bouwer and Rice

The Bouwer and Rice (1976) technique for determining hydraulic conductivity from slug test data was implemented using the computer program "BRISTA (Smith 1992)" (CDM, 1995). The method developed by Bouwer and Rice (1976) for an unconfined aquifer is based on a modified version of the steady state Thiem equation, $Q = 2\pi KL \frac{y}{\ln(R_e r_w)}$, and the rate of rise equation for the well, $dy/dt = -Q/\pi r_c^2$. Combining, intergrating, and solving for K yields

$$K = \frac{r_c^2 \ln(R_e / r_w)}{2L} \frac{1}{t} \ln \frac{y_0}{y_t}$$

$\ln \frac{R_e}{r_w}$ is given by

$$\ln \frac{R_e}{r_w} = \left[\frac{1.1}{\ln(H/r_w)} + \frac{A + B \ln[(D-H)/r_w]}{L/r_w}\right]^{-1}$$

The parameters A and B are found from a graph of L/r_w versus A and B developed by Bouwer and Rice using a resistance network analog to represent axisymmetric flow. r_w is the effective well radius (well casing plus developed zone), L is the screen length, D is the aquifer depth, H is the well depth below the water table, and y_0 is the initial water level in the well. A maximum value of 6 should be used for the factor $\ln[(D-H)/r_w]$.

The field data should yield a straight line when plotted as ln y_t versus t. The term $(1/t)\ln(yo/y_t)$ is obtained from this plot and used in the above equation. Bouwer and Rice state that their method yields values within 10% of the actual values evaluated by analog simulation if L > 0.4H and within 25% if L << H (e.g., L=0.lH).

Grain Size Analysis

Hazen

CDM Federal used two methods for determining hydraulic conductivity from grain size data. The first was developed by Hazen in 1893 and is described in Freeze and Cherry (1979). An empirical relation is found to exist such that $K = d_{10}^2$, where K has units of cm/s and d_{10} is the grain size diameter (mm) at which 10% (by mass) of the grain particles are finer. This approximation was found to be true for uniformly graded sands but it can provide rough, yet useful, estimates for most soils in the fine sand to gravel range.

Alyamani and Sen

The second grain size method used by CDM was developed by Alyamani and Sen (1993). It uses grain sizes d_{10} and d_{50}, the diameters (mm) at which 10% and 50% by mass, respectively, of the grain size particles are finer. It also relates the hydraulic conductivity to the initial slope and intercept of the grain size distribution curve (grain size in mm versus percent by mass passing). An empirical relation was discovered between K values measured using a constant-head permeameter and the expression $[I_0 + 0.025(d_{50} - d_{10})]$ such that a plot on log-log paper produced a nearly straight line. I_0 is the x intercept of the grain size

distribution curve. Values for the parameters a and b shown below were derived from this plot.

$$K = a[I_o + 0.025(d_{50} - d_{10})]^b$$

Since it follows that log K = log a + b log[I_o + 0.025(d_{50}-d_{10})], the parameter a is equal to the K value at $[I_0 + 0.025(d_{50} - d_{10})] = 1$, and the parameter b is equal to the slope of the log-log plot (in decades). The final formula derived by Alyamani and Sen for the sample data used in their investigation was

$$K = 1300[I_o + 0.025(d_{50} - d_{10})]^2 .$$

The sediments used in this analysis are characterized as wadi (alluvium) deposits and Quaternary alluvial deposits, with the most common being slightly coarse (Alyamani et al, 1993).

Bedinger

In addition to the Hazen and Alyamani/Sen methods used by CDM Federal, an additional algorithm developed by Bedinger was used in this study. The formula is K = (267)(d_{50}^2), where K has units of feet/day and d_{50} is the grain size diameter in mm at which 50% (by mass) of the grain particles are finer (Bradbury, et al, 1990).

Figure 3.1: West Cape Cod Glacial Deposits (CDM Federal, 1995)

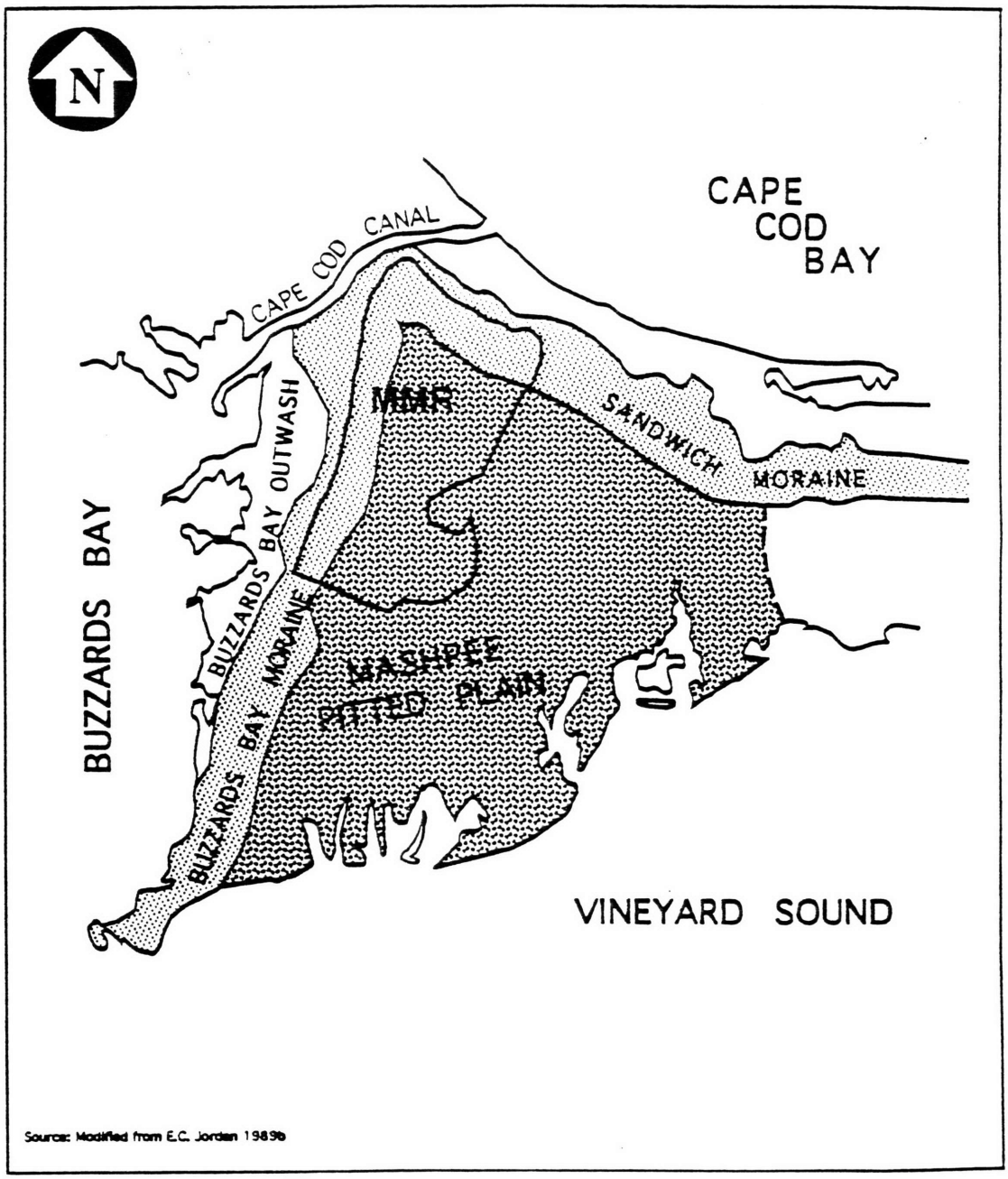

Chapter IV. METHODS

Data Sources

As stated previously, the data used for characterizing the LF-1 plume was taken from the "Remedial Investigation Report" (RI Study) prepared by CDM Federal for the MMR IRP as part of the Superfund process. Data were examined in two areas: groundwater contamination and subsurface hydraulic conductivity (CDM Federal, 1995).

Geographic coordinate information for 66 locations was obtained from the RI Study, Volume II, Table 3-7 (see Figure 5.1 and Appendix A). Well clusters share the same coordinates. The coordinate system used in the RI Study had to be converted to the coordinate system used in the western Cape mapping system created in Dynplot by Bruce Jacobs. The conversion was accomplished by subtracting 838,906 from the RI Study "Easting" coordinate and 213,789 from the RI Study "Northing" coordinate.

Contamination samples were taken utilizing two basic procedures. Field screening samples were tested within a few hours of sampling using mobile laboratory equipment. This method was employed to quickly guide well drilling operations in the directions and depths required to identify the plume extent. In order to fulfill QA/QC (quality assurance/quality control) Superfund requirements, the majority of testing was done at fixed contract laboratories as part of the Contract Laboratory Program (CLP). A total of 73 wells were tested for 34 different contaminants from the beginning of 1993 to the beginning of 1994. Approximately 160 wells were drilled as part of the RI Study, but not all of these were tested for contamination. Some were used for testing water levels and geologic sampling. The

results are posted in Table 5-7A, Detected VOC (Volatile Organic Compound) Values, in Volume II of the RI Study. Contaminant investigations in this work focused on this database.

Slug test data for this report were taken from the RI Study, Volume II, Table 4-1. As stated previously, two analytic techniques were used, Bouwer and Rice and Van Der Kamp. 79 well tests out of 87 were used in the present investigation. Eight of the points were not used because the geographic location of these points was not found in the report.

Grain size data were taken from the RI Study, Volume II, Table 4-2. 140 samples were analyzed from 21 well locations. Nine samples from one well (GB-21) were not used because the geographic location could not be found in the report.

Data Interpretation Tools

The data taken from the RI Study was transcribed into Microsoft Excel spreadsheets. These spreadsheets were used to create appropriate tables and statistically analyze the data. The data files were also reformatted and converted to text files for input into a program developed by Camp Dresser & McKee called DynPlot.

Dynplot is a graphical pre- and post-processor for the DYN system of flow and contaminant transport computer models. It can be used to create displays of data in plan view and vertical cross-section. It was used in this report to map well locations and point data, to contour concentration levels for different categories of contaminant, and to contour values of hydraulic conductivity. It was also used to calculate finite element grid node values from

point data using a gaussian filter algorithm. The additional programming required within the Dynplot code for this project was performed by Bruce Jacobs.

Analysis of Contamination Sample Data

A spreadsheet of all RI Study (Table 5-7A) VOC contamination data is included in Appendix B. This contamination data was aggregated in three different ways for each well location. In the first case the concentration of all contaminants measured at a particular well was totaled. This was done to estimate and track the total mass of VOC contamination. In the second case the sampled concentration values were first divided by the MCL level for that contaminant. The MCL level is the Maximum Contaminant Level allowed in order to pass EPA drinking water quality standards. Those contaminants that have no listed MCL were not included. These normalized values were then totaled for each sampling well location. The third case was similar to the second, except that the maximum normalized contaminant value at each well was used rather than the total. The reason for looking only at the maximum value is the fact that EPA doesn't have a cumulative standard. The standard is met as long as all detected contamination concentrations don't exceed the individual MCL level for that contaminant. This method of characterizing the data provides insight into the level and extent of human health hazard. See Figures 5.2 - 5.7 for two dimensional (plan view) contours of this data.

In addition, concentration contours were made for two of the contaminants with the highest concentrations, tetrachloroethene (PCE) and trichloroethene (TCE) (see Figures 5.8 and 5.9).

Analysis of derived hydraulic conductivity values

A spreadsheet was created to calculate values of hydraulic conductivity (K) from the grain size information in Table 4-2 of the RI Study (see Appendix D). As discussed in the results chapter of this report, several of the calculated values determined in this study using the Alyamani/Sen method were significantly different from the calculated values determined by CDM Federal. See Appendix D for a comparison of the two results.

Twenty-three points among the slug and grain size data are located at approximately the same location. A comparison was made among these derived values to see if a correlation could be found between the various methods. The mean, standard error, median, standard deviation, sample variance, range, minimum, and maximum values were computed (see Table 5.3). In addition, natural log histograms were plotted (see Figures 5.13 and 5.14). Ln Hazen K values were plotted versus ln slug K values and a least squares best fit line was fitted through the plot. Ln Alyamani/Sen values were similarly plotted versus ln Bedinger K values. Out of the 23 points, 8 had the grain size samples pulled from the exact location where the slug test was performed. Similar plots were also made for these 8 points alone (see Figures 5.15 - 5.18). However, it should be noted the grain size analysis applies only to the small amount of material pulled from the well, whereas the slug test determines an average hydraulic conductivity over its zone of influence, a volume substantially larger than the grain sample.

As described previously, two parameters in the original Alyamani/Sen formula were based on K values determined by permeameter tests in the lab. The 23 slug K values were plotted in

the same manner to see if a similar straight line relationship would yield different parameters. This plot is shown in Appendix E.

A three dimensional gauss filter was used to spatially smooth the contaminant and hydraulic conductivity data. Vertical cross section contours of the filtered contaminant values are presented in Figures 5.10 - 5.12. In the case of hydraulic conductivity, this device was used to find trends in the data so that values could be assigned to discrete element blocks in a discrete element flow model. The formula for this filter is

$$K_i^* = \frac{\sum_{j=1}^{n} K_j EXP - \{[(x_j - x_i)/l_x]^2 + [(y_j - y_i)/l_y]^2 + [(z_j - z_i)/l_z]^2\}}{\sum_{j=1}^{n} EXP - \{[(x_j - x_i)/l_x]^2 + [(y_j - y_i)/l_y]^2 + [(z_j - z_i)/l_z]^2\}}$$

where (x_i, y_i, z_i) are the coordinates for a point at which a filtered value for the natural log of K is to be calculated; $ln\, K_i^*$ is the smoothed value of ln K at location point i;

n is the total number of data points; $\ln K_j$ is the natural log of the jth K data point; and l_x, l_y, and l_z are significant length parameters that can be varied to yield different degrees of smoothing (Springer, 1991). See Figures 5.19 - 5.31 for vertical cross section contours of the filtered K data.

This filter is very effective at smoothing and contouring "noisy" data, thereby illustrating trends, but must be used with caution. To illustrate the effect of the length parameter on the results of the algorithm, a one dimensional calculation was performed. The length parameter was varied and values were calculated for the same locations as the data set points. A comparison was then made between the data set value and the calculated value at each

location. As the length parameters varied from 1/10 to 10 times the dimension of the data set, the filtered values varied from the data set value to the data set average. However, if the sample set values were increased in one direction, the values which were calculated at further distances in the same direction increased up to the maximum data set value. Consequently, it can be seen that if there is a trend of increasing sample values in one direction, the values calculated by the algorithm at locations in the same direction, beyond the last sample point, will continue to increase up to the maximum sample value in the data set.

Another value required for the element flow model is the anisotropy in hydraulic conductivity; i.e., the ratio between hydraulic conductivity in the vertical and horizontal directions. This value was determined for the area, as a whole, using the equation

$$EXP\{[\sum_{j=1}^{n} (\ln K_j - \ln K_j^*)^2]/n-1\}$$

where $\ln K_j$ is the natural log of the jth K data point and $\ln K_j^*$ is the filtered value of ln K at location point j.

Chapter V. Results

Groundwater Contamination

The full groundwater contamination database used in this report is presented in Appendix B. Figure 5.1 shows a map of the sampling well locations. A number of two dimensional contaminant concentration contours are developed using this database and the Dynplot program. In all cases, the contour area must be limited to a specified region within the finite element grid. If this is not done, values may be extrapolated for regions where there could not be any contamination; for example, upgradient from the landfill. This problem is similar to the trending produced by the gaussian filter discussed in Chapter IV; that is, if the data shows a trend in one direction, the contours will show a continuation of this trend beyond the data points. This is only a problem where the data values do not decrease when going from the center of the sample area towards the perimeter. This occurs in the area near the border of the landfill. By restricting the contour area to a perimeter just beyond the sample well locations, this problem was avoided.

In addition, Dynplot has the option to create linear or log-linear contours. The log-linear method spaces intervening contours between known or boundary values using a log scale, whereas the linear procedure uses a linear scale. This report uses only the log-linear option.

Figures 5.2 - 5.4 are log-linear contours of total contaminant mass. They show the contaminantion migrating from the landfill in a southwesterly direction and then curving towards the west. This is to be expected given the groundwater contours shown in Figure 2.3.

Groundwater seepage is generally at right angles to water level contour lines. The area which contains a total concentration of 1 part per billion (ppb) or more is about 4.1 square miles.

The figures also show greater concentrations closer to the landfill. One reason for this could be that the contaminants are naturally degrading as they migrate away from the landfill. However, this is not the case with regard to two of the major contamninants, PCE and TCE. Figures 5.5 and 5.6 are maps of PCE and TCE concentration contours, respectively. Comparing the two, one can see the main concentrations of PCE are downgradient from the main concentrations of TCE. This shows that little, if any, biodegradation of PCE is occurring, since TCE is created when PCE biodegrades.

Since the landfill has been operating since 1941, a likely explanation for the variability in concentrations is simply the episodic nature of dumping. Unfortunately, it is not possible to verify this theory, since no records were kept of material deposited in the landfill. However, it is known that unregulated dumping at the landfill ended in 1984. This could explain why the concentration peak closest to the landfill, seen in Figure 5.4, is approximately 3,300 feet away. This distance is equal to the average estimated seepage velocity, 0.9 feet/day (CDM Federal, 1995), times 10 years (3650 days). Since the landfill has been closed and partially capped, it is reasonable to assume that the contaminant concentrations next to the landfill will continue to decline over time.

It should also be noted that Figures 5.3 and 5.5 show a bifurcation at the western end of the plume. Separate northern and southern concentration lobes can clearly be observed. This phenomena is discussed further in the following sections.

Figures 5.7 and 5.8 show contour maps similar to Figures 5.2 - 5.4 (total mass) but the individual contamination concentrations have been normalized by dividing by the EPA specified Maximum Contamination Level (MCL) for that contaminant in drinking water. That is to say, all of the contaminant concentrations found at a particular well were first divided by the listed MCL for that particular contaminant. These numbers were then totaled to yield a single value for that particular well. Contaminants without a designated MCL were excluded. These contours give a picture of the extent of contamination in terms of total MCL exceedance. The area which contains a total MCL-normalized value of 1 or more is about 2.2 square miles.

The EPA drinking water standard does not account for cumulative effects, therefore Figure 5.9 is an additional contour map showing only the maximum individual MCL-normalized level (regardless of type of contaminant). That is, after all of the contaminant concentrations found at a particular well were divided by the listed MCL for that particular contaminant, the highest single value was chosen as the value for that well. The area which contains a maximum MCL-normalized value of 1 or more is about 2.0 square miles. This represents the areal extent of the aquifer which must be remediated in order to meet EPA drinking water standards. This is about half the areal extent of the total mass contour of 1 ppb shown in Figure 5.2.

As mentioned earlier, Figures 5.3 and 5.5 show a bifurcation at the western end of the plume. Separate northern and southern concentration lobes can be observed. Figures 5.10 and 5.11 show vertical cross sections of maximum MCL-normalized contours through the longitudinal axes of the north and south lobes. Figure 5.12 shows a north/south cross section.

As discussed previously, a three dimensional gauss filter was used to assign concentration point values to each of the nodes in the three dimensional finite element grid. The program can then contour these point values in vertical cross section. Dynplot is not capable of contouring the unfiltered contamination data in the vertical plane.

If one projects the vertical cross section contours shown in Figures 5.10 - 5.12 onto a horizontal plane it does not yield the same plan view contours shown in Figure 5.9, although the data is the same. This is because the length parameters used in the filtering process for the vertical cross sections are relatively small compared to the data extent. As explained previously, this will tend to give values closer to the original data. There is less smoothing of the data set, therefore one sees more localized peaks.

One can note a general downward movement of the contamination. Modeling predicts this is due more to the areal recharge than the density of the contaminant (Amarasekera, 1996). One can also observe that the southern lobe is significantly deeper than the northern lobe. This is also predicted by modeling. It is explained by the longer distance traveled by the southern lobe (Amarasekera, 1996).

From Figures 5.2 - 5.4 it is possible to make a very rough approximation of the total mass of groundwater contamination. An estimate is made of the area contained by the innermost contour in a concentric set. The concentration for this area is assumed to be the average of the boundary contour value and the highest point value which lies within the area. The area bounded by the next contour interval going outward is then estimated. The previous (inner) area is subtracted to obtain the area in this contour interval. The concentration for this area is assumed to contain the average concentrations of the two bounding contour intervals.

Continuing to work outward, subsequent areas and concentrations are estimated. The total concentration per unit depth is the result of summing the product of each area and concentration. The more difficult estimation to be made at this point is coming up with an average depth for all the contamination. A rough estimate can be made from looking at the vertical cross sections of contoured contamination shown in Figures 5.10 - 5.12. Using an estimated average depth of 40 feet, the estimated total mass is 160 cubic feet or 22 - 55 gallon drums (see Table 5.2). This mass is distributed over approximately 4.5 square miles. This works out to be an average total contaminant concentration of 32 ppb.

Hydraulic Conductivity

The database used in this report is shown in Appendix D. Values for the three grain size determined K values were calculated in the spreadsheet. It was discovered that a majority of the values calculated by CDM Federal using the Alyamani/Sen method were not correct. Both values are included in Appendix D for comparison. The values calculated in this report were the ones used in the following analysis.

Figures 5.13 and 5.14 show histograms of the distribution of natural log K values from slug tests and grain size determinations for 23 common (approximately) locations. The Alyamani/Sen data most approximates a normal distribution. The next best fit is the Bedinger data. The slug test data has the narrowest spread. This could be due to the fact that the grain size data applies to the hydraulic conductivity in a sample less than 0.2 cubic feet, whereas the slug test averages the hydraulic conductivity over a much wider volume.

A statistical description of the natural log of the 23 approximately common K data locations is shown in Table 5.3. The Bedinger method shows the highest mean, 3.957 and the lowest sample variance. Looking at the correlation values, the best correlation (0.572) was found between the Alyamani/Sen and Bedinger methods. Examining a plot of ln Alyamani/Sen vs. ln Bedinger (Figure 5.15), one can see that a marked improvement in the correlation will occur if the 5 lowest Alyamani/Sen values (those below 4.1 feet/day) are ignored. Table 5.4 represents this reduced data set. Wells GB-22, MW-25, MW-64A, MW-569C, and MW-567D were removed. There is no correlation between these wells with respect to depth or location, only the fact they all had a low Alyamani/Sen value for K. The improved correlation seen in Table 5.4 is 0.874. A linear regression fit of the reduced data is seen in Figure 5.16. The straight-line equation is ln Bedinger = 0.809(ln Alyamani/Sen) + 1.25, representing 18 data points. This result could be explained, in part, by the fact that the Alyamani/Sen formula depends on the d_{10} and d_{50} grain sizes, whereas the Bedinger is a function of the d_{50} size alone. Low Alyamani/Sen values would be the result of a greater percentage of d_{10}. When these values are thrown out, what is left are the values more dependent on d_{50}, the Bedinger parameter.

As stated previously, the 23 common data points for K values were not always in the exact same well and location. Samples taken within the same well cluster and close to the same depth were considered common. There are 8 data points out of the 23 which are in the same well and depth. Although the data set is very small, it was examined since it represents "exactly" common locations. The reduced data set is seen in Table 5.5. Once again, there is poor correlation between all data sets except for Sen vs. Bedinger, which has a correlation of

0.863. If the one Sen data point below a K value of 4 feet/day is removed, the correlation becomes 0.967. Plots of linear regression approximations of Sen vs. Bedinger are shown in Figure 5.17. The line representing the best correlation is ln Bedinger = 0.883(ln Alyamani/Sen) + 1.38. The close correlation between the Sen and Bedinger methods is not surprising since they both depend upon the same grain size fraction, d_{50}.

As described previously, two parameters in the original Alyamani/Sen formula were based on K values determined by permeameter tests in the lab. The 23 slug determined K values were plotted in the same manner to see if a similar straight line relationship would yield different parameters. This plot is shown in Appendix E. The data does not form a straight line but drawing a line which matches the parameters of the Alyamani/Sen equation gives what appears to be a reasonable fit approximation.

The 23 common location K value data sets were put through a gauss filter with horizontal length parameter 3000 feet and vertical length parameter 40 feet. This represents approximately 1/6 of the greatest horizontal and vertical extent of the data sets. The results of this are seen in Table 5.6. There was a marked improvement in the correlation between the slug and Hazen data sets after filtering. The correlation went from 0.13 to 0.62. The Sen and Bedinger correlation also improved, going from 0.57 to 0.71. With the the three smallest slug K data points removed (those less than 4.6 feet/day), the correlation between slug and Hazen improved to 0.72. Figure 5.18 is a graph of ln Hazen vs. ln slug using this reduced data set.

A value for anisotropy was determined by calculating the variance between the filtered and unfiltered ln K slug values. The same filtering length parameters were used as above: 3000 ft. horizontal and 40 ft. vertical. The results of this calculation are shown in Appendix C. The

variance of 1.22 is close to the value determined by Springer of 1.16. Values for horizontal conductivity, to be used for modeling, can be calculated by multiplying the filtered slug values by exp(variance/2) (personal communication, Professor Lynn Gelhar, 1996). This factor is 1.84 given the calculated variance of 1.22.

The arithmetic and geometric means of the slug K values and the sample variance of the ln slug values, both filtered and unfiltered, are shown at the bottom of page 2 of Appendix C. The sample variance of 2.76 is greater in this data set than the variance of 2.25 Springer found in his data set. The means are quite a bit lower than Springer found: 33 ft/day vs. 171 ft/day for the geometric mean, and 75 ft/day vs. 410 ft/day for the arithmetic mean. This is reasonable given that Springer's data was taken completely from the Mashpee Pitted Plain and about half the data for this report came from within the Buzzard's Bay moraine. Comparing the filtered and unfiltered values one can see that, although the geometric mean is nearly the same, the filtering process has substantially reduced the arithmetic mean and cut the peak value in half.

Gaussian Filtered K Cross Sectional Contours

Dynplot was used to filter all 4 sets of K value data (Hazen, Sen, Bedinger, and slug), using the same filter parameters as previously: 3000 ft. horizontal and 40 ft. vertical. The resulting log-linear contours were drawn in cross section as seen in Figures 5.19 - 5.30. Three cross sections were made for each data set; two from east to west through the two separate lobes of the plume, and one north to south through the moraine. A duplicate cross section (Figure 5.19) was made of the northern lobe using the slug test data. This shows, for

comparison purposes, some of the point values associated with the contours. One can see how the data was smoothed by the filtering process.

These diagrams illustrate, as noted previously, a good correlation between the Hazen and slug data and between the Sen and Bedinger data. They all illustrate the general trend of lower conductivity in the moraine and decreasing conductivity with depth. This agrees with previous analysis of the general Cape Cod hydrogeology. The Buzzard's Bay Moraine is clearly seen in Figure 5.20 as having significantly lower conductivity. In addition, looking at the north/south cross section, there is a zone of lower conductivity in the region where the plume is seen to split into a north and south lobe. This zone of lower conductivity may partially explain the split.

Pumping test comparison

A pumping test was performed on the Bourne public supply well number 5 (PS-5) in 1981 (CDM, 1995). The well screen is at a depth of 55 to 65 feet below the ground surface. The closest test well, from the CDM RI study (the data used in this report), is located at MW-567B, about 300 feet south at a depth of approximately -20 ft. msl. (The slug test well screen was located at the depth interval -19 to -24 ft. msl.) The ground surface at this location is 35 ft. msl.

The transmissivity calculated from the pumping test on PS-5 was 14.5 ft^2/min. Dividing by an aquifer thickness of 175 feet (CDM Federal, 1995), and converting time units, gives a hydraulic conductivity of 119 ft/day. Hydraulic conductivity values for well 567B can be

seen on pages 4 and 8 in Appendix D. The slug test value was 123 ft/day, Hazen - 41 ft/day, Sen - 1 ft/day, and Bedinger - 96 ft/day. The slug test value represents a local average, which apparently was representative of the wider area measured by the pumping test. The values determined from grain size don't correlate very well except for the Bedinger value. It is less likely a single grain size measurement will be representative of the larger localized area, when there is a lot of heterogeneity, since the sampling zone is so small.

Depth of draw for private well

A rough calculation of the approximate depth of draw for a private well can be made by assuming that the upgradient cross sectional area from which water will be drawn to a well located just below the water table is a half circle. (If one were to assume some horizontal to vertical anisotropy, the shape would be an ellipse, so the present assumption will yield a greater, more conservative, depth than actual.) Assuming steady-state and using Darcy's equation:

$$\frac{\pi d^2}{2} = \frac{Q}{K\frac{dh}{dx}} \quad \Rightarrow \quad d = \sqrt{\frac{2Q}{\pi K \frac{dh}{dx}}}$$

Given 100 gpd for 10 people = 1000 gpd for one private well. This equals 134 ft^3/day. Assuming a conservative value for K = 50 ft/day and for $\frac{dh}{dx} = 10^{-2}$ yields a value of d (depth of draw) equal to 13 feet.

Capture Wells

A rough calculation of the total pumping rate of capture wells required to stop the plume migration may be made using the formula

$w = \frac{Q}{T\frac{dh}{dx}}$ where w is the capture zone width, Q is the total well pumping rate, T is the aquifer transmissivity, and $\frac{dh}{dx}$ is the ambient hydraulic gradient. Assuming conservative values of K=100 ft/day, aquifer thickness = 150 ft., $\frac{dh}{dx}$=2.5 x 10^{-3}, and assuming Q = 1000 gpm = 1.925 x 10^5 ft^3/day, the capture width would be 5130 feet. This distance is slightly less than the full plume width. The pumping rate of 1000 gpm is the same as that suggested in the IRP Plume Response Plan Fact Sheet dated June 1994.

Figure 5.1 Contaminant Test Well Names and Locations

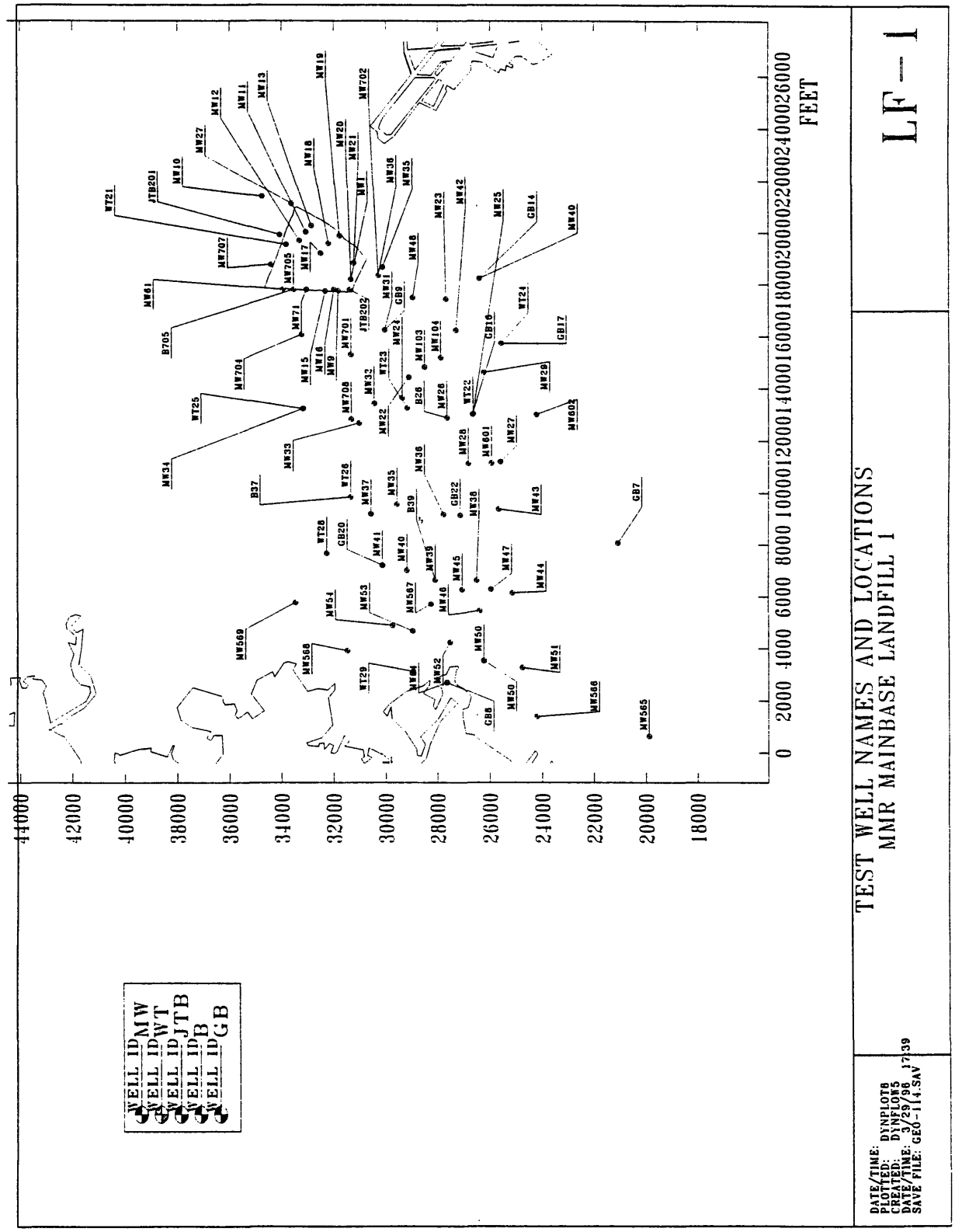

Figure 5.2 Contours of Total Contamination, 1 and 2 PPB

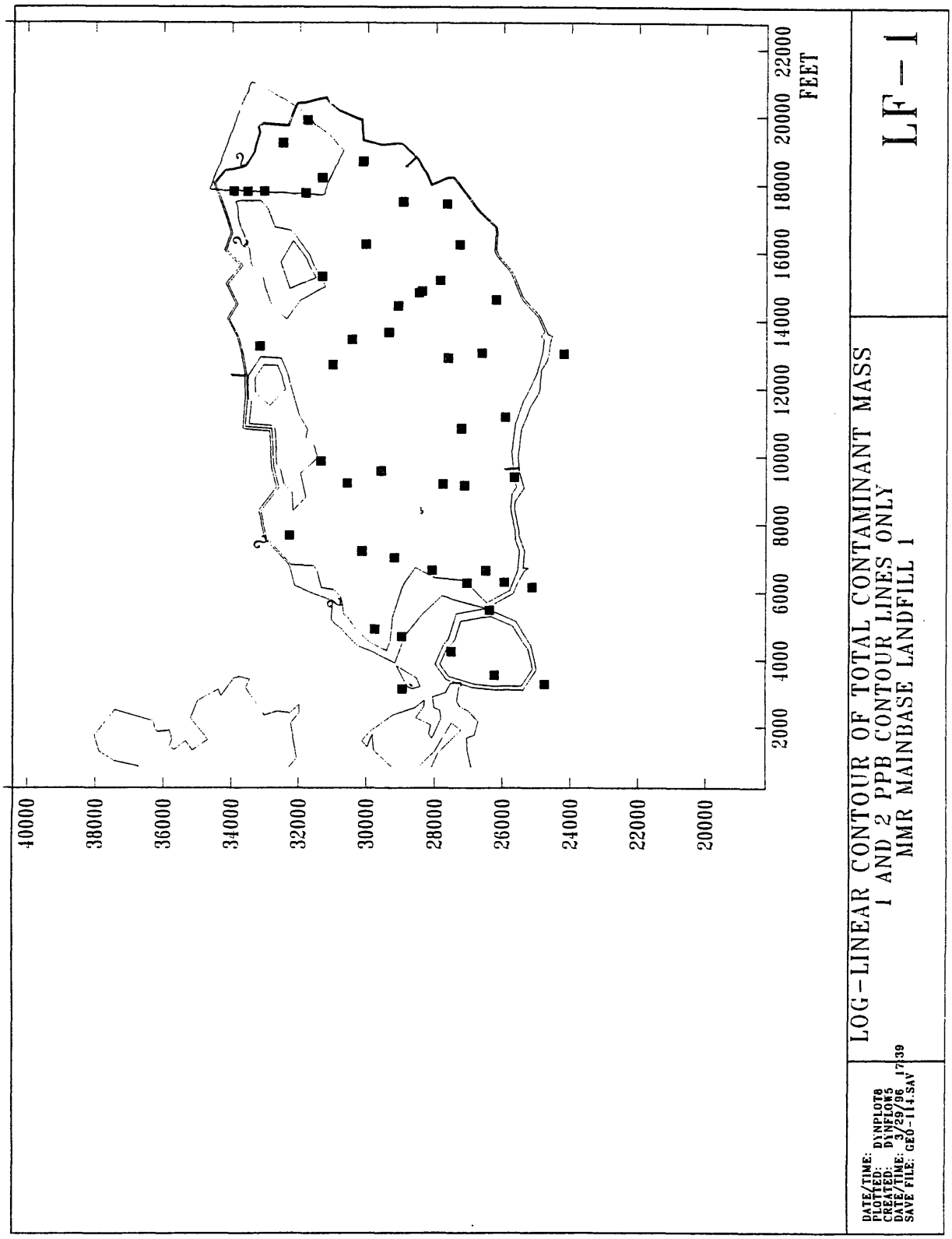

Figure 5.3 Contours of Total Contamination, 20 to 100 PPB

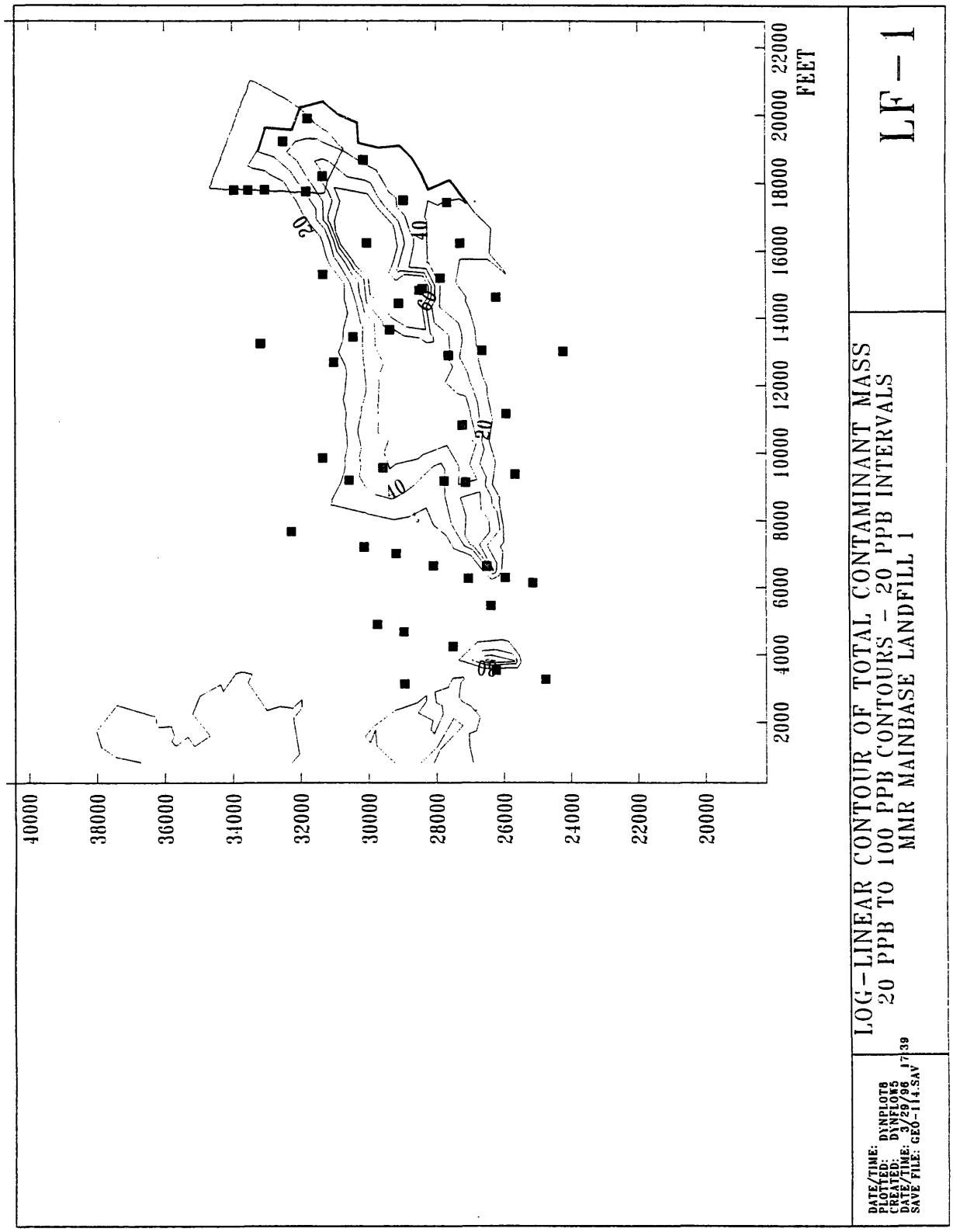

Figure 5.4 Contours of Total Contamination, 100 and greater PPB

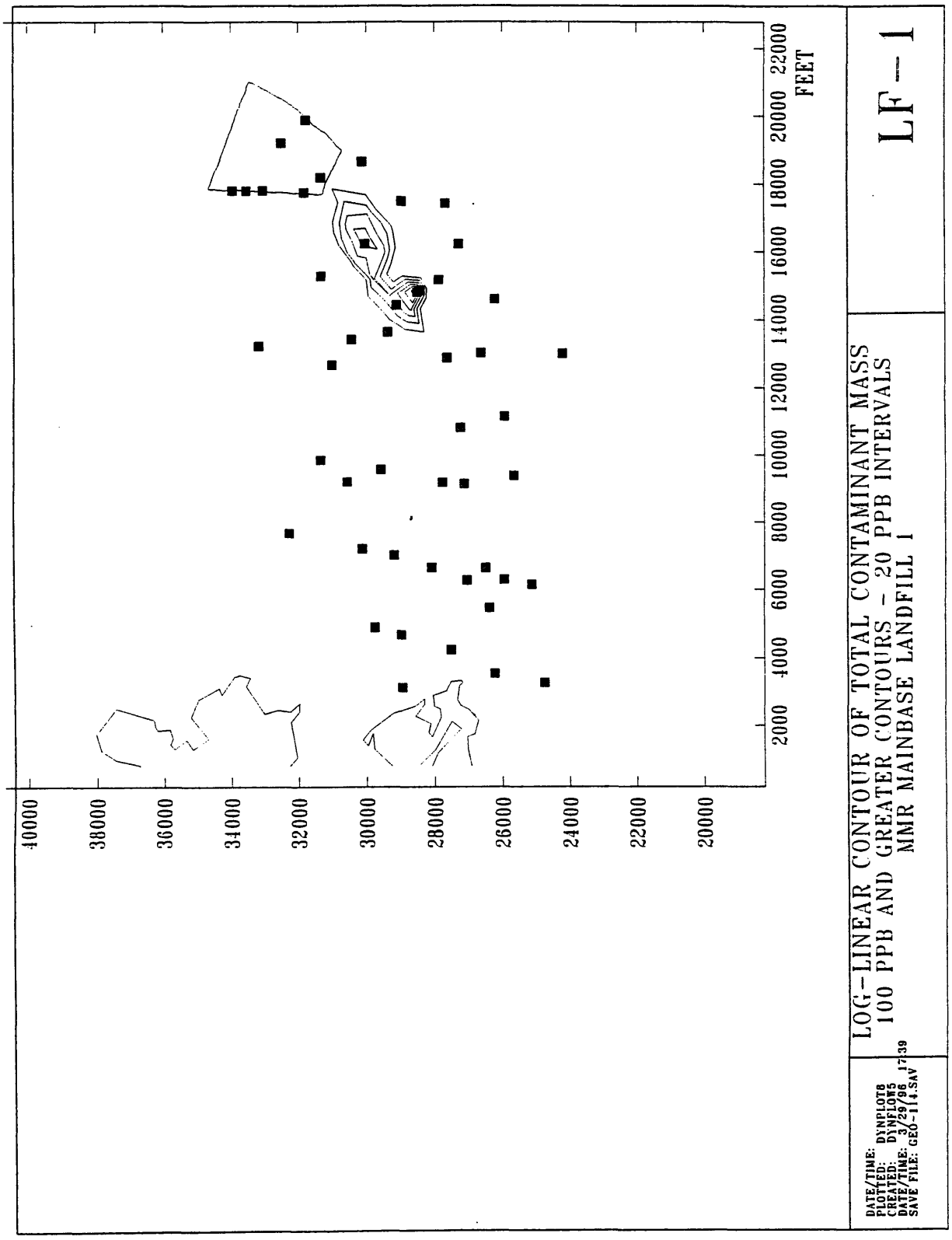

Figure 5.5 Contours of PCE Contamination

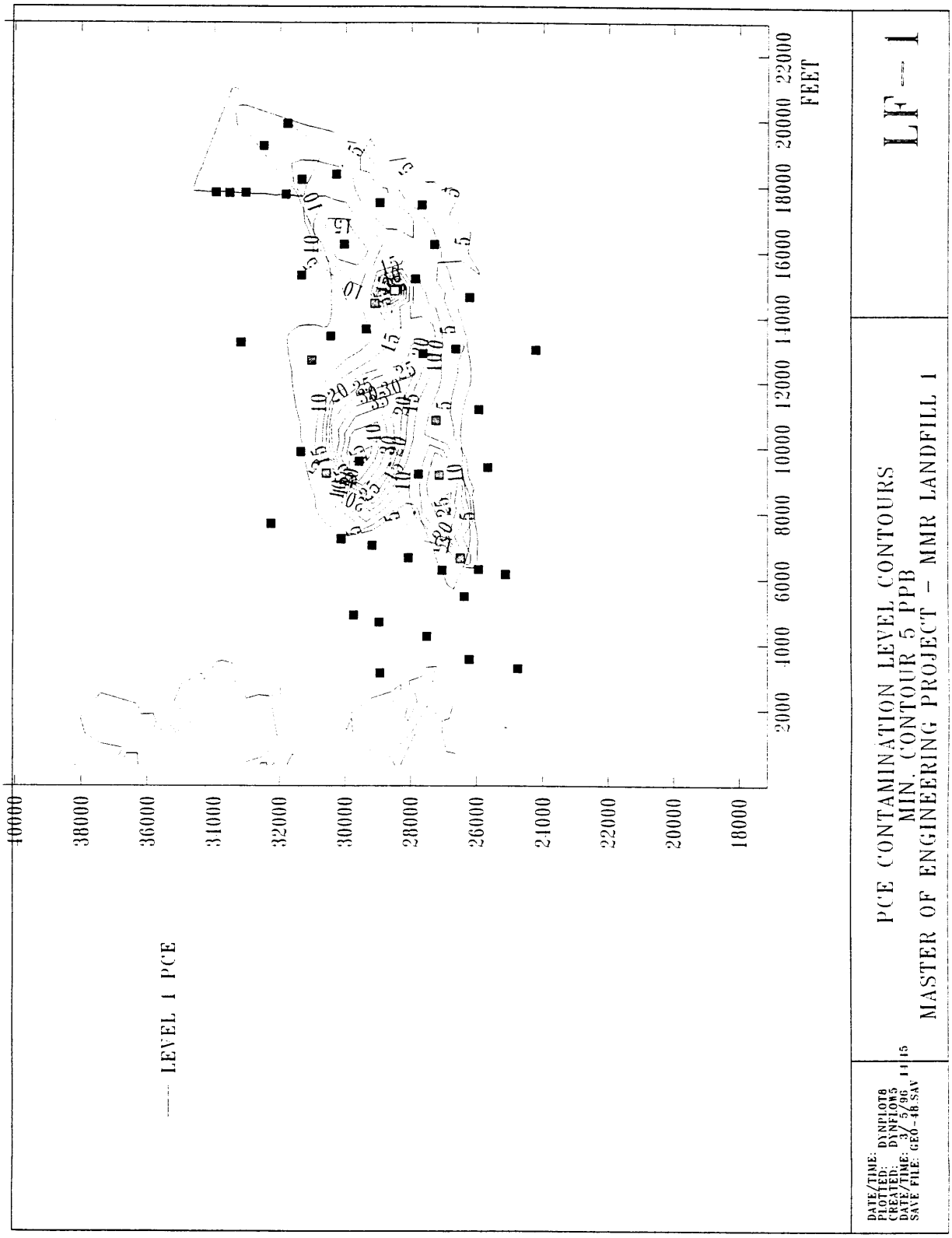

Figure 5.6 Contours of TCE Contamination

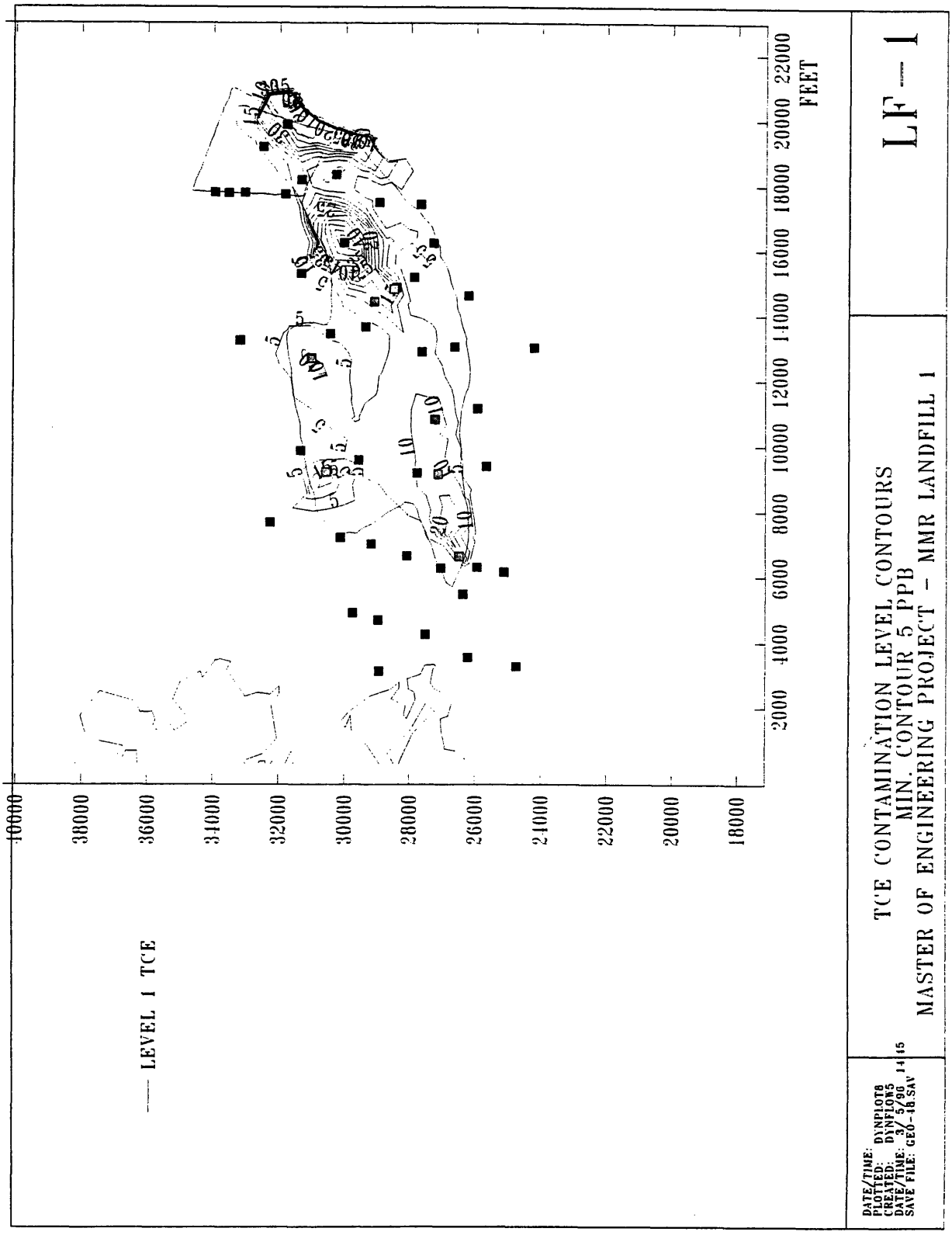

Figure 5.7 Contours of Total MCL-Normalized Contamination, 1 and 2 Contours

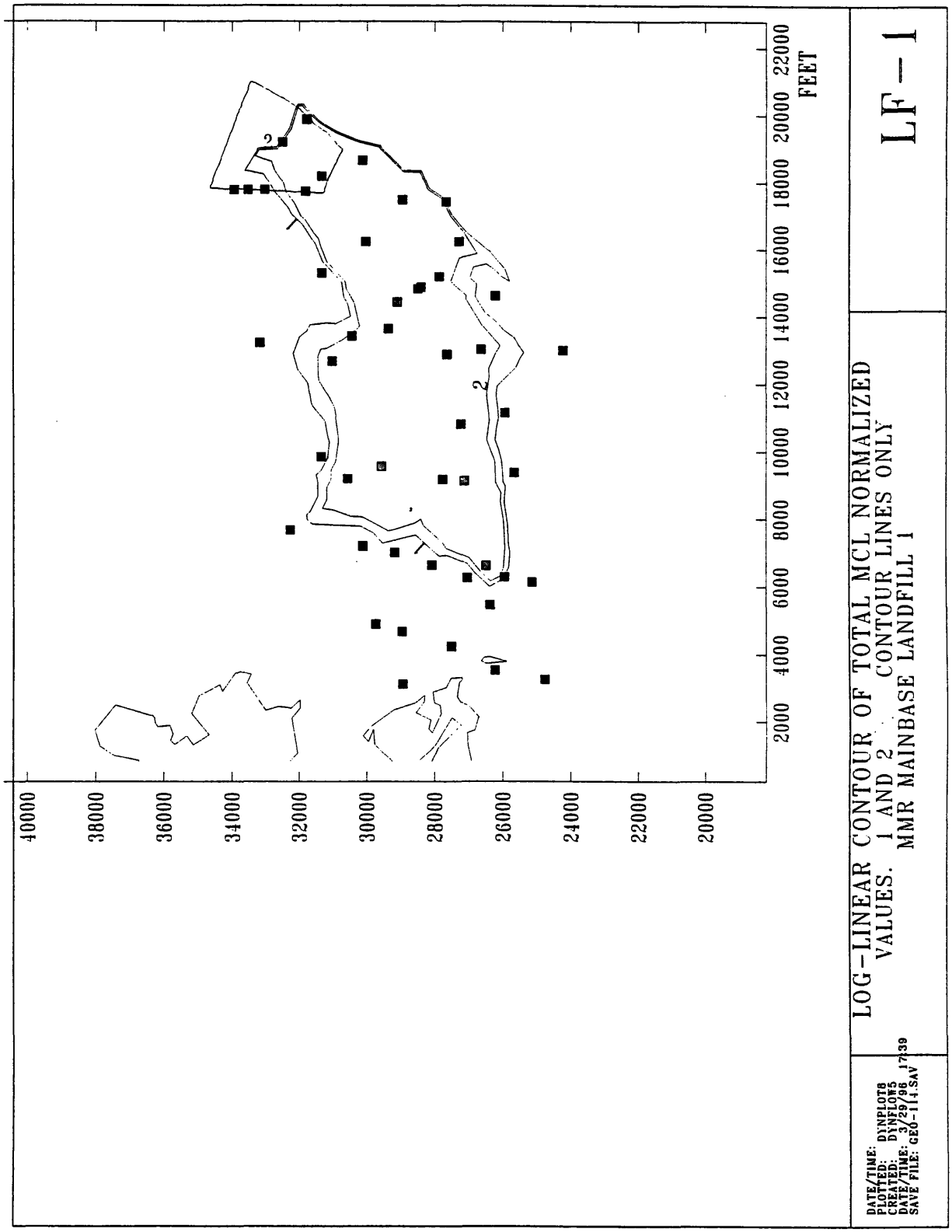

Figure 5.8 Contours of Total MCL-Normalized Contamination, 5 and greater Contours

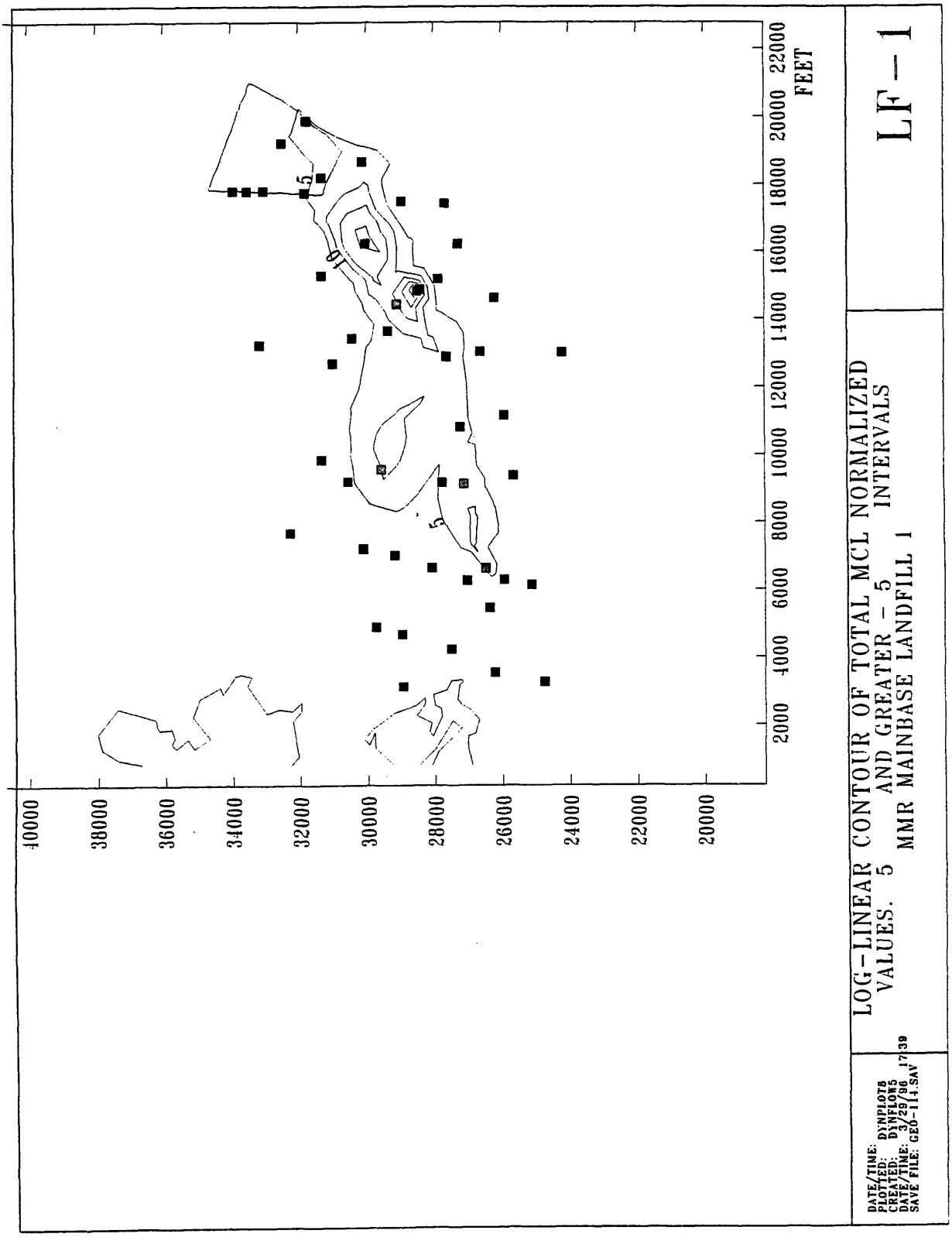

Figure 5.9 Contours of Maximum MCL-Normalized Contamination

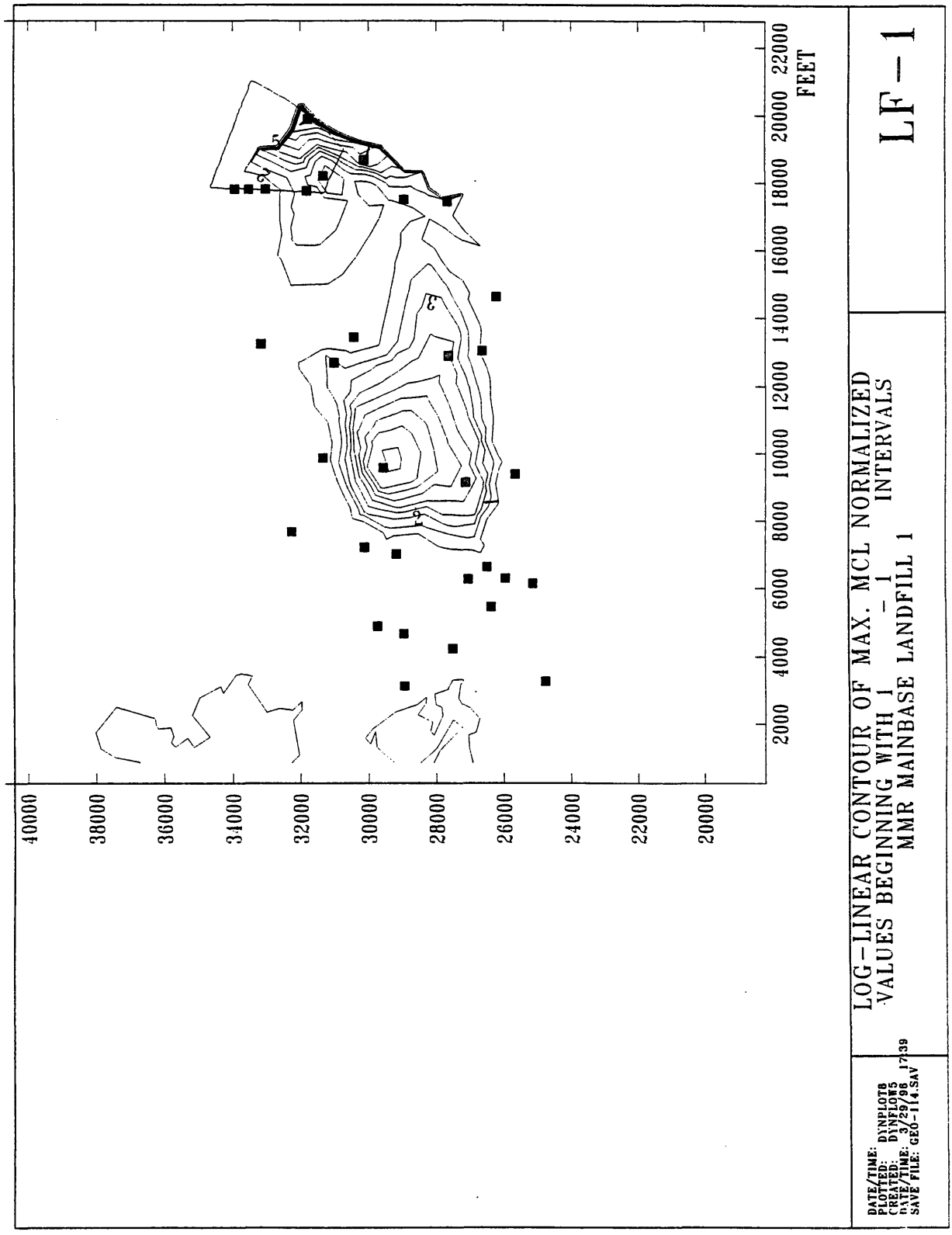

Figure 5.10 Northern Lobe Vertical Cross Section of MCL-Normalized Contamination

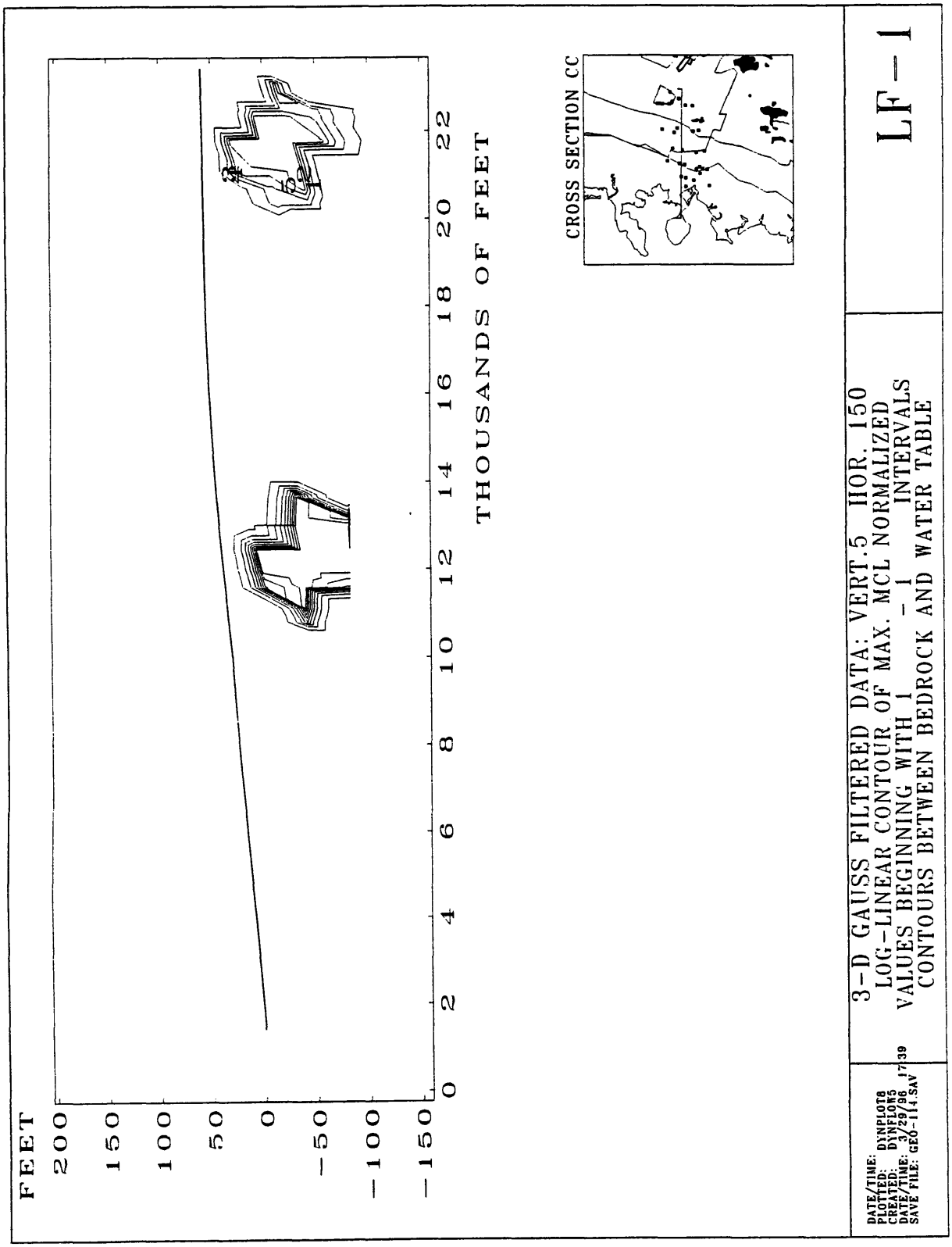

Figure 5.11 Southern Lobe Vertical Cross Section of MCL-Normalized Contamination

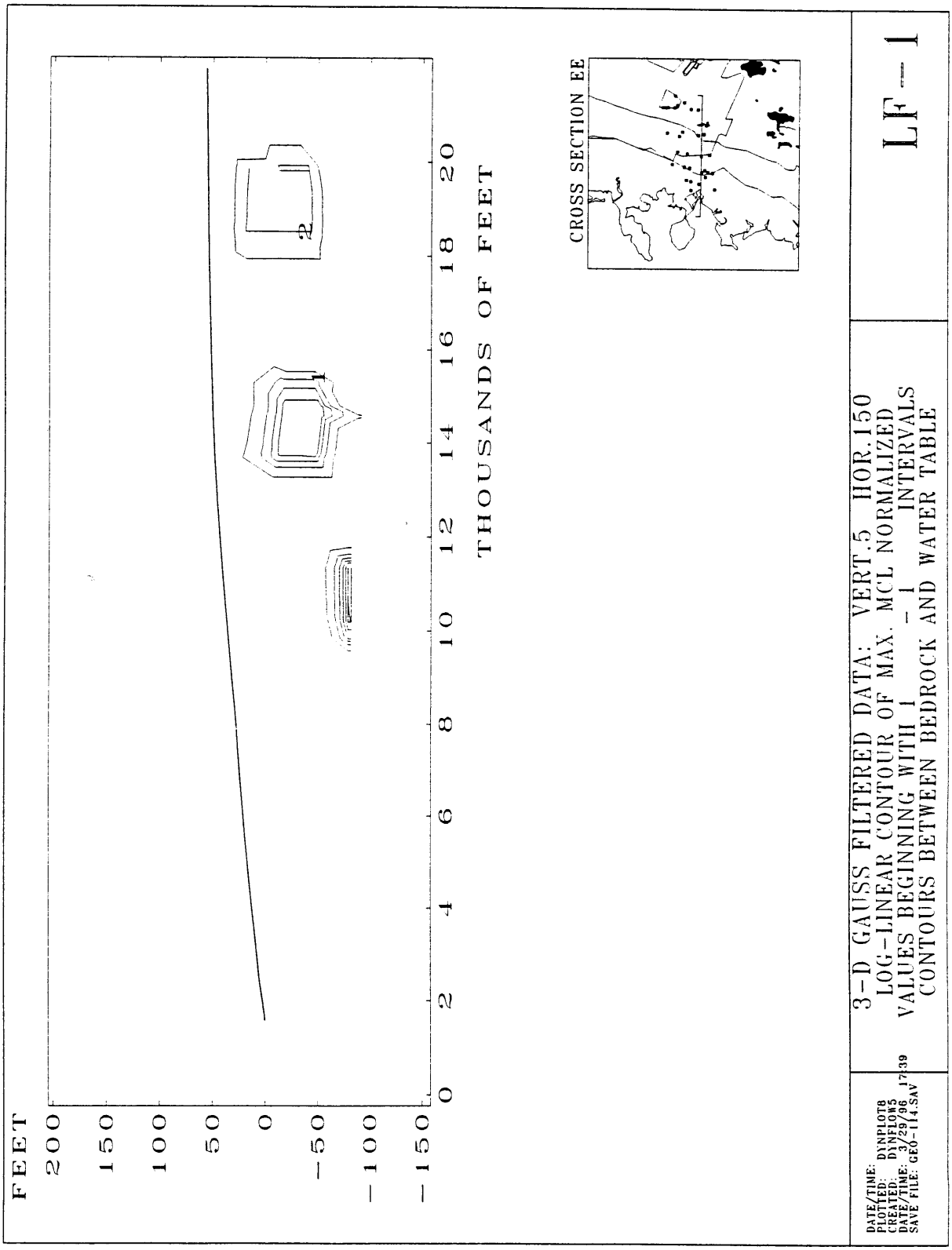

Figure 5.12 North/South Vertical Cross Section of MCL-Normalized Contamination

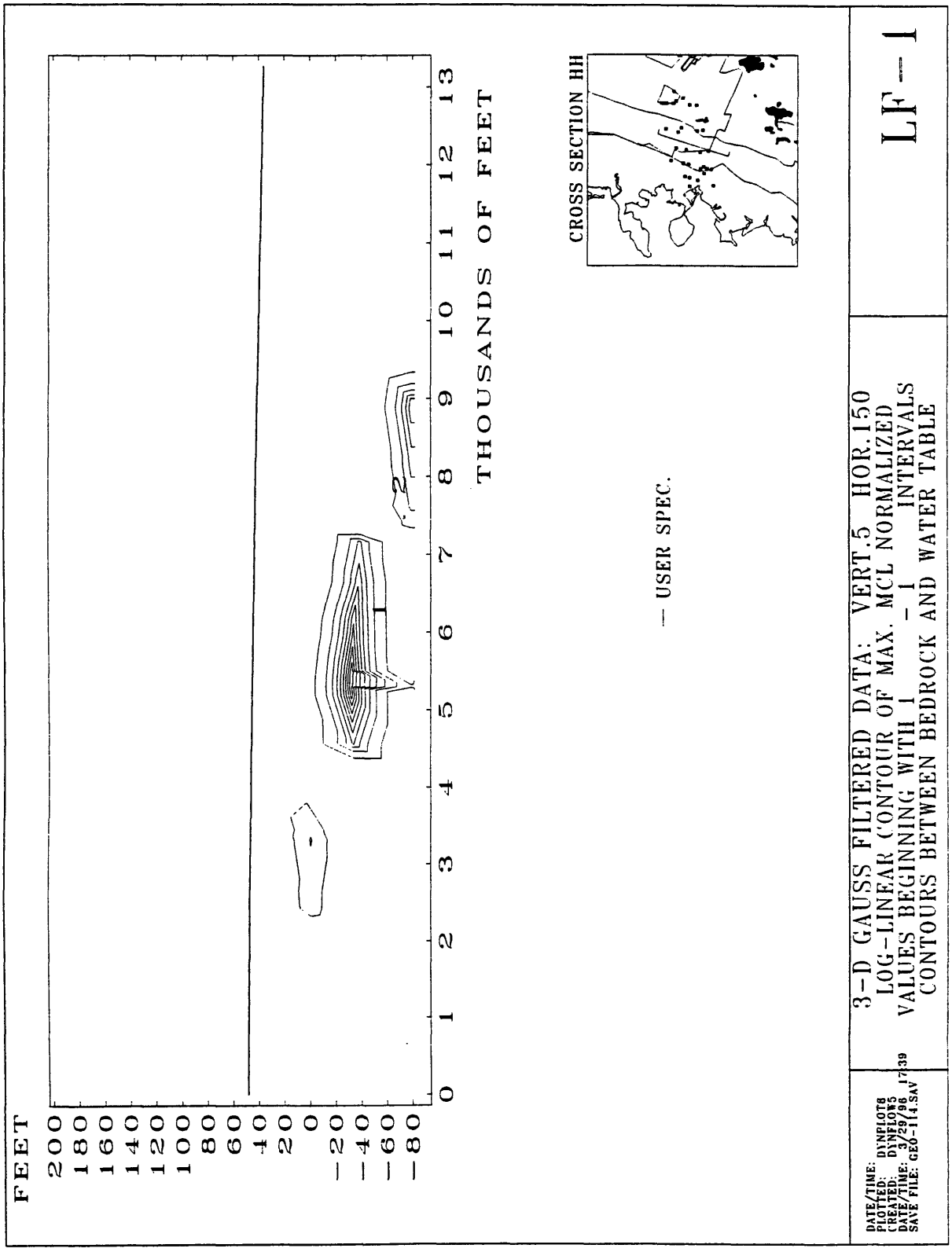

Figure 5.13 Frequency Histogram Total Natural Log Hazen and Sen K Values

FREQUENCY HISTOGRAM OF NATURAL LOG OF K VALUES
INCLUDES ALL DATA POINTS

Bin	requency
-9	0
-8	0
-7	0
-6	1
-5	4
-4	3
-3	5
-2	4
-1	8
0	14
1	14
2	8
3	8
4	37
5	17
6	19
7	1
8	0
9	0
10	0
11	0
12	0
13	0
More	0

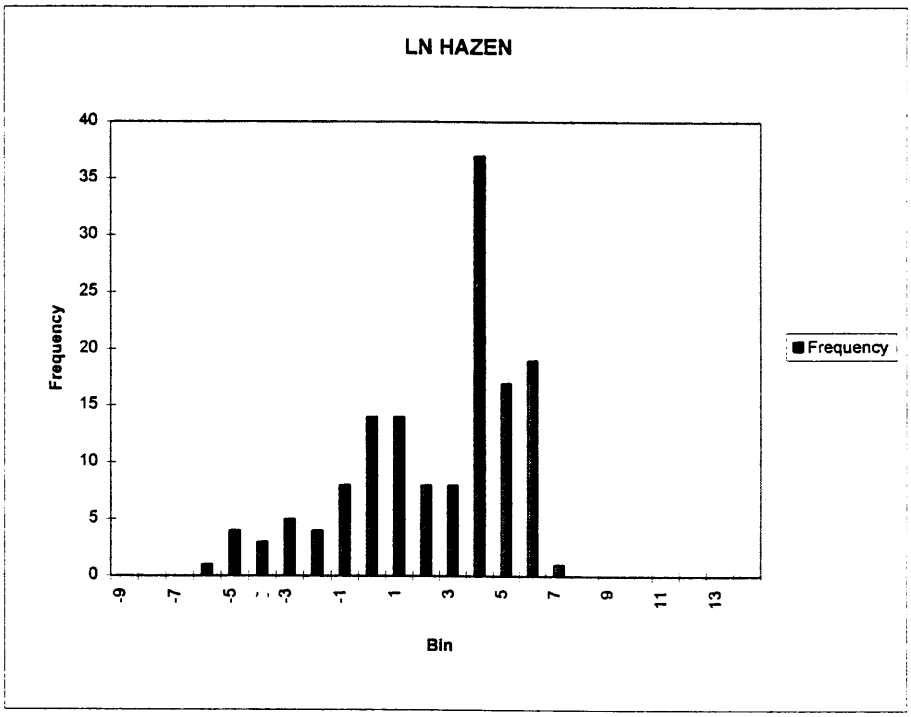

Bin	requency
-9	0
-8	1
-7	0
-6	2
-5	1
-4	2
-3	1
-2	1
-1	2
0	8
1	12
2	15
3	41
4	24
5	16
6	12
7	2
8	1
9	0
10	1
11	0
12	1
13	0
More	0

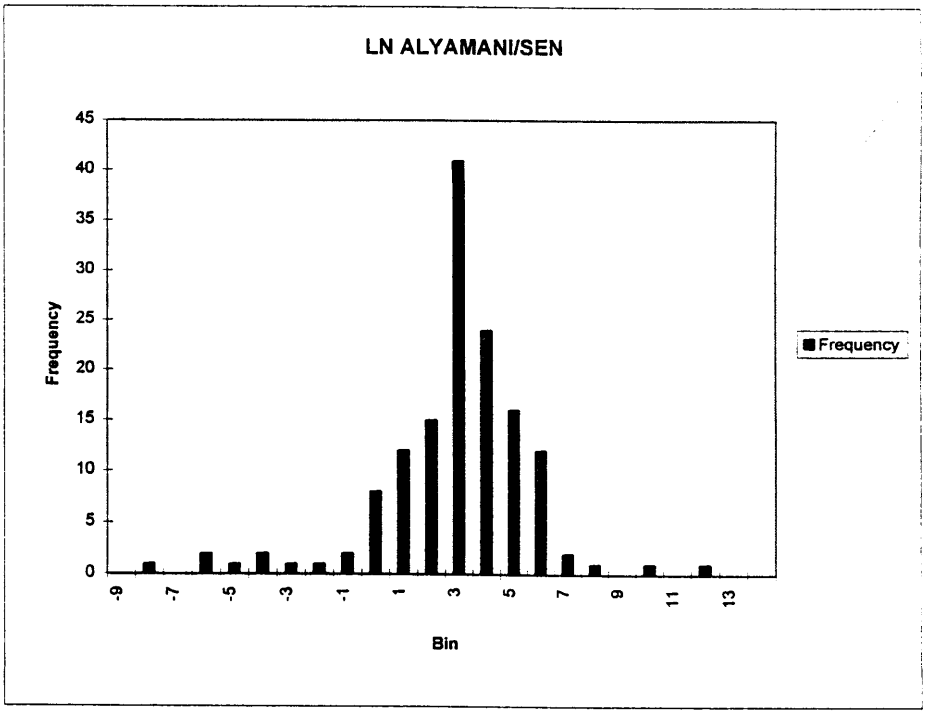

Figure 5.14 Frequency Histogram Total Natural Log Bedinger and Slug K Values

FREQUENCY HISTOGRAM OF NATURAL LOG OF K VALUES
INCLUDES ALL DATA POINTS

Bin	requency
-9	0
-8	0
-7	0
-6	1
-5	1
-4	0
-3	0
-2	1
-1	3
0	1
1	1
2	8
3	21
4	41
5	47
6	10
7	5
8	0
9	1
10	0
11	1
12	1
13	0
More	0

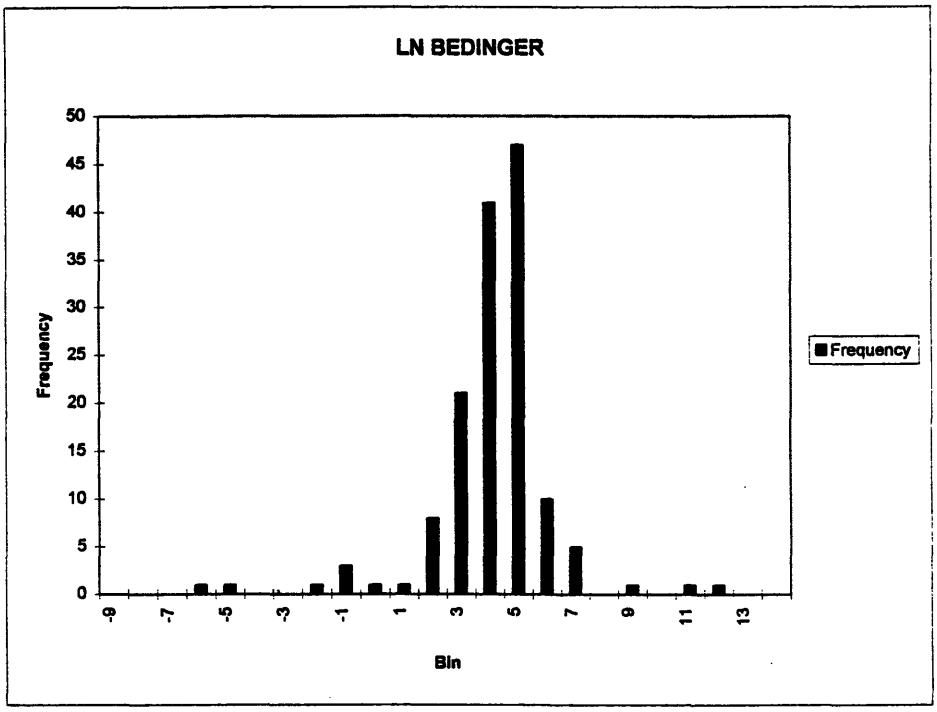

Bin	requency
-9	0
-8	0
-7	0
-6	0
-5	0
-4	0
-3	0
-2	1
-1	1
0	0
1	4
2	10
3	10
4	11
5	27
6	14
7	0
8	0
9	0
10	0
11	0
12	0
13	0
More	0

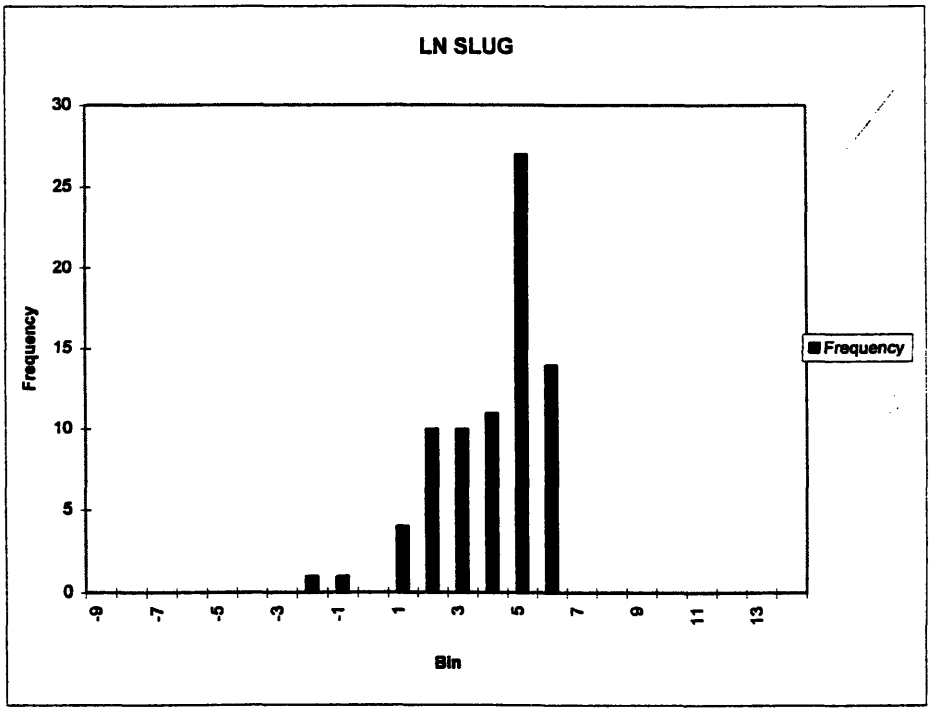

Figure 5.15 Natural Log 23 Common Alyamani/Sen vs. Bedinger K Values

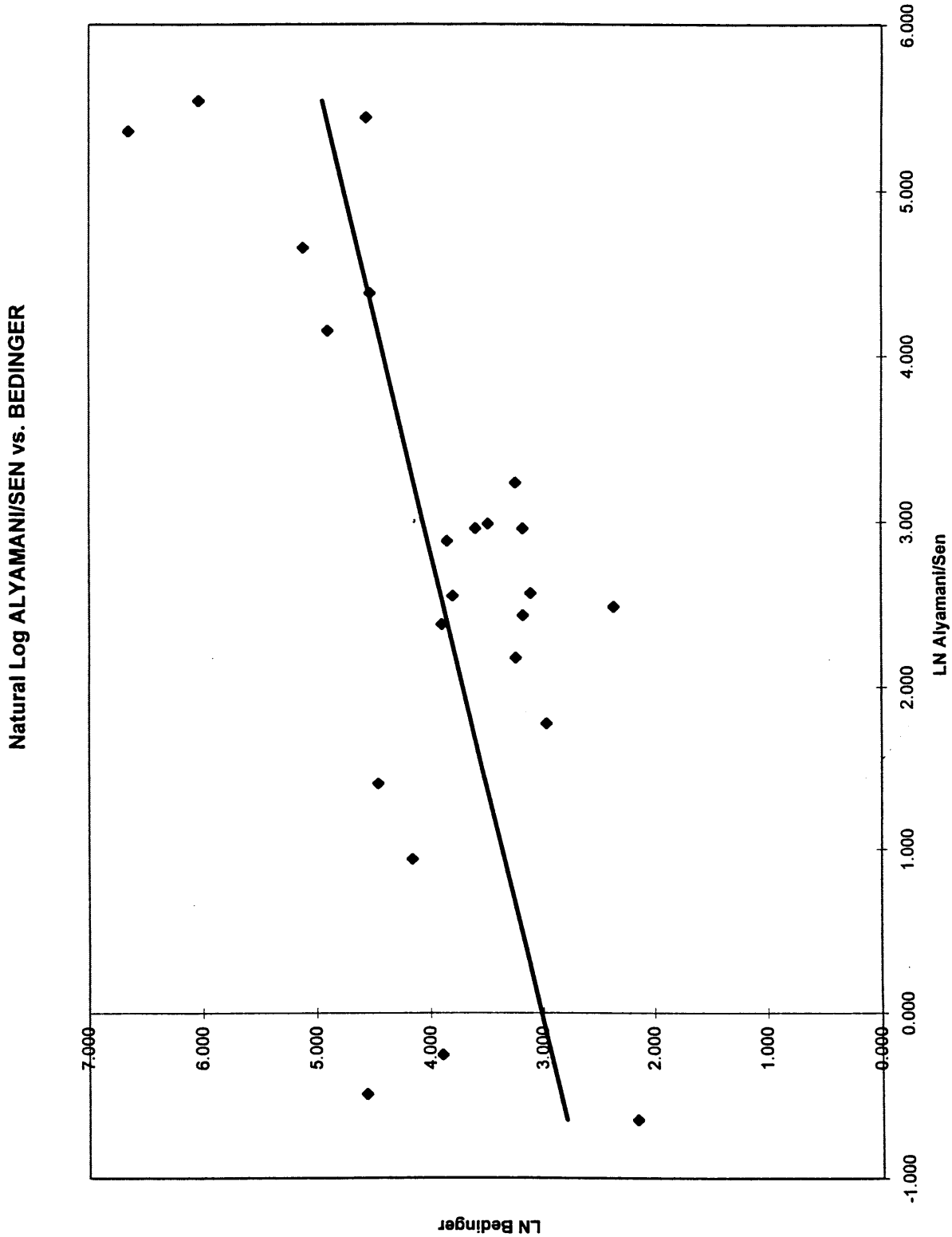

Figure 5.16 Natural Log 18 Common Alyamani/Sen vs. Bedinger K Values

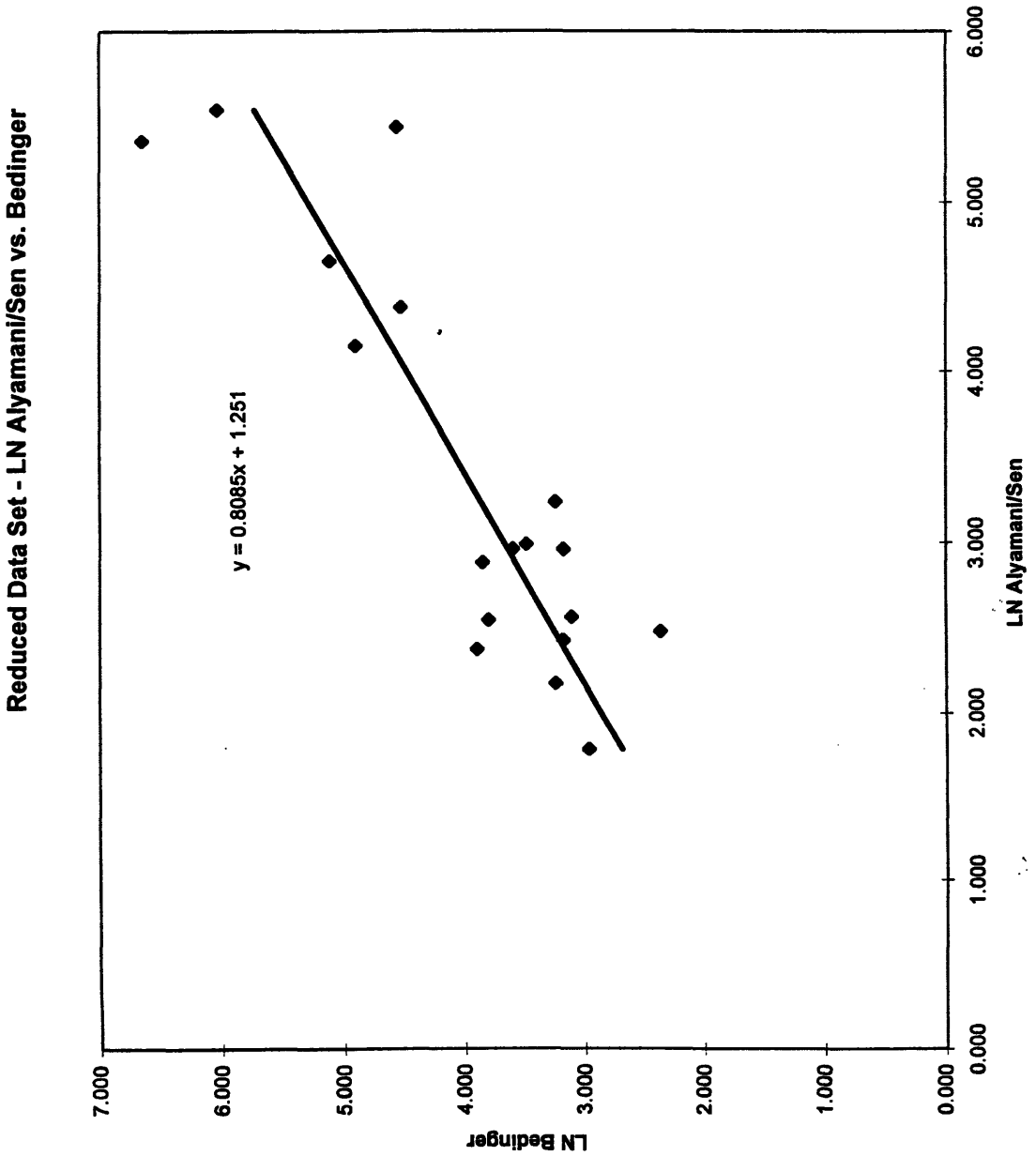

Figure 5.17 Natural Log 7 and 8 Common Alyamani/Sen vs. Bedinger K Values

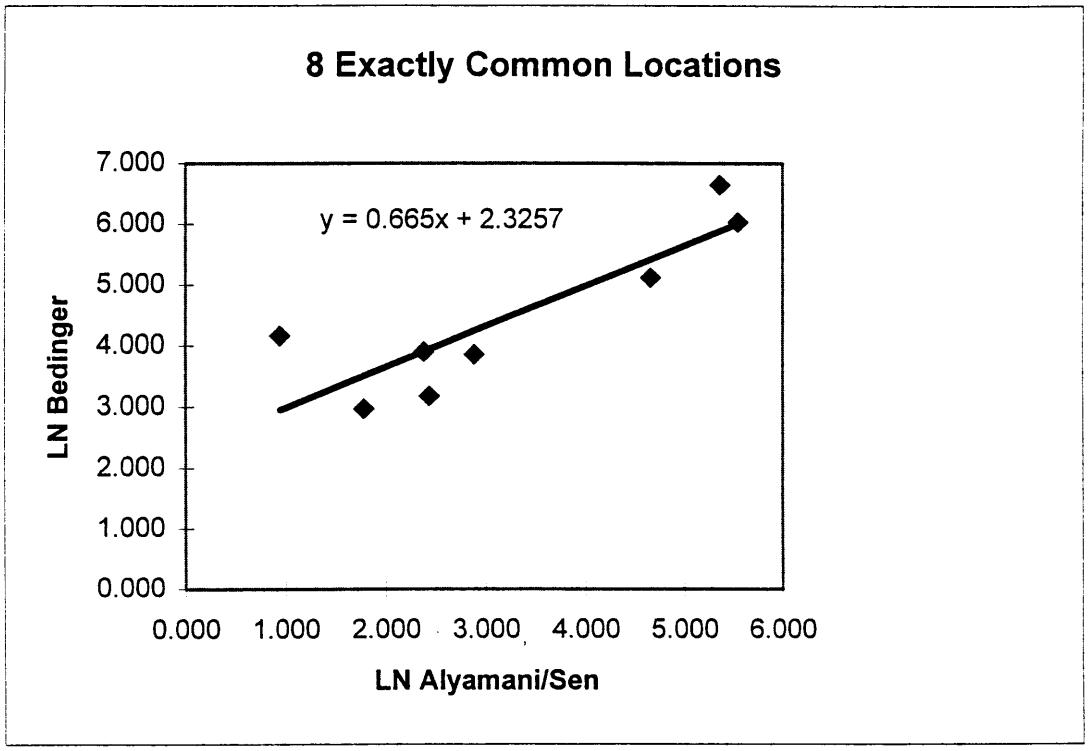

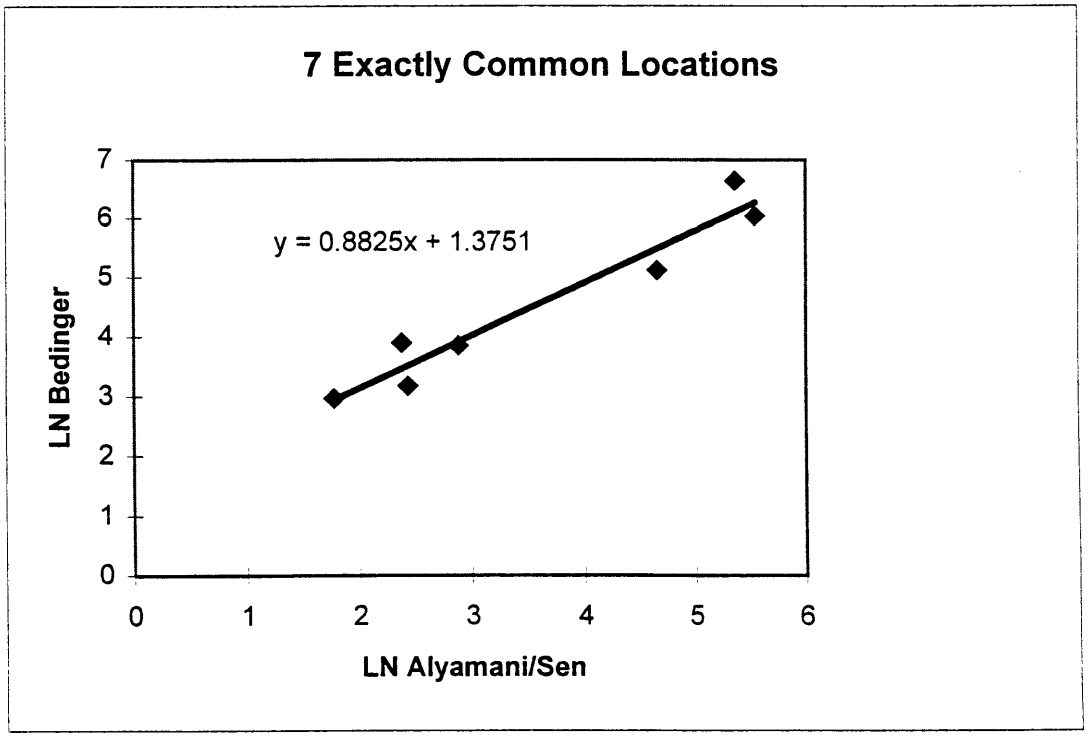

Figure 5.18 Natural Log Gaussian Filtered 23 Common Slug vs. Hazen K Values

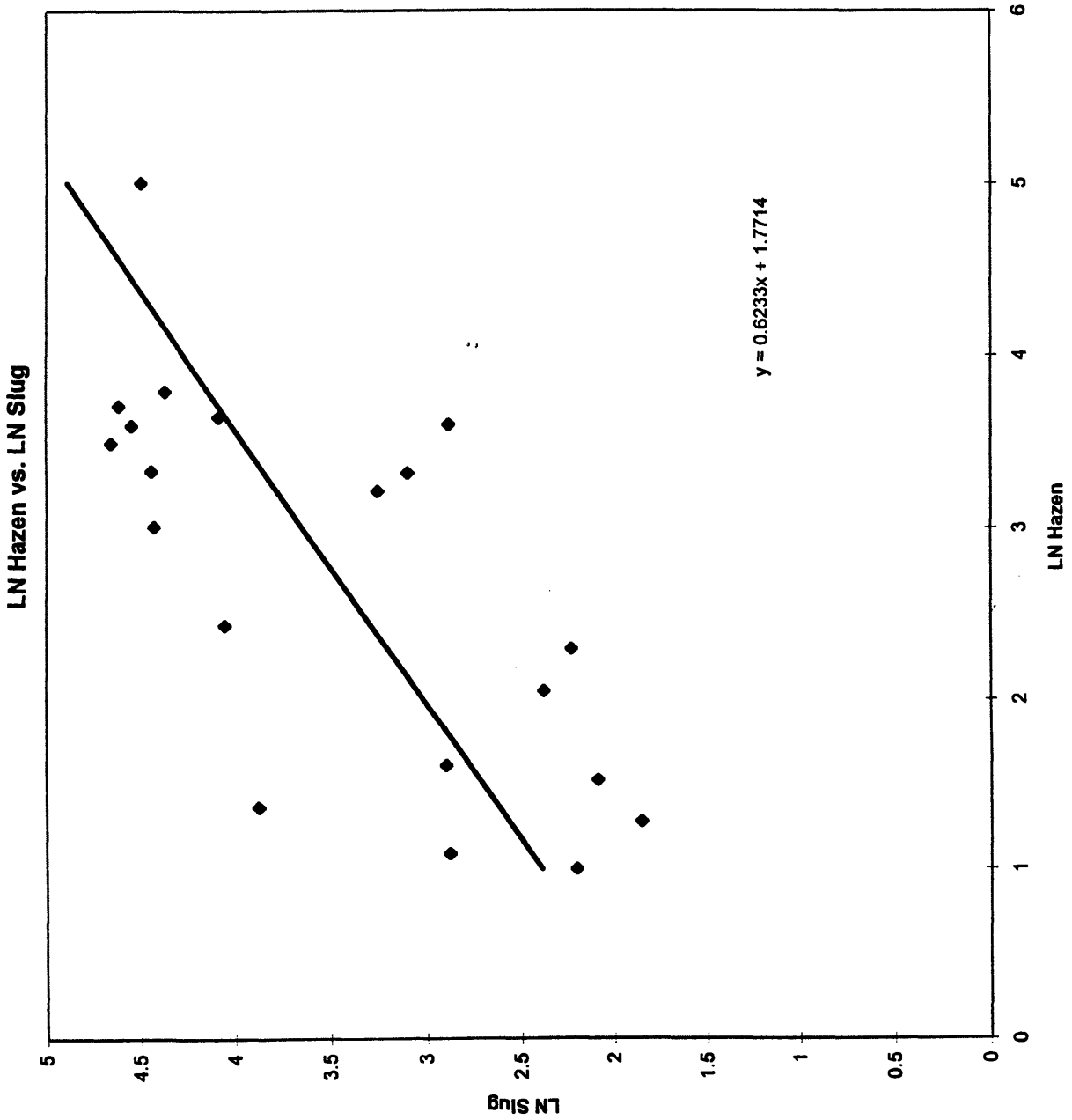

Figure 5.19 Vertical Cross Section Contours of Filtered Slug Data with Point Values

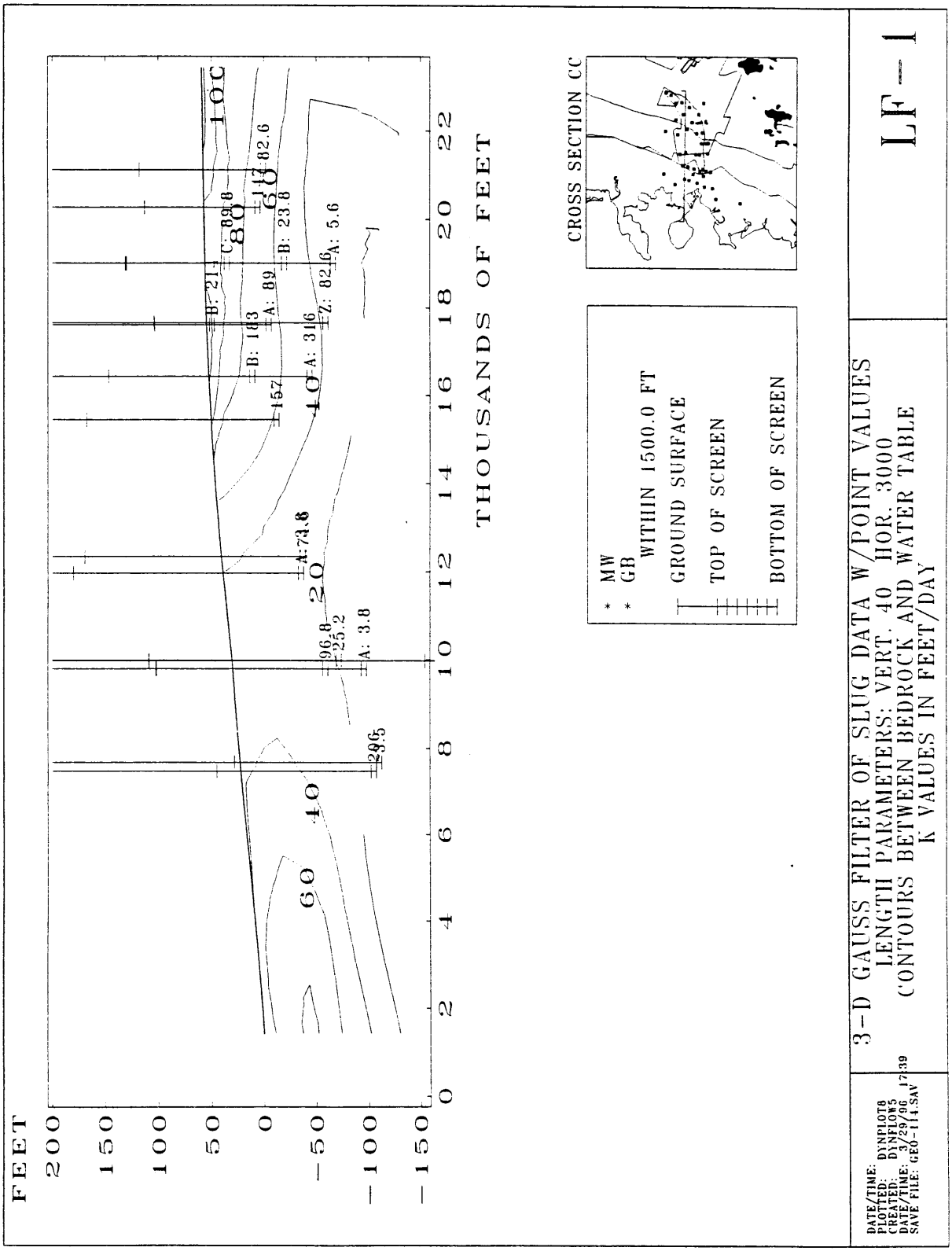

Figure 5.20 Northern Lobe Vertical Cross Section Contours of Filtered Slug Data

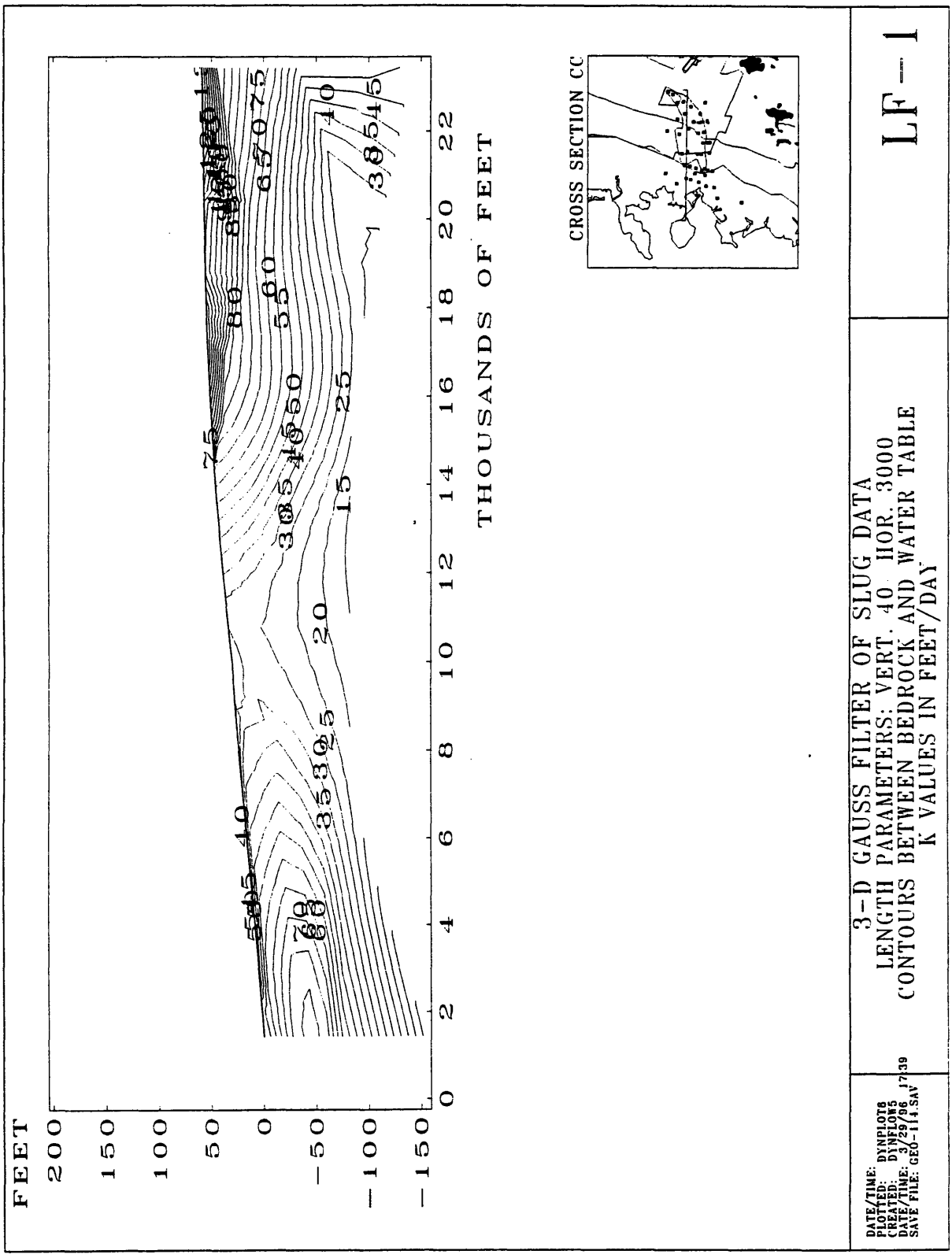

Figure 5.21 Southern Lobe Vertical Cross Section Contours of Filtered Slug Data

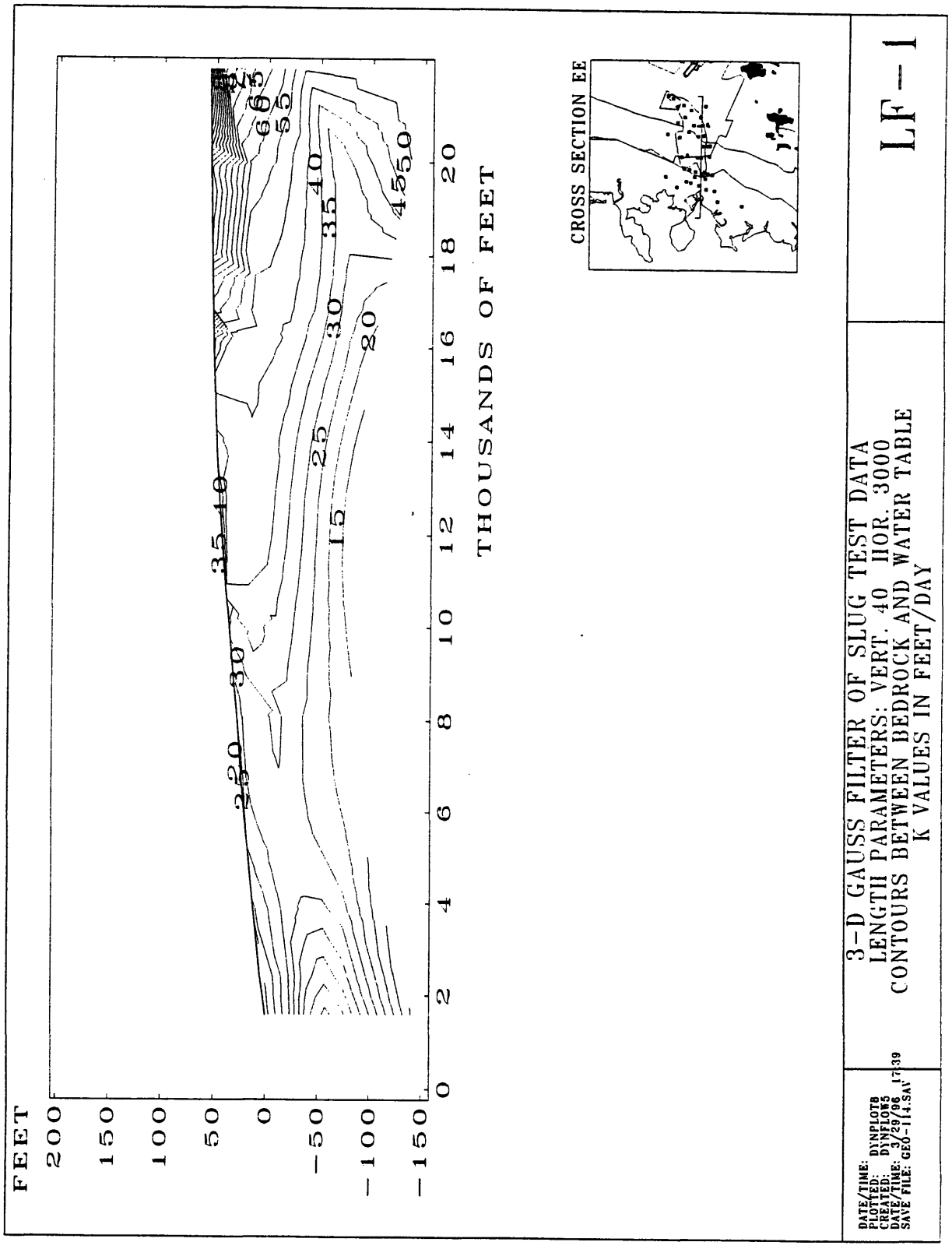

Figure 5.22 North/South Vertical Cross Section Contours of Filtered Slug Data

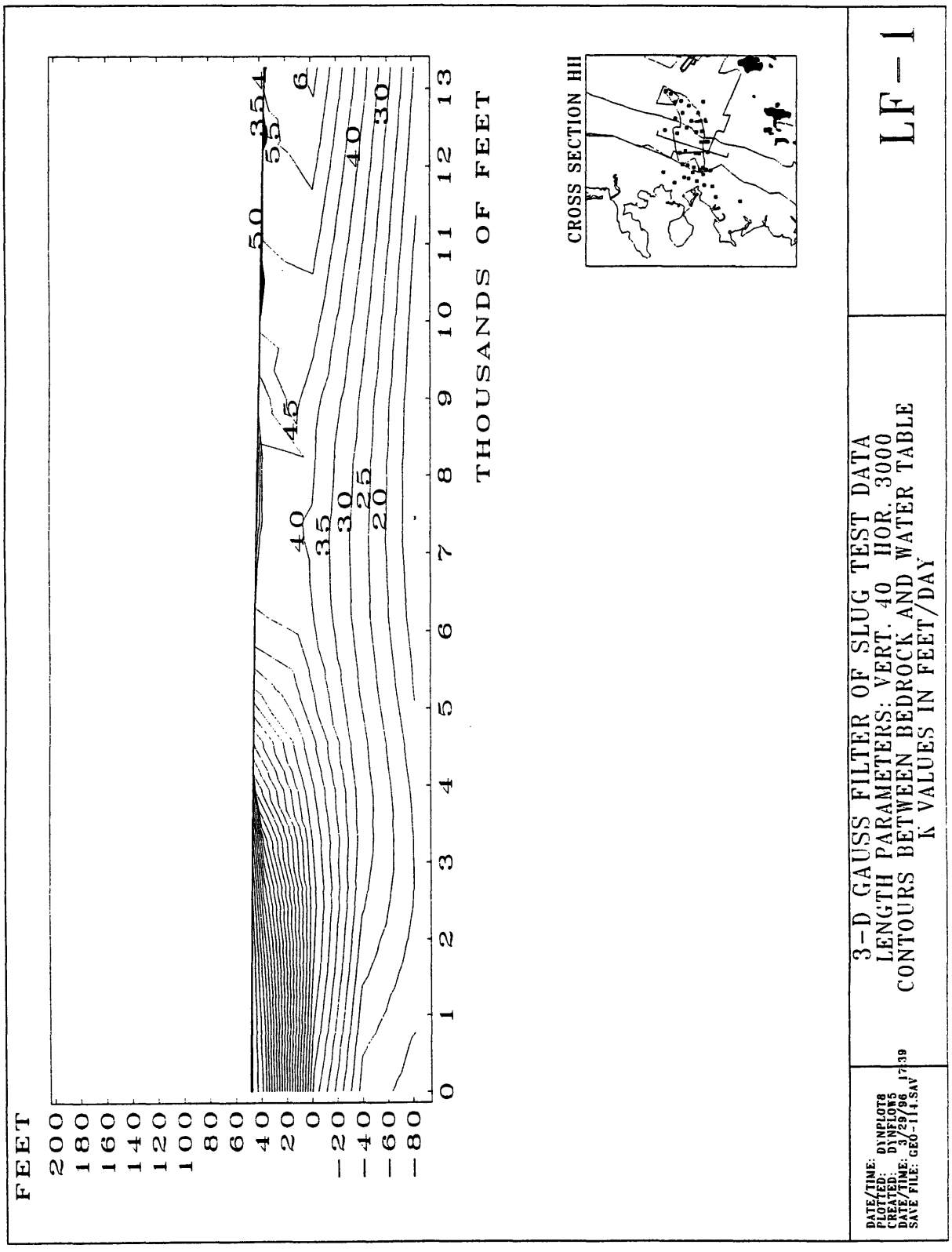

Figure 5.23 Northern Lobe Vertical Cross Section Contours of Filtered Hazen Data

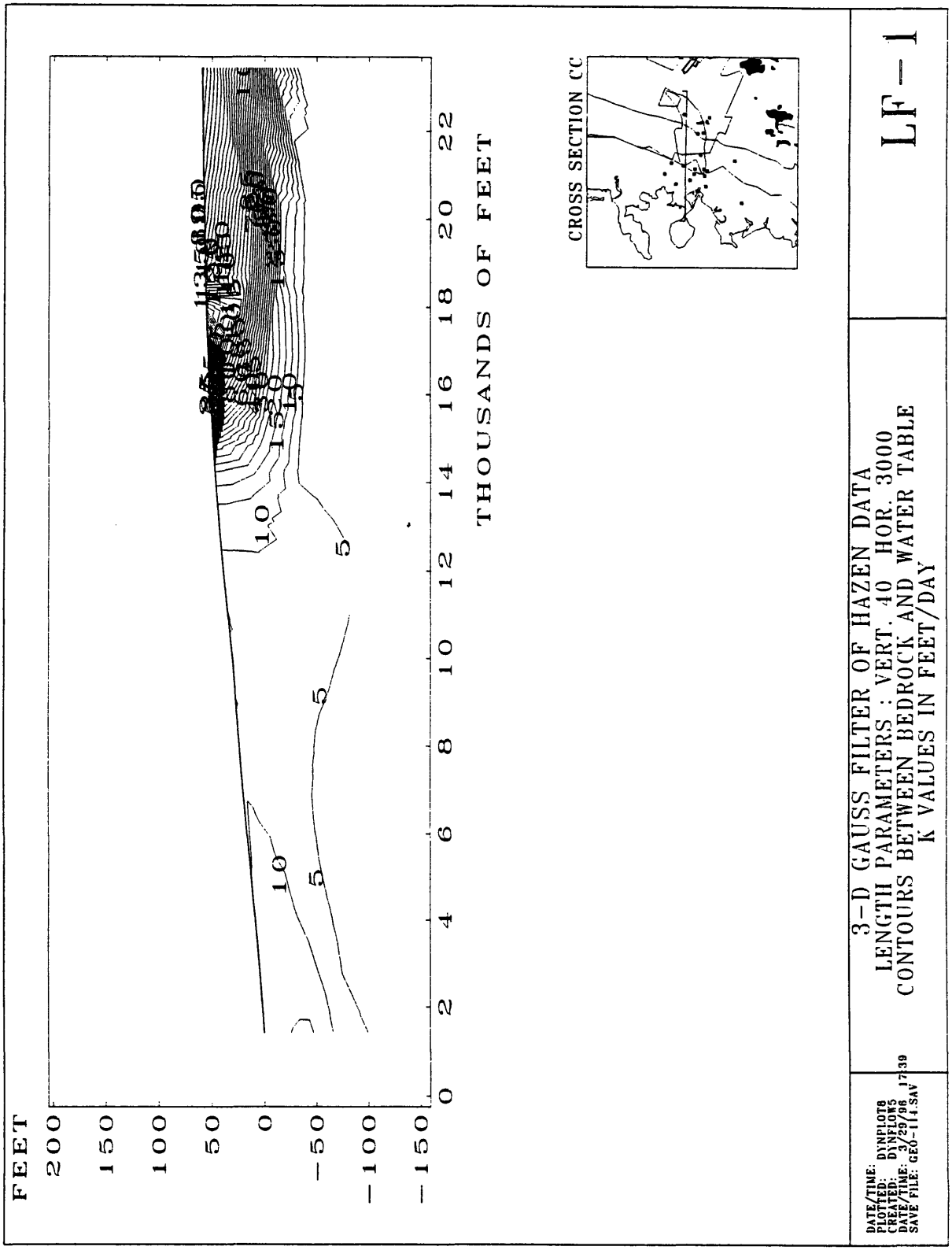

Figure 5.24 Southern Lobe Vertical Cross Section Contours of Filtered Hazen Data

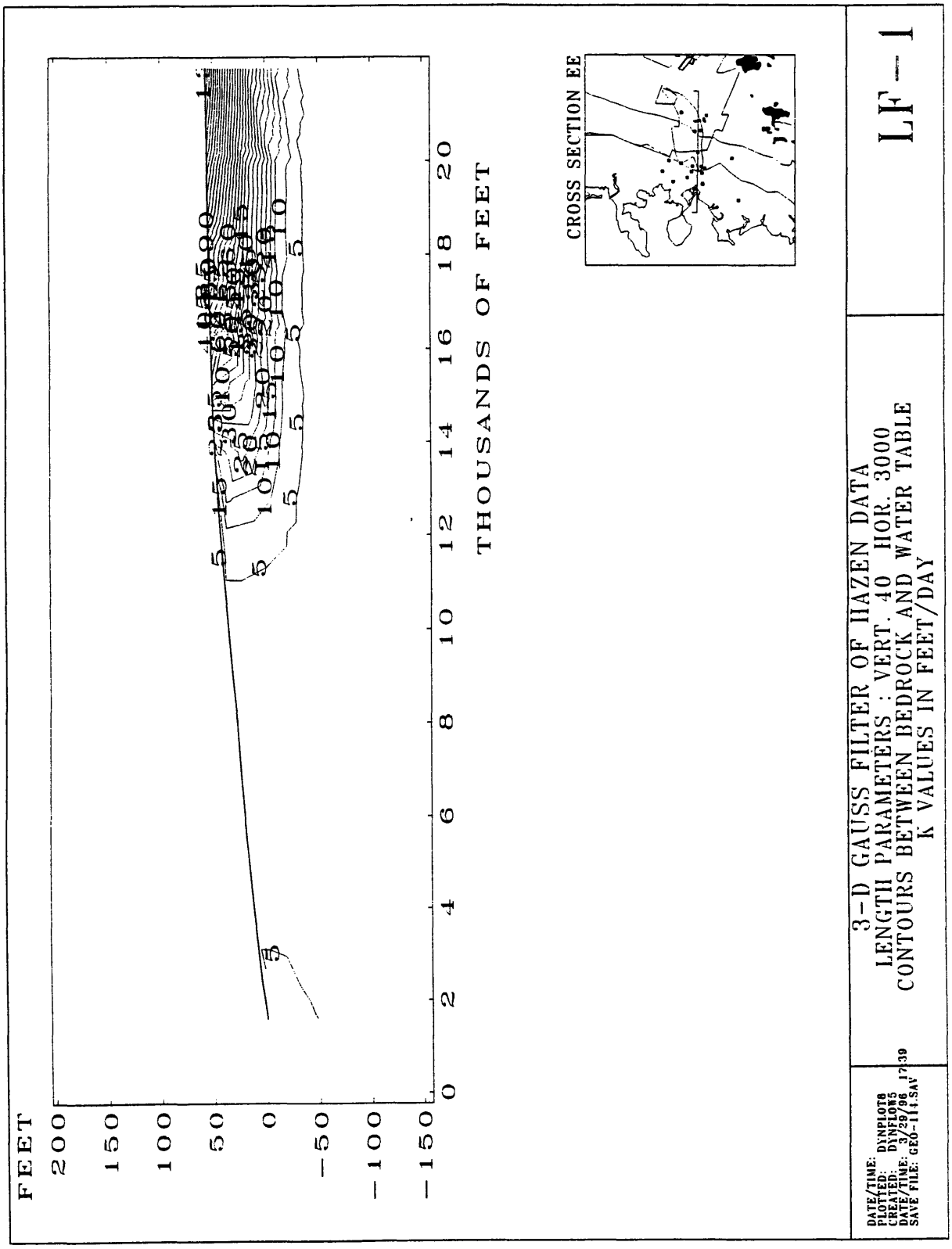

Figure 5.25 North/South Vertical Cross Section Contours of Filtered Hazen Data

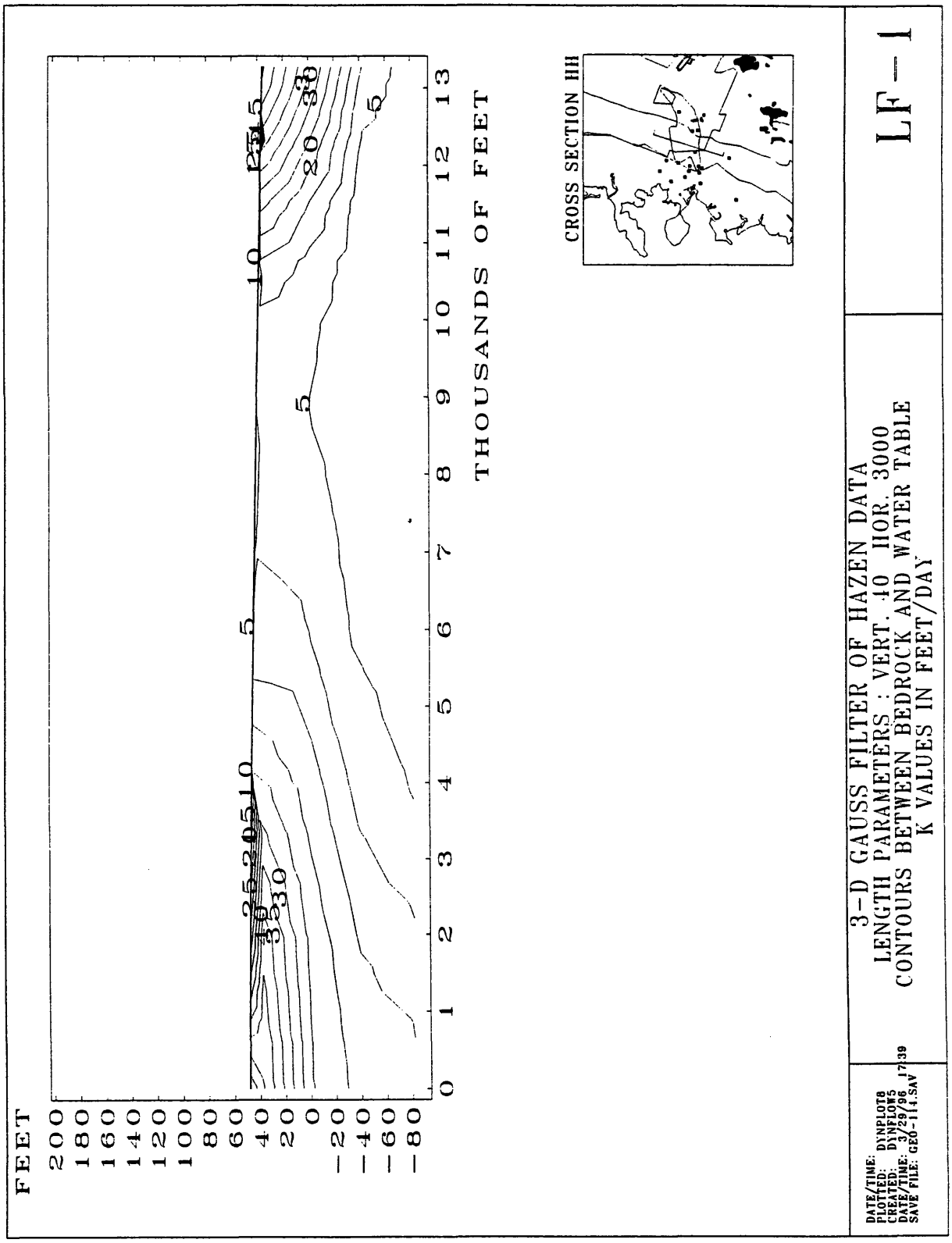

Figure 5.26 Northern Lobe Vertical Cross Section Contours of Filtered Alyamani/Sen Data

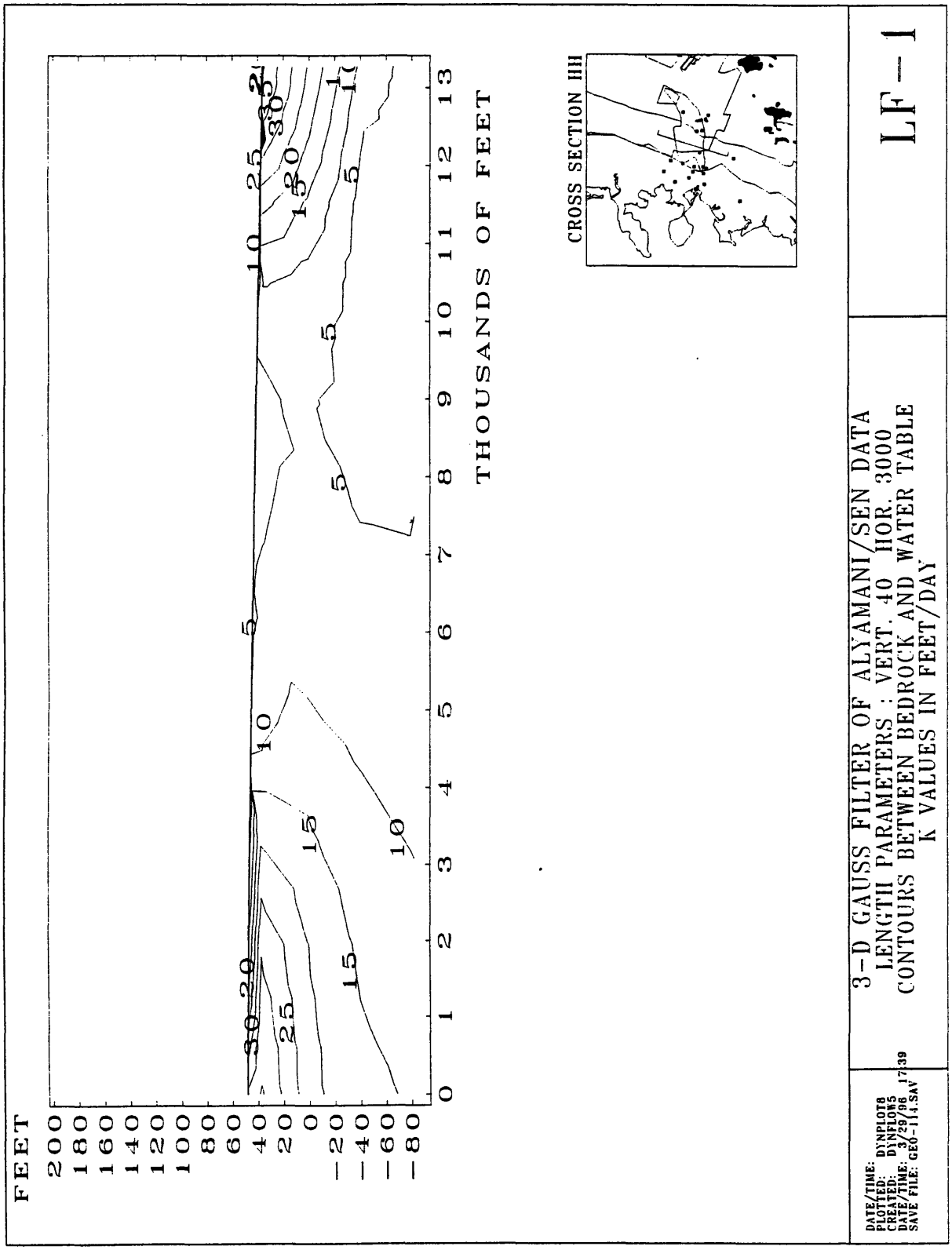

Figure 5.27 Southern Lobe Vertical Cross Section Contours of Filtered Alyamani/Sen Data

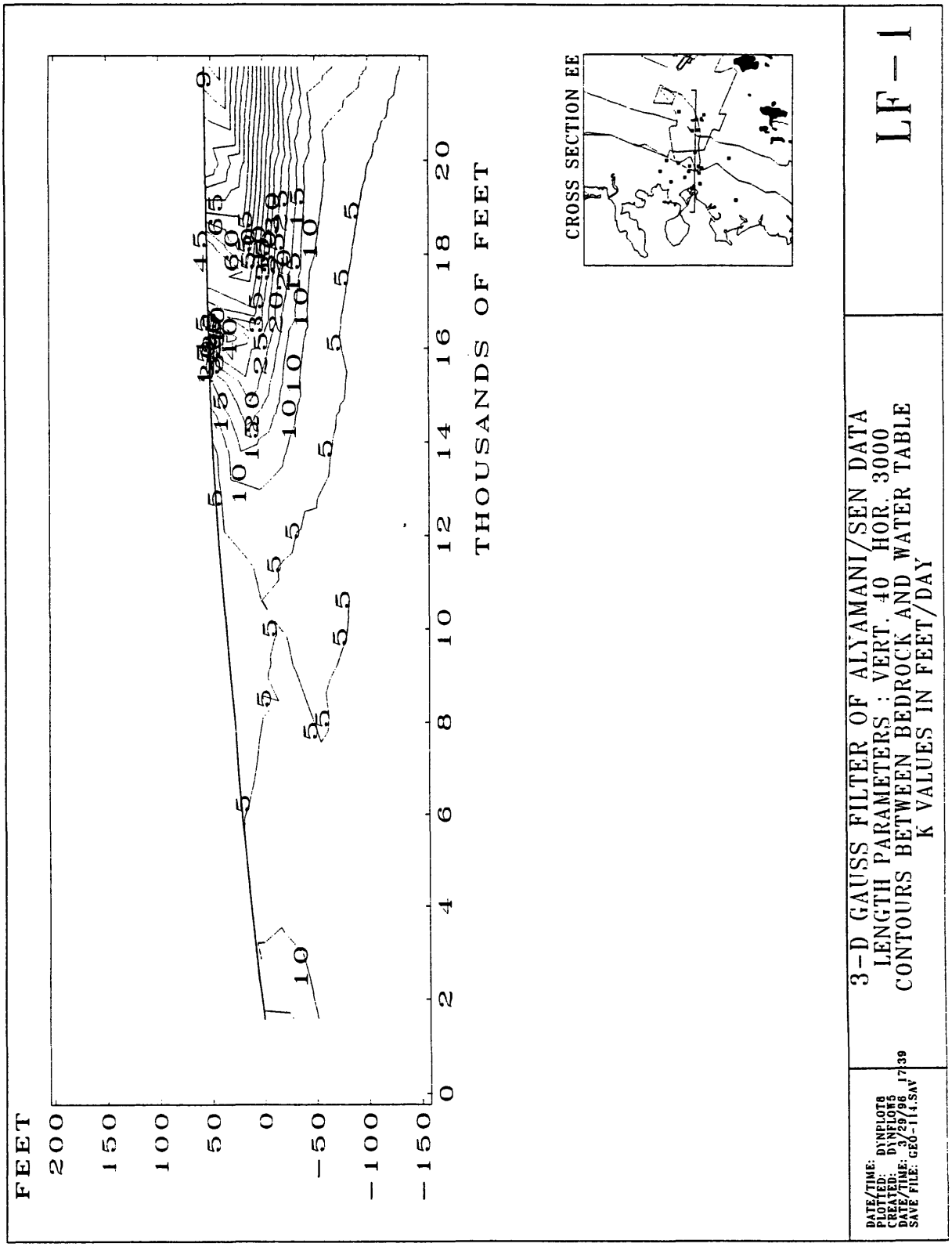

Figure 5.28 North/South Vertical Cross Section Contours of Filtered Alyamani/Sen Data

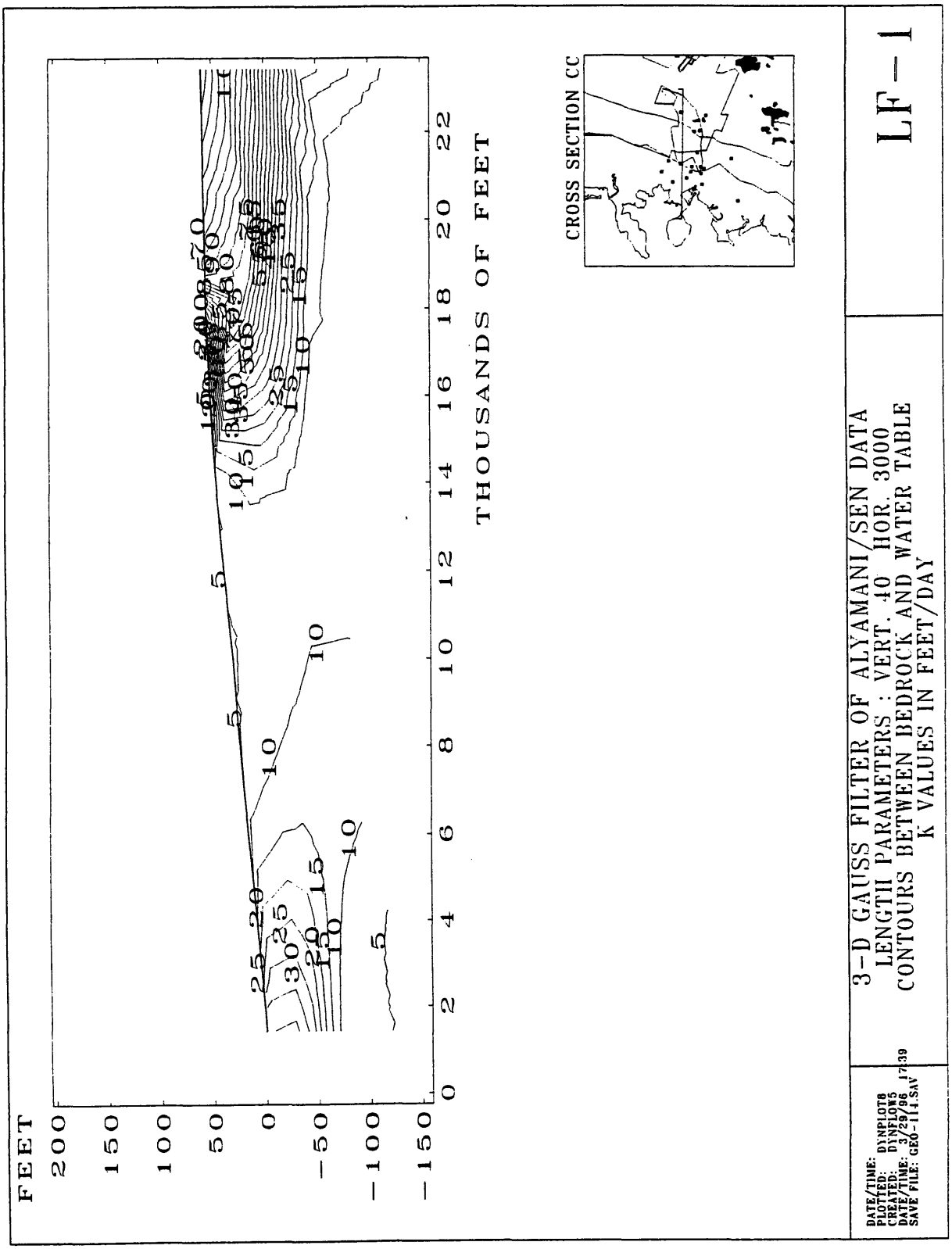

Figure 5.29 Northern Lobe Vertical Cross Section Contours of Filtered Bedinger Data

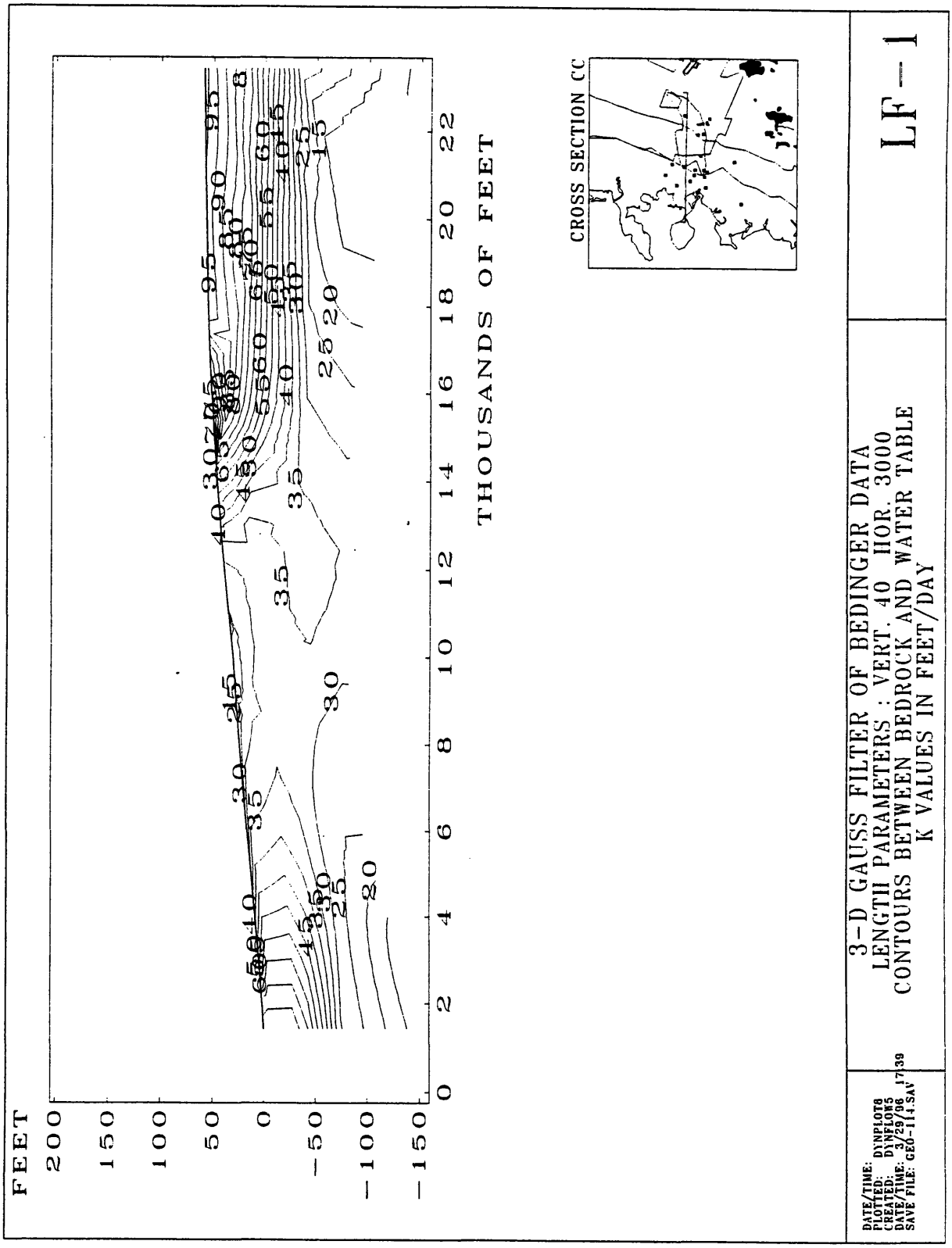

Figure 5.30 Southern Lobe Vertical Cross Section Contours of Filtered Bedinger Data

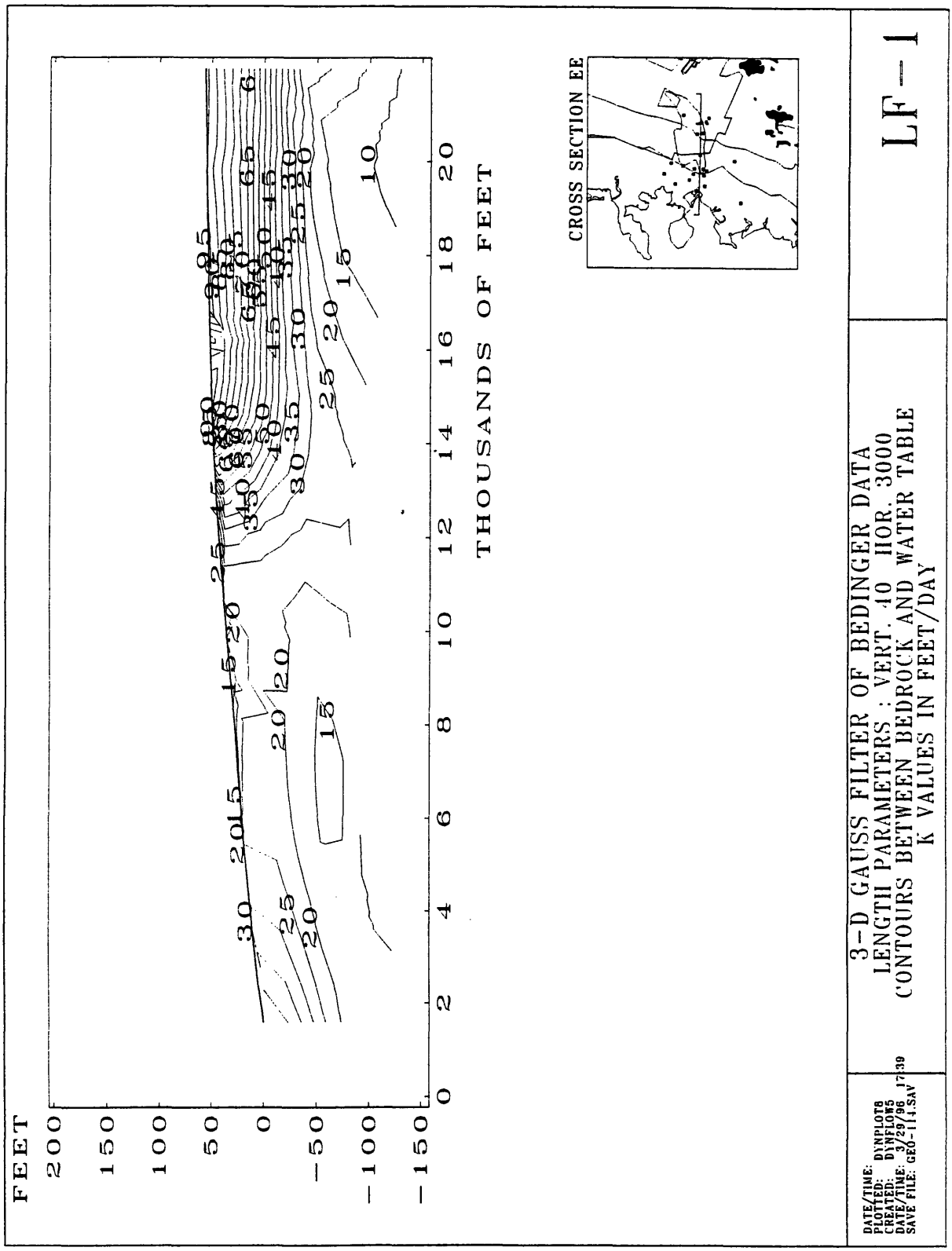

Figure 5.31 North/South Vertical Cross Section Contours of Filtered Bedinger Data

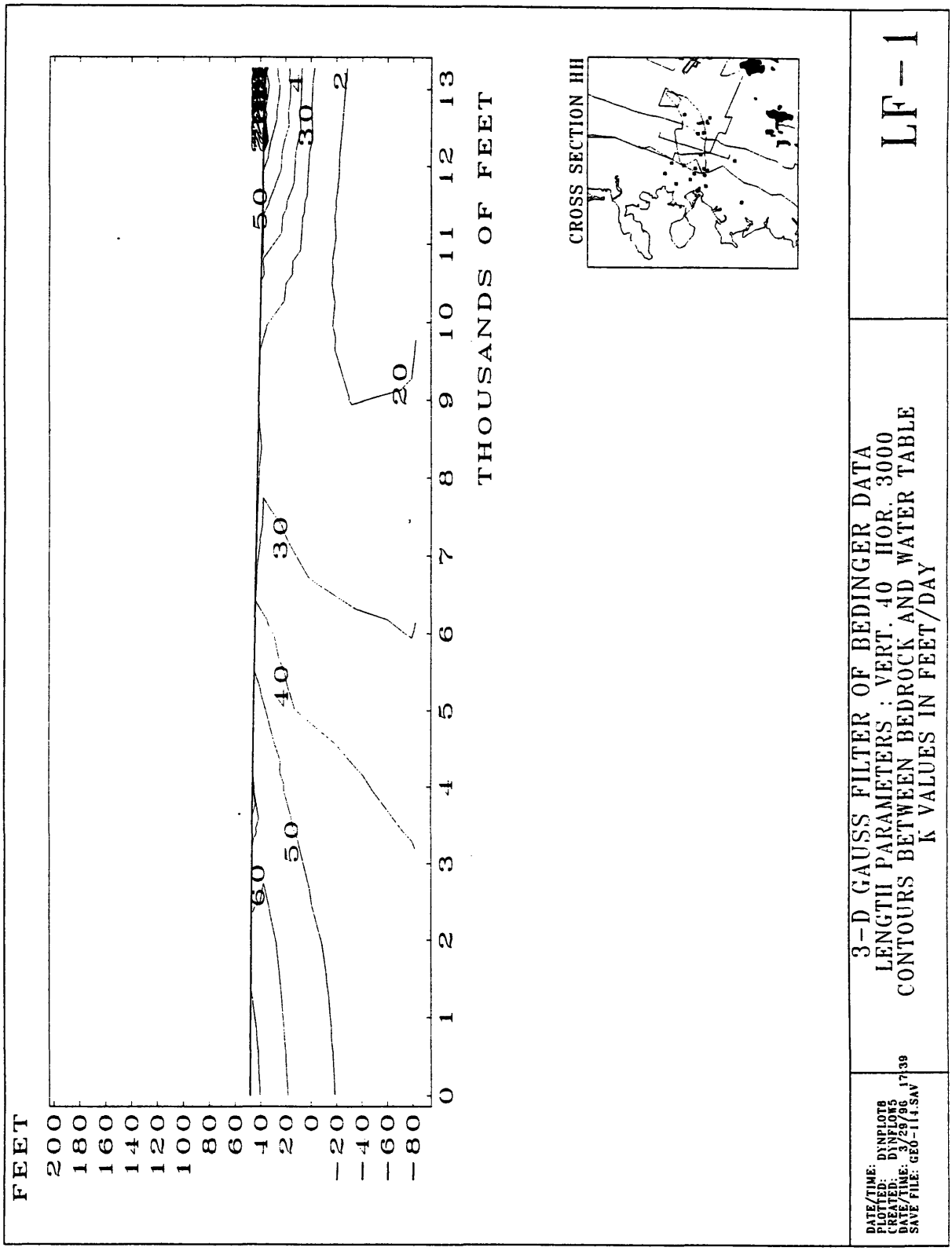

Table 5.1 VOC Contamination Sample Data for wells with at Least One Contaminant Exceeding the EPA MCL

VOC Contamination Sample Data													
For wells with at least one contaminant exceeding the EPA MCL													
				Ground	Top of								
				surface	screen elev.		1993 Data (micrograms per liter - ppb)						
Well Identification				(ft msl)	(ft msl)	VC	CF	CT	TCE	PCE	B	1,4-DCB	Total
CS-10	MW	35		123.2	-11.8		4.6	27	1.3	4.4			37.3
CS-10	MW	36		117.85	3.04		1.5	26	2.1	6.6			36.2
LF-1	GB	22		177.9	-109.1		1	4.7	14	30			49.7
LF-1	MW	9		127.3	67	1.7	0.4		0.4	0.9	1.2	14	18.6
LF-1	MW	17	A	141.72	7.72	1			0.6	1.3	1.1	9.2	13.2
LF-1	MW	17	B	141.6	37.6	0.8			0.5	1.1	0.9	6.8	10.1
LF-1	MW	19		129.7	1.3				44			0.3	44.3
LF-1	MW	20	B	133.7	10.7		1.3	8	8.2	7.6	0.2	0.4	25.7
LF-1	MW	20	Z	133.4	-39.6		1.1		5	5.2			11.3
LF-1	MW	22	A	128.8	-20.7	8.5		8.5	12	7.4	1.3	6.4	44.1
LF-1	MW	23		111.18	-8.12			0.4	2.2	10			12.6
LF-1	MW	24	B	146.7	13.6	7.1	0.1		1.9	2.9	1.1	11	24.1
LF-1	MW	26		105.6	-37.4		4	12	8.8	23	0.2		48
LF-1	MW	26	B	107.2	-97.8		1.7	6.7	8.9	20			37.3
LF-1	MW	28	Z	114.17	-40.83		1.1	2.5	12	7.6			23.2
LF-1	MW	31	A	130.62	-63.58	3	9	47	26	18			103
LF-1	MW	31	B	130.03	-16.97		5		64	20	4		93
LF-1	MW	33		167.53	-9.47		0.2		11	0.7			11.9
LF-1	MW	35		169.32	-34.68		1.7	0.1	5.2	48			55
LF-1	MW	36	B	198.56	-4.44		0.6	1	9.6	9.2			20.4
LF-1	MW	37	A	179.87	-33.13		0.8		19	0.7			20.5
LF-1	MW	38	A	72.21	-62.79		1.35	5.8	26	20			53.15
LF-1	MW	50	B	31.6	-137.9		0.2				7.05		7.25
LF-1	MW	103	A	103.31	-2.04	0.8	6.2	60	30	65			162
LF-1	MW	103	Z	103.71	-56.29		0.8	5	1.8	1.8			9.4
LF-1	MW	104	A	109.4	-2.42			1.4	1.1	11			13.5
					MAXIMUM	8.5	9	60	64	65	7.05	14	
					MCL	2	5	5	5	5	5	5	

Table 5.2 Total Mass Calculation

	APPROXIMATE TOTAL MASS CALCULATION					
				Difference		
Concentratio	Dimensions (feet)		Area (sq. ft.)	(sq. ft.)	Avg. Conc.	Product
1 ppb	16000	8000	1.28E+08			
20 ppb	13000	4000	5.20E+07	7.60E+07	10	7.60E+08
60 ppb	10000	2000	2.00E+07	3.20E+07	40	1.28E+09
80 ppb	4500	2000	9.00E+06	1.10E+07	70	7.70E+08
100 ppb	4000	1750	7.00E+06	2.00E+06	90	1.80E+08
140 ppb	2000	1000	2.00E+06	5.00E+06	120	6.00E+08
160 ppb	100	1000	1.00E+05	1.90E+06	150	2.85E+08
200 ppb	50	500	2.50E+04	7.50E+04	180	1.35E+07
			Parts per billion over total area			3.89E+09
		1.00E-09	times depth	of 40 feet =	156	cubic feet

Table 5.3 Statistical Description of 23 Common K data locations

	Statistical Description Of			
	Hydraulic Conductivity at 23 Common Locations			
	Determined by 3 Grain Size Methods and 1 Slug Test			
	Elevation	**Natural Log of (feet/day) K values**		
Well No.	**(ft. msl)**	**Hazen**	**Sen (calc.)**	**Bedinger**	**Slug**
GB-8	-145.0	3.869	2.884	3.854	1.609
MW-50B	-138.4	0.937	5.541	6.035	0.956
GB-22	-112.0	3.535	0.940	4.162	-1.609
MW-53	-110.2	-0.199	4.654	5.117	5.328
MW-46A	-103.9	3.869	5.359	6.650	1.459
MW-26B	-98.0	3.709	2.377	3.901	1.872
MW-38Z	-93.0	-1.657	2.565	3.113	4.673
MW-25	-90.0	0.490	-0.643	2.159	1.629
MW-64A	-85.0	3.869	1.411	4.464	4.575
MW-569A	-83.7	2.898	1.778	2.970	4.439
MW-569B	-53.7	3.709	2.989	3.489	4.430
MW-46	-48.9	-0.736	2.962	3.600	2.322
MW-567A	-39.7	-0.736	2.429	3.181	1.435
MW-39A	-39.5	3.221	2.174	3.246	0.833
MW-565B	-37.5	3.709	3.237	3.246	4.615
MW-64B	-35.0	5.542	5.440	4.567	4.256
MW-569C	-23.7	3.134	-0.252	3.901	4.868
MW-568C	-9.4	4.922	4.379	4.533	5.517
MW-567C	0.3	3.535	2.960	3.181	3.329
MW-568D	10.6	2.898	2.483	2.370	3.223
MW-569D	16.3	3.709	2.548	3.805	5.024
MW-567D	20.4	3.709	-0.487	4.567	2.332
MW-31C	35.0	5.010	4.151	4.904	4.498
		HAZEN	**SEN**	**BEDINGER**	**SLUG**
	Mean	2.737	2.690	3.957	3.114
	Standard Error	0.418	0.367	0.223	0.387
	Median	3.535	2.565	3.854	3.329
	Standard Deviation	2.005	1.760	1.071	1.858
	Sample Variance	4.020	3.097	1.147	3.453
	Range	7.199	6.185	4.491	7.127
	Minimum	-1.657	-0.643	2.159	-1.609
	Maximum	5.542	5.541	6.650	5.517
		CORRELATION			
		HAZEN	**SEN**	**BEDINGER**	**SLUG**
	HAZEN	1.000			
	SEN	0.105	1.000		
	BEDINGER	0.237	0.572	1.000	
	SLUG	0.134	0.177	-0.060	1.000

Table 5.4 Statistical Description of 18 Common K data locations

	Statistical Description Of				
	Hydraulic Conductivity at 18 Common Locations				
	Determined by 3 Grain Size Methods and 1 Slug Test				
	Elevation	**Natural Log of (feet/day) K values**			
Well No.	**(ft. msl)**	**Hazen**	**Sen (calc.)**	**Bedinger**	**Slug**
GB-8	-145.0	3.869	2.884	3.854	1.609
MW-50B	-138.4	0.937	5.541	6.035	0.956
MW-53	-110.2	-0.199	4.654	5.117	5.328
MW-46A	-103.9	3.869	5.359	6.650	1.459
MW-26B	-98.0	3.709	2.377	3.901	1.872
MW-38Z	-93.0	-1.657	2.565	3.113	4.673
MW-569A	-83.7	2.898	1.778	2.970	4.439
MW-569B	-53.7	3.709	2.989	3.489	4.430
MW-46	-48.9	-0.736	2.962	3.600	2.322
MW-567A	-39.7	-0.736	2.429	3.181	1.435
MW-39A	-39.5	3.221	2.174	3.246	0.833
MW-565B	-37.5	3.709	3.237	3.246	4.615
MW-64B	-35.0	5.542	5.440	4.567	4.256
MW-568C	-9.4	4.922	4.379	4.533	5.517
MW-567C	0.3	3.535	2.960	3.181	3.329
MW-568D	10.6	2.898	2.483	2.370	3.223
MW-569D	16.3	3.709	2.548	3.805	5.024
MW-31C	35.0	5.010	4.151	4.904	4.498
		HAZEN	**SEN**	**BEDINGER**	**SLUG**
	Mean	2.678	3.384	3.987	3.323
	Standard Error	0.512	0.285	0.264	0.383
	Median	3.622	2.961	3.703	3.792
	Standard Deviation	2.174	1.211	1.119	1.624
	Sample Variance	4.724	1.466	1.253	2.638
	Range	7.199	3.763	4.280	4.685
	Minimum	-1.657	1.778	2.370	0.833
	Maximum	5.542	5.541	6.650	5.517
		CORRELATION			
		HAZEN	**SEN**	**BEDINGER**	**SLUG**
	HAZEN	1.000			
	SEN	0.190	1.000		
	BEDINGER	0.142	0.874	1.000	
	SLUG	0.167	0.044	-0.149	1.000

Table 5.5 Statistical Description of 8 Common K data locations

	Statistical Description Of				
	Hydraulic Conductivity at 8 Common Locations				
	Determined by 3 Grain Size Methods and 1 Slug Test				
	Elevation	**Natural Log of (feet/day) K values**			
Well No.	**(ft. msl)**	**Hazen**	**Sen (calc.)**	**Bedinger**	**Slug**
GB-8	-145.0	3.869	2.884	3.854	1.609
MW-50B	-138.4	0.937	5.541	6.035	0.956
GB-22	-112.0	3.535	0.940	4.162	-1.609
MW-53	-110.2	-0.199	4.654	5.117	5.328
MW-46A	-103.9	3.869	5.359	6.650	1.459
MW-26B	-98.0	3.709	2.377	3.901	1.872
MW-569A	-83.7	2.898	1.778	2.970	4.439
MW-567A	-39.7	-0.736	2.429	3.181	1.435
		HAZEN	**SEN**	**BEDINGER**	**SLUG**
	Mean	2.235	3.245	4.484	1.936
	Standard Error	0.682	0.609	0.469	0.755
	Median	3.217	2.656	4.031	1.534
	Standard Deviation	1.930	1.721	1.327	2.134
	Sample Variance	3.726	2.963	1.761	4.556
	Range	4.605	4.601	3.680	6.937
	Minimum	-0.736	0.940	2.970	-1.609
	Maximum	3.869	5.541	6.650	5.328
		CORRELATION			
		HAZEN	**SEN**	**BEDINGER**	**SLUG**
	HAZEN	1.000			
	SEN	-0.274	1.000		
	BEDINGER	0.030	0.863	1.000	
	SLUG	-0.342	0.257	-0.109	1.000
BEDINGER vs. SEN correlation with GB-22 removed			0.967		

Table 5.6 Statistical Description of Gaussian Filtered 23 Common K Data Locations

Correlation Analysis For Hydraulic Conductivity at 23 Common Locations					
Using Gauss Filtered Natural Log K Values					
Filter Length Parameters: 3000 ft. horizontal, 30 ft. vertical					
	Elevation	**LN**	**LN**	**LN**	**LN**
Well No.	**(ft. msl)**	**Hazen**	**Sen (calc.)**	**Bedinger**	**Slug**
GB-8	-145.0	2.586	4.008	4.809	1.533
MW-50B	-138.4	2.166	4.438	5.218	1.516
GB-22	-112.0	2.304	1.805	4.079	0.799
MW-53	-110.2	1.361	3.818	4.962	3.875
MW-46A	-103.9	1.606	3.821	5.024	2.897
MW-26B	-98.0	2.296	1.044	3.214	2.232
MW-38Z	-93.0	1.087	3.293	4.503	2.879
MW-25	-90.0	2.048	0.744	3.052	2.380
MW-64A	-85.0	2.435	2.866	4.705	4.051
MW-569A	-83.7	3.015	2.152	3.218	4.423
MW-569B	-53.7	3.335	2.014	3.508	4.438
MW-46	-48.9	0.995	2.910	3.580	2.205
MW-567A	-39.7	1.519	2.813	3.489	2.088
MW-39A	-39.5	1.275	2.642	3.412	1.853
MW-565B	-37.5	3.708	3.238	3.248	4.614
MW-64B	-35.0	3.216	4.007	4.012	3.253
MW-569C	-23.7	3.494	1.624	3.783	4.653
MW-568C	-9.4	3.793	2.913	3.705	4.364
MW-567C	0.3	3.321	2.265	3.607	3.095
MW-568D	10.6	3.644	2.698	3.432	4.080
MW-569D	16.3	3.596	2.471	3.560	4.545
MW-567D	20.4	3.600	1.065	3.928	2.882
MW-31C	35.0	5.007	4.150	4.903	4.497
		Hazen	**Sen**	**Bedinger**	**Slug**
	Hazen	1.000			
	Sen	-0.061	1.000		
	Bedinger	-0.131	0.708	1.000	
	Slug	0.622	0.018	-0.149	1.000
Correlation with 3 smallest slug K values removed (those < 4.6 ft./day)					
		Hazen	**Sen**	**Bedinger**	**Slug**
	Hazen	1.000			
	Sen	-0.037	1.000		
	Bedinger	-0.090	0.653	1.000	
	Slug	0.716	0.208	0.151	1.000

VI. Conclusions

Site characterization investigations followed two main topics with respect to this report. The first involved describing the nature and extent of the chemical contamination in the groundwater. The second involved analyzing tests for hydraulic conductivity to determine parameters that could be used for modeling contaminant migration.

Groundwater Contamination

As part of the Superfund Remedial Investigation process, 73 wells at different locations and different depths were tested for 34 of the most likely compounds. The EPA standard for drinking water sets individual maximum contamination levels (MCLs) for most of these compounds. 28 out of the 73 wells had at least one contaminant which exceeded the MCL. 7 out of the 34 possible contaminants were at levels which exceeded the MCL. These contaminants are vinyl chloride (VC), carbon tetrachloride (CT), trichloroethene (TCE), tetrachloroethene (PCE), 1,4 dichlorobenzene (1,4 DCB), benzene (B), and chloroform (CF). All of these compounds have an MCL of 5 ppb, except for vinyl chloride which has an MCL of 2 ppb. The highest total of all 7 of these contaminants at any one well was 162 ppb (see Table 5.1).

The highest total of all contaminants sampled at any one well was 236 ppb. (Some of these contaminants have an MCL much higher than 5 ppb.) The highest three individual contaminant readings were CT at 60 ppb, TCE at 64 ppb, and PCE at 65 ppb. One ppb by volume is equivalent to one drop in 15,000 gallons. 162 ppb, the highest total concentration of the 7 contaminants mentioned above, is equivalent to about 1/3 ounce per 15,000 gallons.

Looking at two dimensional log-linear contours of the contamination data points and vertical section filtered contours (see Figures 5.2 - 5.4 and 5.10), a very rough estimate of the total volume of contamination can be made. This is estimated to be about 160 cubic feet or 22 - 55 gallon drums. This mass is distributed over approximately 4.5 square miles. This works out to be an average total contaminant concentration of 32 ppb. The area where any single MCL level is exceeded is about 2 square miles.

Contamination contours show that little degradation of PCE is occurring. TCE is the degraded product of PCE. The contours show the center of PCE concentration to be downgradient from the center of TCE concentration, therefore the TCE could not be the result of PCE degradation. Instead, this indicates that TCE must be one of the originally dumped contaminants.

Examining cross sectional contours of contamination (see Figure 5.10), it is seen that a contamination level exceeding the MCL comes within 10 feet of the top of the aquifer. It is estimated that the withdrawal depth of a hypothetical private well pulling 1000 gallons per day to be 13 feet, given a conservative figure for hydraulic conductivity (50 ft/day) and hydraulic gradient (1/100). Therefore, it is possible that private wells located directly over the uppermost levels of contamination could draw in water exceeding the MCL levels for drinking water.

Hydraulic Conductivity

Hydraulic conductivity (K) was determined using 140 grain size samples from 21 well locations and 79 slug test well locations. A comparison of values from these two different tests generally shows very poor correlation. However, a better correlation was seen between the Alyamani/Sen (Alyamani, et al, 1993) and Bedinger (Bradbury, et al, 1990) grain size methods. This is due to the fact that both depend on the grain size fraction d_{50}. Both grain size and slug test data were put through a 3-D gauss filtering process. The resulting data and corresponding contours exhibit a significant correlation between the Hazen and slug methods. However, the Hazen values are much lower.

The filtered slug contours match the general geology of the area, showing a decline in conductivity from north to south and with depth. In addition, the Buzzard's Bay Moraine is clearly seen in Figure 5.20 as having significantly lower conductivity. The contours also point out a zone of lower conductivity in a region where the contaminant plume appears to be dividing. This finding may provide part of the explanation for the observed migration path. The arithmetic mean of the unfiltered slug test data was 75 feet/day, ranging from less than 1 ft/day to 316 feet/day. The calculated horizontal conductivity from the filtered slug test data had a mean of 85 feet/day and a maximum of 272 feet/day. In addition to hydraulic conductivity, a determination of overall hydraulic anisotropy was made using the filtered slug K values. The number was approximately 3.4. It is very similar to the value of 3.2 determined by Springer for the Mashpee Pitted Plain (Springer, 1991).

Summary

In summary, a large area of groundwater has been contaminated by the MMR Mainbase Landfill 1 with halogenated volatile organic compounds. The contaminant plume is heading west through the Buzzards Bay Moraine. Public and private drinking supply wells are in danger of possibly drawing water with concentration levels exceeding EPA drinking water standards. Assuming 236 ppb (the highest total concentration sampled at any one well) and 60 gallons per day of individual water use (an average for all domestic needs), an individual could be exposed to one drop of contaminant per day.

Hydraulic conductivity trends can be ascertained using gaussian filtered slug test data. Values for horizontal and vertical hydraulic conductivity may be calculated from the filtered data. These values may be used to model migration of the plume.

REFERENCES

ABB Environmental Services, Inc. *Installation Restoration Program, Massachusetts Military Reservation, Interim Remedial Investigation, Main Base Landfill (AOC LF-1),* Portland, Maine, March 1992.

Alyamani, M.S., and Z. Sen. "Determination of Hydraulic Conductivity from Complete Grain-Size Distribution Curves," *Ground Water*, v. 31, no. 4, p. 551-555, 1993.

Amarasekera, K. *A Groundwater Model Of The Landfill Site At The Massachusetts Military Reservation,* MEng Thesis Massachusetts Institute of Technology, Cambridge, Massachusetts, 1996.

Automated Sciences Group, Inc., Hazardous Waste Remedial Actions Program, and Oak Ridge National Laboratory. *Risk Assessment Handbook*, Oak Ridge, Tennessee, 1994.

Bouwer, Herman and R.C. Rice. "A Slug Test for Determining Hydraulic Conductivity of Unconfined Aquifers With Completely or Partially Penetrating Wells," *Water Resources Research*, v. 12, no. 3, p. 423-428, 1976.

Bradbury and Muldoon. "Hydraulic Conductivity Determinations in Unlithified Glacial and Fluvial Materials," ASTM STP 1053, *Ground Water and Vadose Zone Monitoring*, 1990.

Camp Dresser & McKee Inc. *Dyntrack, A 3-Dimensional Contaminant Transport Model For Groundwater Studies*, Camp Dresser & McKee Inc., Boston, MA, 1984.

Cape Cod Commission. *Cape Trends, Demographic and Economic Characteristics and Trends*, Barnstable County, Cape Cod, MA, 1996.

CDM Federal Programs Corp. *Remedial Investigation Report Main Base Landfill (AOC LF-1) and Hydrogeological Region I Study*, Boston, Massachusetts, April 1995.

E.C. Jordan Co. *Hydrogeologic Summary, Task 1-8, Installation Restoration Program, Massachusetts Military Reservation*, Portland, Maine, April 1989.

Freeze, R.A., and J.A. Cherry. *Groundwater*, Prentice-Hall, Inc., Englewood Cliffs, NJ, 1979.

Garabedian, S. P., L. W. Gelhar, and M. A. Celia, *Large-scale dispersive Transport in Aquifers: Field Experiments and Reactive Transport Theory.* Ralph M. Parsons Laboratory Report 315, Massachusetts Institute of Technology, Cambridge, MA, 290p., 1988.

Gelhar, L. W., C. Welty and K. R. Rehfeldt, "A critical review of data on field-scale dispersion in aquifers," *Water Resources Research*, 28(7), 1958-1974, 1992.

LaGrega, D.M., P.L. Buckingham, and J.C. Evans. *Hazardous Waste Management*, McGraw-Hill, New York, 1994.

LeBlanc, D.R., J.H. Guswa, M.H. Frimpter, and C.J. Londquist. *Groundwater Resources of Cape Cod, Massachusetts*, U.S. Dept. of the Interior, U.S. Geological Survey, Hydrologic Investigations Atlas HA-692, 1986.

Masterson, J. P. and P. M. Barlow, *Effects of Simulated Ground-Water Pumping and Recharge on Ground-Water Flow in Cape Cod, Martha's Vineyard, and Nantucket Island Basins, Massachusetts*.. U.S. Geological Survey Open-File Report 94-316, 1994.

Oldale, R.N. "Glaciotectonic Origin of the Massachusetts Coastal End Moraines and a Fluctuating Late Wisconsinian Ice Margin," *Geological Society of America Bulletin*, v. 95, 1984.

Operation Technologies Corporation (Op-Tech). *Technical Memorandum - Containment of Landfill-1 Plume*.Oak Ridge, TN, 1996.

Springer, R.K. *Application Of An Improved Slug Test Analysis To The Large-Scale Characterization Of Heterogeneity in a Cape Cod Aquifer*, MS Thesis Massachusetts Institute of Technology, Cambridge, Massachusetts, 1991.

Thompson, K. D. *The Stochastic Characterization of Glacial Aquifers Using Geologic Information*, PhD Thesis Massachusetts Institute of Technology, Cambridge, Massachusetts, 1994.

U.S. Environmental Protection Agency (USEPA). *Guidance for Conducting Remedial Investigations and Feasibility Studies under CERCLA*, Office of Solid Waste and Emergency Response, OSWER Directive 9335.3-01, March 1988.

Van Der Kamp, G. "Determining Aquifer Transmissivity by Means of Well Response Tests: The Underdamped Case," *Water Resources Research*, v. 12, no. 1, p. 71-77, 1976.

Appendix A.			Contaminant Sampling Well Designations and Locations						
Page 1 of 2									
						Ground	Top of	Bottom of	
	Well	Well		Coordinates		surface	screen	screen elev.	Sampling
Site	Type	No.	Letter	Northing	Easting	(ft msl)	(ft msl)	(ft msl)	Year
CS-10	MW	35		43914.8	57575.7	123.2	-11.8	-16.8	1993
CS-10	MW	42	A	41078.1	55131.1	102.86	-72.14	-77.14	1993
CS-10	MW	42	B	41102.8	55134.8	103.26	-11.61	-16.61	1993
CS-10	MW	42	C	41091.4	55132.3	102.8	7.64	2.64	1993
CS-10	MW	48		42750.3	56391.4	112.84	8.34	3.34	1993
CS-9	MW	1		45120	57100	133.7			1993
LF-1	GB	20		43918.5	46110.4	108.66	-154.34	-164.34	1993
LF-1	GB	22		40924.1	48048.8	177.9	-109.1	-114.1	1993
LF-1	MW	9		45610.5	36649.3	127.3	67	-14.3	1993
LF-1	MW	17	A	46284.8	58115	141.72	7.72	2.72	1993
LF-1	MW	17	B	46284.8	58115	141.6	37.6	32.6	1993
LF-1	MW	19		45560	58790	129.7	1.3	-3.7	1993
LF-1	MW	20	A	45120	57100	133.7	-4.9	-9.9	1993
LF-1	MW	20	B	45120	57100	133.7	10.7	5.7	1993
LF-1	MW	20	C	45120	57100	133.7	44.7	39.7	1993
LF-1	MW	20	Z	45120	57100	133.4	-39.6	-44.6	1993
LF-1	MW	22	A	42920.1	53314	128.8	-20.7	-25.7	1993
LF-1	MW	23		41465.5	56328.8	111.18	-8.12	-13.12	1993
LF-1	MW	24	A	43160	52550	146.7	-41.1	-46.1	1993
LF-1	MW	24	B	43160	52550	146.7	13.6	8.6	1993
LF-1	MW	25		40430	51937.5	86.9	33.6	23.6	1993
LF-1	MW	25	A	40443.5	51931.1	87.84	-107.16	-112.16	1993
LF-1	MW	26		41429	51789.8	105.6	-37.4	-42.4	1993
LF-1	MW	26	B	41464.1	51820.9	107.2	-97.8	-102.8	1993
LF-1	MW	28	Z	41026.4	49728.9	114.17	-40.83	-45.83	1993
LF-1	MW	29		40013	53517	63.87	-27.13	-32.13	1993
LF-1	MW	31	A	43830	55139.2	130.62	-63.58	-68.58	1993
LF-1	MW	31	B	43812.9	55164.2	130.03	-16.97	-21.97	1993
LF-1	MW	31	C	43836.5	55115.8	131.26	37.7	32.7	1993
LF-1	MW	32		44234.8	52334.8	146.38	-8.12	-13.12	1993
LF-1	MW	33		44806.2	51589.8	167.53	-9.47	-14.47	1993
LF-1	MW	34		46957.1	52143.2	134.33	-40.67	-45.67	1993
LF-1	MW	35		43368.7	48476.1	169.32	-34.68	-39.68	1993
LF-1	MW	36	B	41563.1	48085.3	198.56	-4.44	-9.44	1993

Appendix A.			Contaminant Sampling Well Designations and Locations						
Page 2 of 2									
						Ground	Top of	Bottom of	
	Well	Well		Coordinates		surface	screen	screen elev.	Sampling
Site	Type	No.	Letter	Northing	Easting	(ft msl)	(ft msl)	(ft msl)	Year
LF-1	MW	37	A	44362.8	48110.1	179.87	-33.13	-38.13	1993
LF-1	MW	38	A	40291.5	45536.8	72.21	-62.79	-67.79	1993
LF-1	MW	38	Z	40290.1	45562.9	74.16	-90.34	-95.34	1993
LF-1	MW	38		40291.5	45536.8	74.08	30.58	20.58	1993
LF-1	MW	39	A	41878.2	45549.8	97.46	-42.04	-47.04	1993
LF-1	MW	40		42976.9	45919	101.54	-56.06	-61.06	1993
LF-1	MW	40	A	42984.2	45911.8	102.26	-92.74	-97.74	1993
LF-1	MW	41		43926.5	46119.5	108.8	-69	-74	1993
LF-1	MW	43		39457.5	48290.7	173.33	-24.67	-29.67	1993
LF-1	MW	44		38928.7	45049.6	85.41	-100.99	-105.99	1993
LF-1	MW	45		40843.4	45175.5	52.04	-102.96	-107.96	1993
LF-1	MW	46		40172.4	44368.3	96.4	-47.95	-52.95	1993
LF-1	MW	46	A	40166.5	44355.1	96.1	-102.9	-107.9	1993
LF-1	MW	47		39743.7	45198.4	91.4	-21.6	-26.6	1993
LF-1	MW	50	A	40022	42451.5	31.98	-75.02	-80.02	1993
LF-1	MW	50	B	40012.7	42444.3	31.6	-137.9	-142.9	1993
LF-1	MW	51		38550.2	42179	45.14	-97.06	-102.06	1993
LF-1	MW	52		41307.1	43150.6	42.26	-127.74	-132.74	1993
LF-1	MW	53		42760.4	43588.2	44.84	-102.26	-107.26	1993
LF-1	MW	54		43543.2	43804.4	28.21	-107.64	-112.64	1993
LF-1	MW	61		47734.7	56702.5	129.55	63.55	53.55	1993
LF-1	MW	71		46828	56699.5	135.27	63.27	53.27	1993
LF-1	MW	103	A	42290	53720	103.31	-2.04	-7.04	1993
LF-1	MW	103	B	42290	53720	103.33	51.69	47.19	1993
LF-1	MW	103	Z	42200.3	53768.8	103.71	-56.29	-61.29	1993
LF-1	MW	104	A	41664.5	54082	109.4	-2.42	-7.42	1993
LF-1	MW	104	B	41664.5	54082	109.4	51.67	46.73	1993
LF-1	MW	601	A	39728	50064	144.4	-25.6	-30.6	1993
LF-1	MW	601	B	39728	50064	142.1	-6.37	-11.37	1993
LF-1	MW	601	C	39728	50064	141.06	9.14	4.14	1993
LF-1	MW	602	B	38014.5	51912.8	126.2	-7.8	-12.8	1993
LF-1	MW	602	C	38014.5	51912.8	126.23	11.23	6.23	1993
LF-1	MW	701	A	45136.5	54193.9	143.23	-31.77	-36.77	1993
LF-1	MW	705		47321.5	56693.5	141.88	68.18	57.98	1993
LF-1	WT	25		46971.6	52135.3	132.36	58.36	48.36	1993
LF-1	WT	26		45137.6	48766.9	161.6	37.6	26.6	1993
LF-1	WT	28		46060.5	46580.8	124.18	41.18	31.18	1993
LF-1	WT	29		42736.6	42038.6	59.3	4.46	-5.54	1993

Appendix B. VOC Contamination Sample Data

Page 1 of 6 — Values in micrograms per liter (ppb). Blank cells represent non-detect.

Well Identification				DCDFM	VC	CMA	CE	TCFM	1,1-DCE	t 1,2-DCE	1,1-DCA	c 1,2-DCE	CF	1,1,1-TCA	CT
CS-10	MW	35		13				6.4	0.3				4.6	3.9	27
CS-10	MW	42	A												
CS-10	MW	42	B												
CS-10	MW	42	C										1		
CS-10	MW	48		4.6				2.7						1.4	4
CS-9	MW	1													
LF-1	GB	20		0.75									0.65		
LF-1	GB	22		11				1.5			1.1	4.4	1	1.1	4.7
LF-1	MW	9		3.8	1.7						1.8	4.4	0.4		
LF-1	MW	17	A	5.4	1		0.5				6	17			
LF-1	MW	17	B	3.8	0.8						3.4	17			
LF-1	MW	19										1.6		0.8	
LF-1	MW	20	A	3.2				1.8		0.2	2.2	34		1	
LF-1	MW	20	B	4.3				3.8	0.5		2.6	3.3	1.3	3	8
LF-1	MW	20	C					0.6							
LF-1	MW	20	Z	16						1	3.2	59	1.1	0.9	
LF-1	MW	22	A	3.1	8.5			0.2	2.8	0.9	6.4	62		8.6	8.5
LF-1	MW	23		16				8.4	0.4					3.5	0.4
LF-1	MW	24	A		1.6						1.4	20	0.3		
LF-1	MW	24	B		7.1					0.2	1.8	45	0.1		
LF-1	MW	25						0.8	0.5				0.7	2.7	4.4
LF-1	MW	25	A						0.2				0.8		2.1
LF-1	MW	26		5.8				0.9		0.1		1.8	4	0.6	12
LF-1	MW	26	B	19				1.4	0.8		0.9	0.6	1.7	2.3	6.7
LF-1	MW	28	Z	8.1					5.9	0.2	1.7	13	1.1	21	2.5
LF-1	MW	29											0.6		
LF-1	MW	31	A		3						5	68	9		47
LF-1	MW	31	B						2		4	25	5		
LF-1	MW	31	C												
LF-1	MW	32											0.3		
LF-1	MW	33										0.8	0.2		
LF-1	MW	34													
LF-1	MW	35		3.8				2.7					1.7	0.5	0.1
LF-1	MW	36	B	7.2				0.5				0.4	0.6		1

DCDFM	dichlorodifluoromethane	t1,2-DCE	trans-1,2-dichloroethene
VC	vinyl chloride	1,1-DCA	1,1-dichloroethane
CMA	chloromethane	C1,2-DCE	cis-1,2-dichloroethene
CE	chloroethane	CF	chloroform
TCFM	thrchlorofluoromethane	1,1,1-TCA	1,1,1-trichloroethane
1,1-DCE	1,1 dichloroethene	CT	carbon tetrachloride

Appendix B. VOC Contamination Sample Data															
Page 2 of 6				Values in micrograms per liter (ppb). Blank cells represent non-detect.											
Well Identification				DCDFM	VC	CMA	CE	TCFM	1,1-DCE	t 1,2-DCE	1,1-DCA	c 1,2-DCE	CF	1,1,1-TCA	CT
LF-1	MW	37	A										0.8		
LF-1	MW	38	A	4.2				0.5	1.9	0.65	0.9	8.8	1.35	15	5.8
LF-1	MW	38	Z											0.8	0.4
LF-1	MW	38											1.6		
LF-1	MW	39	A										1.4		
LF-1	MW	40											0.2		
LF-1	MW	40	A	1.2											
LF-1	MW	41											0.6		
LF-1	MW	43											0.5		
LF-1	MW	44				0.4									
LF-1	MW	45				0.3							0.6		
LF-1	MW	46													
LF-1	MW	46	A			0.6									0.4
LF-1	MW	47											0.3		
LF-1	MW	50	A												
LF-1	MW	50	B										0.2		
LF-1	MW	51				0.3									
LF-1	MW	52											0.3		
LF-1	MW	53													
LF-1	MW	54				0.2									
LF-1	MW	61													1.2
LF-1	MW	71		1.6				0.2					1.5		
LF-1	MW	103	A	22	0.8			11	5.5		1.7	1.4	6.2	32	60
LF-1	MW	103	B										0.8		
LF-1	MW	103	Z	2.5				0.1				1.8	0.8		5
LF-1	MW	104	A	17				2.4							1.4
LF-1	MW	104	B										1.5		
LF-1	MW	601	A										0.3	1.1	0.4
LF-1	MW	601	B										0.3	0.7	
LF-1	MW	601	C												
LF-1	MW	602	B												
LF-1	MW	602	C												
LF-1	MW	701	A												
LF-1	MW	705											1.4		
LF-1	WT	25													
LF-1	WT	26											1.7		
LF-1	WT	28											2.1		
LF-1	WT	29													
Maximum out of previous page and this page:				22	8.5	0.6	0.5	11	5.9	1	6.4	68	9	32	60
EPA MCL Standard:				1400	2	none	none	none	7	100	70	70	5	200	5

Appendix B. VOC Contamination Sample Data

Page 3 of 6

Values in micrograms per liter (ppb). Blank cells represent non-detect.

Well Identification				1,2-DCA	TCE	1,2-DCP	PCE	DBCM	CB	B	T	E	X	ACE	STY
CS-10	MW	35			1.3		4.4								
CS-10	MW	42	A												
CS-10	MW	42	B		4		5							10	
CS-10	MW	42	C		8		2								
CS-10	MW	48			1.9		2.2			1.9	13	2	13.6		
CS-9	MW	1					0.6								
LF-1	GB	20			0.7		3.95								
LF-1	GB	22		2.5	14		30								
LF-1	MW	9			0.4		0.9		2.3	1.2	0.2	0.3			0.1
LF-1	MW	17	A		0.6		1.3			1.1		0.9	0.5		
LF-1	MW	17	B		0.5		1.1			0.9		2			
LF-1	MW	19			44										
LF-1	MW	20	A	0.4	4.5		3.9			0.3	0.7		0.5		
LF-1	MW	20	B		8.2		7.6			0.2					
LF-1	MW	20	C		0.9		1.5								
LF-1	MW	20	Z		5		5.2								
LF-1	MW	22	A	1.6	12		7.4			1.3	0.5		1.3		
LF-1	MW	23			2.2		10								
LF-1	MW	24	A		0.9		2.8			0.3					
LF-1	MW	24	B	0.9	1.9		2.9		0.2	1.1					
LF-1	MW	25			1.9		4.7								
LF-1	MW	25	A				0.4								
LF-1	MW	26			8.8		23			0.2	1.2	0.3	2.2		
LF-1	MW	26	B		8.9		20								
LF-1	MW	28	Z	0.8	12		7.6								
LF-1	MW	29					0.8								
LF-1	MW	31	A	1	26		18								
LF-1	MW	31	B		64		20		4	4	4				
LF-1	MW	31	C												
LF-1	MW	32			0.6		0.7			0.9	7.1	1.7	10.1		
LF-1	MW	33			11		0.7								
LF-1	MW	34						0.5	1	0.4	0.9				
LF-1	MW	35			5.2		48								
LF-1	MW	36	B	0.9	9.6		9.2								

1,2-DCA	1,2-dichloroethane	B	benzene
TCE	trichloroethene	T	toluene
1,2-DCP	1,2-dichloropropane	E	ethylbenzene
PCE	tetrachloroethene	X	xylenes
DBCM	dibromochloromethane	ACE	acetone
CB	chlorobenzene	STY	styrene

Appendix B. VOC Contamination Sample Data

Page 4 of 6 — Values in micrograms per liter (ppb). Blank cells represent non-detect.

Well Identification				1,2-DCA	TCE	1,2-DCP	PCE	DBCM	CB	B	T	E	X	ACE	STY
LF-1	MW	37	A		19		0.7								
LF-1	MW	38	A	1.95	26	0.4	20								
LF-1	MW	38	Z				0.3								
LF-1	MW	38													
LF-1	MW	39	A												
LF-1	MW	40					0.4				0.2				
LF-1	MW	40	A				1.5								
LF-1	MW	41					0.7								
LF-1	MW	43													
LF-1	MW	44													
LF-1	MW	45													
LF-1	MW	46		0.6							0.2				
LF-1	MW	46	A												
LF-1	MW	47					2.5								
LF-1	MW	50	A												
LF-1	MW	50	B					0.25		7.05	29.9	7.1	41	8.4	
LF-1	MW	51			0.6										
LF-1	MW	52													
LF-1	MW	53					0.9								
LF-1	MW	54			3		0.6								
LF-1	MW	61					0.5				0.4		0.2		
LF-1	MW	71													
LF-1	MW	103	A		30		65				0.2		0.4		0.1
LF-1	MW	103	B												
LF-1	MW	103	Z		1.8		1.8								
LF-1	MW	104	A		1.1		11					0.2	0.2		
LF-1	MW	104	B												
LF-1	MW	601	A				1								
LF-1	MW	601	B				0.4								
LF-1	MW	601	C												
LF-1	MW	602	B												
LF-1	MW	602	C												
LF-1	MW	701	A								0.2				
LF-1	MW	705			0.2										
LF-1	WT	25													
LF-1	WT	26													
LF-1	WT	28													
LF-1	WT	29													
Maximum out of previous page and this page:				2.5	64	0.4	65	0.5	4	7.05	29.9	7.1	41	10	0.1
EPA MCL Standard:				5	5	5	5	none	100	5	1000	900	10000	none	100

Appendix B. VOC Contamination Sample Data

Page 5 of 6

Values in micrograms per liter (ppb). Blank cells represent non-detect.

Well Identification				ISOPB	1,1,2,2-PCE	NPB	1,3,5-TMB	1,2,4-TMB	1,3-DCB	1,4-DCB	1,2-DCB	n-BB	NAPH	TOTAL
CS-10	MW	35												60.9
CS-10	MW	42	A											0
CS-10	MW	42	B											19
CS-10	MW	42	C											11
CS-10	MW	48					0.5	2.2					0.9	50.9
CS-9	MW	1												0.6
LF-1	GB	20												6.05
LF-1	GB	22												71.3
LF-1	MW	9							0.3	14	1.4	0.1		33.3
LF-1	MW	17	A				0.3			9.2	0.5	0.3	13	57.6
LF-1	MW	17	B	0.7						6.8	0.3	0.2	12	49.5
LF-1	MW	19								0.3				46.7
LF-1	MW	20	A											52.7
LF-1	MW	20	B							0.4				43.2
LF-1	MW	20	C											3
LF-1	MW	20	Z											91.4
LF-1	MW	22	A	1	4.7					6.4				137.2
LF-1	MW	23												40.9
LF-1	MW	24	A							1.3	0.3			28.9
LF-1	MW	24	B	0.6						11	0.6			73.4
LF-1	MW	25												15.7
LF-1	MW	25	A											3.5
LF-1	MW	26			1.1		0.6	0.7						63.3
LF-1	MW	26	B											62.3
LF-1	MW	28	Z		1									74.9
LF-1	MW	29												1.4
LF-1	MW	31	A											177
LF-1	MW	31	B											132
LF-1	MW	31	C											0
LF-1	MW	32					0.6	2						24
LF-1	MW	33			2.5									15.2
LF-1	MW	34												2.8
LF-1	MW	35												62
LF-1	MW	36	B											29.4

ISOPB	isopropylbenzene	1,4-DCB	1,4-dichlorobenzene
1,1,2,2-PCE	1,1,2,2-tetrachloroethylene	1,2-DCB	1,2-dichlorobenzene
NPB	n-propylbenzene	n-BB	n-butylbenzene
1,3,5-TMB	1,3,5-trimethylbenzene	NAPH	naphthalene
1,2,4-TMB	1,2,4-trimethylbenzene		
1,3-DCB	1,3-dichlorobenzene		

Appendix B. VOC Contamination Sample Data															
Page 6 of 6				Values in micrograms per liter (ppb). Blank cells represent non-detect.											
Well Identification				ISOPB	1,1,2,2-PCE	NPB	1,3,5-TMB	1,2,4-TMB	1,3-DCB	1,4-DCB	1,2-DCB	n-BB	NAPH	TOTAL
LF-1	MW	37	A		11									31.5
LF-1	MW	38	A											87.45
LF-1	MW	38	Z											1.5
LF-1	MW	38												1.6
LF-1	MW	39	A											1.4
LF-1	MW	40												0.8
LF-1	MW	40	A											2.7
LF-1	MW	41												1.3
LF-1	MW	43												0.5
LF-1	MW	44												0.4
LF-1	MW	45												0.9
LF-1	MW	46												0.8
LF-1	MW	46	A											1
LF-1	MW	47												2.8
LF-1	MW	50	A											0
LF-1	MW	50	B	0.3		0.8	2.5	7.4					0.8	105.7
LF-1	MW	51												0.9
LF-1	MW	52												0.3
LF-1	MW	53												0.9
LF-1	MW	54												3.8
LF-1	MW	61												2.3
LF-1	MW	71												3.3
LF-1	MW	103	A											236.3
LF-1	MW	103	B											0.8
LF-1	MW	103	Z											13.8
LF-1	MW	104	A											33.3
LF-1	MW	104	B											1.5
LF-1	MW	601	A											2.8
LF-1	MW	601	B											1.4
LF-1	MW	601	C											0
LF-1	MW	602	B											0
LF-1	MW	602	C											0
LF-1	MW	701	A											0.2
LF-1	MW	705												1.6
LF-1	WT	25												0
LF-1	WT	26												1.7
LF-1	WT	28												2.1
LF-1	WT	29												0
Maximum out of previous page and this page:				1	11	0.8	2.5	7.4	0.3	14	1.4	0.3	13	
EPA MCL Standard:				none	none	none	none	none	none	5	600	none	none	

Appendix C: Gaussian Filtered Slug Data Values								
Page 1 of 2							Feet/day	
	Coordinates (feet)			Feet/day		FILTERE	FILTERED	Calculated
Well ID	X	Y	Z	SLUG	LN SLUG	LN SLUG	SLUG	K_x
CS-10MW36	18344.80	30287.00	3.00	82.60	4.41	4.27	71.34	131.27
CS-10MW40A	18227.50	26399.50	-116.80	54.00	3.99	3.87	47.87	88.09
CS-10MW42B	16225.10	27289.10	-11.60	83.30	4.42	3.92	50.46	92.85
CS-10MW42C	16225.10	27289.10	7.60	10.50	2.35	3.96	52.50	96.59
CS-10MW48	17485.40	28961.30	8.30	147.00	4.99	4.21	67.17	123.58
HG-1MW565B	643.30	19889.40	-31.50	101.00	4.62	4.44	85.10	156.59
HG-1MW566A	1392.90	24204.10	-61.90	150.00	5.01	4.07	58.69	107.98
HG-1MW566B	1392.90	24204.10	-41.90	57.70	4.06	3.94	51.23	94.26
HG-1MW566D	1392.90	24204.10	10.60	1.40	0.34	1.32	3.76	6.91
HG-1MW567A	5715.90	28249.70	-38.70	4.20	1.44	3.17	23.76	43.72
HG-1MW567B	5715.90	28249.70	-18.60	122.70	4.81	3.35	28.56	52.55
HG-1MW567C	5715.90	28249.70	1.80	27.90	3.33	3.44	31.16	57.33
HG-1MW567D	5715.90	28249.70	26.20	10.30	2.33	3.25	25.79	47.45
HG-1MW568A	3927.60	31479.10	-47.60	203.00	5.31	4.27	71.30	131.19
HG-1MW568B	3927.60	31479.10	-27.60	70.50	4.26	4.36	78.07	143.65
HG-1MW568C	3927.60	31479.10	-7.60	249.00	5.52	4.33	75.77	139.43
HG-1MW568D	3927.60	31479.10	12.50	25.10	3.22	4.19	65.95	121.34
HG-1MW569A	5776.60	33461.50	-76.20	84.70	4.44	4.14	62.81	115.56
HG-1MW569B	5776.60	33461.50	-48.40	83.90	4.43	4.38	80.13	147.43
HG-1MW569C	5776.60	33461.50	-23.00	130.00	4.87	4.50	89.57	164.82
HG-1MW569D	5776.60	33461.50	24.70	152.00	5.02	4.55	94.85	174.52
LF-1GB20	7204.40	30129.50	-154.30	0.10	-2.30	-0.76	0.47	0.86
LF-1GB22	9142.80	27135.10	-109.10	0.20	-1.61	1.46	4.31	7.93
LF-1MW103A	14814.00	28501.00	-2.00	89.00	4.49	4.07	58.30	107.27
LF-1MW103B	14814.00	28501.00	51.70	214.00	5.37	4.37	78.83	145.05
LF-1MW103Z	14862.80	28411.30	-56.30	82.60	4.41	3.61	37.12	68.30
LF-1MW11A	20034.00	33060.00	-11.10	142.00	4.96	4.35	77.63	142.84
LF-1MW11B	20034.00	33060.00	16.20	84.60	4.44	4.50	89.72	165.08
LF-1MW11C	20034.00	33060.00	28.20	102.80	4.63	4.55	94.26	173.43
LF-1MW11D	20034.00	33060.00	36.90	99.40	4.60	4.58	97.86	180.06
LF-1MW18A	19594.80	32198.80	-23.20	54.60	4.00	4.14	63.07	116.04
LF-1MW18B	19594.80	32198.80	2.60	88.10	4.48	4.39	80.45	148.03
LF-1MW18C	19594.80	32198.80	23.50	91.60	4.52	4.51	90.83	167.13
LF-1MW20A	18194.00	31331.00	-4.90	153.00	5.03	4.22	67.75	124.66
LF-1MW20B	18194.00	31331.00	10.70	25.00	3.22	4.36	78.44	144.34
LF-1MW20C	18194.00	31331.00	44.70	306.00	5.72	4.66	105.70	194.48
LF-1MW20Z	18194.00	31331.00	-39.60	9.00	2.20	3.65	38.58	70.99
LF-1MW24A	13644.00	29371.00	-41.10	316.00	5.76	3.82	45.54	83.80
LF-1MW24B	13644.00	29371.00	13.60	183.00	5.21	4.26	70.48	129.68
LF-1MW25	13031.50	26641.00	33.60	5.10	1.63	3.72	41.34	76.06
LF-1MW25A	13031.50	26641.00	-107.20	33.00	3.50	2.53	12.61	23.21
LF-1MW26	12883.80	27640.00	-37.40	7.00	1.95	3.54	34.56	63.59
LF-1MW26B	12883.80	27640.00	-97.80	6.50	1.87	2.57	13.00	23.93
LF-1MW27	11212.30	25596.00	-50.90	18.00	2.89	3.21	24.66	45.38
LF-1MW28A	11144.00	26821.00	-47.40	10.00	2.30	3.23	25.30	46.54

Appendix C: Gaussian Filtered Slug Data Values								
Page 2 of 2							Feet/day	
	Coordinates			Feet/day		FILTERED	FILTERED	Calculated
Well ID	X	Y	Z	SLUG	LN SLUG	LN SLUG	SLUG	K_x
LF-1MW28B	11144.00	26821.00	-17.40	17.00	2.83	3.59	36.16	66.53
LF-1MW31A	16233.20	30041.00	-63.60	5.60	1.72	3.30	26.99	49.66
LF-1MW31B	16233.20	30041.00	-17.00	23.80	3.17	4.00	54.76	100.76
LF-1MW31C	16233.20	30041.00	37.70	89.80	4.50	4.54	93.84	172.66
LF-1MW33	12683.80	31017.20	-9.50	157.00	5.06	4.15	63.33	116.52
LF-1MW34	13237.20	33168.10	-40.70	8.10	2.09	3.34	28.25	51.99
LF-1MW35	9570.10	29579.70	-34.70	74.60	4.31	3.22	24.96	45.92
LF-1MW36B	9179.30	27774.10	-4.40	24.90	3.21	3.55	34.67	63.80
LF-1MW37A	9204.10	30573.80	-33.10	3.80	1.34	3.20	24.41	44.92
LF-1MW38A	6630.80	26502.50	-62.80	46.40	3.84	2.99	19.89	36.60
LF-1MW38Z	6630.80	26502.50	-90.30	107.00	4.67	2.61	13.62	25.07
LF-1MW39A	6643.80	28089.20	-42.00	2.30	0.83	3.11	22.33	41.08
LF-1MW40	7013.00	29187.90	-56.10	96.80	4.57	3.06	21.28	39.15
LF-1MW40A	7013.00	29187.90	-92.70	3.80	1.34	2.49	12.07	22.20
LF-1MW41	7213.50	30137.50	-69.00	25.20	3.23	3.05	21.12	38.86
LF-1MW43	9384.70	25668.50	-24.70	66.00	4.19	3.59	36.14	66.50
LF-1MW44	6143.60	25139.70	-101.00	17.40	2.86	2.58	13.16	24.21
LF-1MW45	6269.50	27054.40	-103.00	7.00	1.95	2.38	10.83	19.92
LF-1MW46	5462.30	26383.40	-48.00	10.20	2.32	3.13	22.79	41.93
LF-1MW46A	5462.30	26383.40	-102.90	4.30	1.46	2.49	12.10	22.27
LF-1MW47	6292.40	25954.70	-21.60	192.00	5.26	3.46	31.93	58.76
LF-1MW50A	3545.50	26233.00	-75.00	22.40	3.11	3.10	22.21	40.87
LF-1MW50B	3545.50	26233.00	-137.90	2.60	0.96	1.66	5.25	9.67
LF-1MW51	3273.00	24761.20	-97.10	39.70	3.68	2.96	19.33	35.57
LF-1MW52	4244.60	27518.10	-127.70	1.60	0.47	1.88	6.56	12.07
LF-1MW53	4682.20	28971.40	-102.30	206.00	5.33	2.54	12.67	23.32
LF-1MW54	4898.40	29754.20	-107.60	3.50	1.25	2.44	11.46	21.09
LF-1MW601A	11158.00	25939.00	-25.60	80.40	4.39	3.53	34.11	62.77
LF-1MW601B	11158.00	25939.00	-6.40	55.70	4.02	3.73	41.88	77.07
LF-1MW601C	11158.00	25939.00	9.10	101.00	4.62	3.84	46.46	85.49
LF-1MW601D	11158.00	25939.00	32.20	194.00	5.27	3.80	44.90	82.61
LF-1MW601E	11158.00	25939.00	54.70	16.00	2.77	3.60	36.47	67.11
LF-1MW701A	15288.10	31331.20	-31.80	70.90	4.26	3.82	45.49	83.71
LF-1WT25	13229.30	33182.60	58.40	156.40	5.05	4.99	147.66	271.69
These figures include		**Mean**		74.74	3.50	3.53	46.15	84.91
values from pages 1		**Maximum**		316.00	5.76	4.99	147.66	271.69
and 2		**Geometric Mean**		33.04			34.25	63.02
		Sample Variance		5501.69	2.76	1.09	911.75	3086.80
Variance between LN K and Filtered LN K				1.223		**ANISOTROPY**	3.396	
Multiply the filtered K values by EXP(variance/2) = 1.84 to get K_x								

Appendix D. Hydraulic Conductivity Database

Appendix D. HYDRAULIC CONDUCTIVITY DATABASE									
		10%	50%	90%					Y
	Elevation	Passing	Passing	Passing	Hazen	Delta Y	Delta X	Slope	intercept
Well No.	(ft. msl)	(mm)	(mm)	(mm)	(ft./day	(%)	(mm)	(DY/DX)	
HG-1	103	0.00	0.02	0.10	0.01	40.00	0.01	3100.78	3.49
GB-7	93	0.18	0.70	9.20	91.85	40.00	0.52	76.92	-3.85
	83	0.12	0.60	9.20	40.82	40.00	0.48	83.33	0.00
	73	0.24	10.00	20.70	163.30	40.00	9.76	4.10	9.02
	63	0.30	4.90	16.00	255.15	40.00	4.60	8.70	7.39
	53	0.25	0.73	4.90	177.19	40.00	0.48	83.33	-10.83
	43	0.13	0.34	0.80	47.91	40.00	0.21	190.48	-14.76
	38	0.16	0.58	2.40	72.58	40.00	0.42	95.24	-5.24
	33	0.13	0.44	1.50	47.91	40.00	0.31	129.03	-6.77
	28	0.26	0.52	1.30	191.65	40.00	0.26	153.85	-30.00
	23	0.13	0.34	1.00	47.91	40.00	0.21	190.48	-14.76
	18	0.11	0.20	0.38	34.30	40.00	0.09	444.44	-38.89
	13	0.22	0.57	1.90	137.21	40.00	0.35	114.29	-15.14
	8	0.18	0.54	5.50	91.85	40.00	0.36	111.11	-10.00
	3	0.04	0.14	0.28	4.54	40.00	0.10	400.00	-6.00
	-2	0.11	0.26	0.80	34.30	40.00	0.15	266.67	-19.33
	-7	0.11	0.23	0.71	34.30	40.00	0.12	333.33	-26.67
HG-1	-10	0.00	0.47	1.60	0.05	40.00	0.47	85.84	9.66
GB-8	-14	0.50	1.70	7.80	708.75	40.00	1.20	33.33	-6.67
W-64A,	-35	0.30	0.60	1.90	255.15	40.00	0.30	133.33	-30.00
	-85	0.13	0.57	1.70	47.91	40.00	0.44	90.91	-1.82
	-125	0.01	0.02	0.10	0.08	40.00	0.02	2272.73	-2.27
	-145	0.13	0.42	0.80	47.91	40.00	0.29	137.93	-7.93
	-150	0.00	0.23	2.30	0.05	40.00	0.23	176.99	9.29
LF-1	50	0.27	0.63	5.60	206.67	40.00	0.36	111.11	-20.00
GB-9	45	0.28	0.62	1.90	222.26	40.00	0.34	117.65	-22.94
MW-31	40	0.27	0.60	1.70	206.67	40.00	0.33	121.21	-22.73
	35	0.23	0.71	3.00	149.97	40.00	0.48	83.33	-9.17
	30	0.26	0.62	3.00	191.65	40.00	0.36	111.11	-18.89
	25	0.24	0.66	4.30	163.30	40.00	0.42	95.24	-12.86
	20	0.26	0.52	1.40	191.65	40.00	0.26	153.85	-30.00
	15	0.27	0.52	1.50	206.67	40.00	0.25	160.00	-33.20
	10	0.17	0.49	1.80	81.93	40.00	0.32	125.00	-11.25
	0	0.12	0.36	1.20	40.82	40.00	0.24	166.67	-10.00
	-30	0.00	0.21	0.80	0.05	40.00	0.21	194.17	9.22
	-75	0.00	0.20	0.96	0.01	40.00	0.20	202.33	9.53
LF-1	3	0.16	0.63	10.00	72.58	40.00	0.47	85.11	-3.62
GB-16	-27	0.16	0.50	2.80	72.58	40.00	0.34	117.65	-8.82
MW-25	-57	0.06	0.30	0.80	10.90	40.00	0.24	168.07	-0.42
	-90	0.02	0.18	0.58	1.63	40.00	0.16	256.41	3.85
	-125	0.01	0.13	0.37	0.24	40.00	0.12	331.13	6.95
	-145	0.02	0.17	7.20	1.50	40.00	0.15	272.11	3.74

Appendix D. Hydraulic Conductivity Database

Appendix D. HYDRAULIC CONDUCTIVITY DATABASE									
		10%	50%	90%					Y
	Elevation	Passing	Passing	Passing	Hazen	Delta Y	Delta X	Slope	intercept
Well No.	(ft. msl)	(mm)	(mm)	(mm)	(ft./day	(%)	(mm)	(DY/DX)	
LF-1	54	0.21	0.60	9.30	125.02	40.00	0.39	102.56	-11.54
GB-17	34	0.24	0.54	1.90	163.30	40.00	0.30	133.33	-22.00
WT-24	4	0.01	0.40	1.70	0.07	40.00	0.40	101.27	9.49
	-26	0.13	0.39	1.20	47.91	40.00	0.26	153.85	-10.00
	-46	0.09	0.19	0.50	22.96	40.00	0.10	400.00	-26.00
	-81	0.00	0.13	0.50	0.01	40.00	0.13	312.74	9.34
LF-1	29	0.01	0.08	0.20	0.11	40.00	0.07	541.27	6.70
GB-20	-21	0.09	0.42	3.20	21.46	40.00	0.33	120.12	-0.45
MW-41	-61	0.13	1.00	4.30	47.91	40.00	0.87	45.98	4.02
	-101	0.01	0.14	0.24	0.48	40.00	0.13	314.96	5.91
LF-1	-9	0.11	0.32		34.30	40.00	0.21	190.48	-10.95
GB-21	-14	0.08	0.23		19.06	40.00	0.15	270.27	-12.16
	-42	0.11	0.28		34.30	40.00	0.17	235.29	-15.88
	-52	0.11	0.22		34.30	40.00	0.11	363.64	-30.00
	-62	0.01	0.43		0.07	40.00	0.43	94.12	9.53
	-72	0.03	0.63		1.92	40.00	0.60	66.23	8.28
	-82	0.03	1.10		2.38	40.00	1.07	37.35	8.92
	-92	0.05	0.41		7.09	40.00	0.36	111.11	4.44
	-102	0.19	0.63		102.34	40.00	0.44	90.91	-7.27
LF-1	158	0.01	0.34		0.34	40.00	0.33	121.58	8.66
GB-22	138	0.01	0.13		0.34	40.00	0.12	336.13	6.30
	128	0.00	0.02		0.01	40.00	0.01	2721.09	3.74
	98	0.05	0.43		7.37	40.00	0.38	105.54	4.62
	48	0.05	0.39		7.67	40.00	0.34	118.34	3.85
	18	0.08	0.23		18.14	40.00	0.15	266.67	-11.33
	0	0.02	0.20		1.63	40.00	0.18	227.27	4.55
	-72	0.04	0.16		5.00	40.00	0.12	338.98	-4.24
	-112	0.11	0.49		34.30	40.00	0.38	105.26	-1.58
	-122	0.02	1.70		1.13	40.00	1.68	23.81	9.52
LF-1	102	0.01	0.45		0.41	40.00	0.44	91.32	8.90
MW-26B	97	0.07	0.45		15.11	40.00	0.38	106.10	2.25
	77	0.14	0.73		55.57	40.00	0.59	67.80	0.51
	42	0.13	1.00		47.91	40.00	0.87	45.98	4.02
	7	0.15	0.39		63.79	40.00	0.24	166.67	-15.00
	-48	0.00	0.24		0.00	40.00	0.24	167.57	9.78
	-58	0.07	0.53		13.89	40.00	0.46	86.96	3.91
	-63	0.01	0.30		0.41	40.00	0.29	138.89	8.33
	-93	0.01	0.42		0.25	40.00	0.41	97.39	9.09
	-98	0.12	0.43		40.82	40.00	0.31	129.03	-5.48

Appendix D. Hydraulic Conductivity Database

Appendix D. HYDRAULIC CONDUCTIVITY DATABASE									
		10%	50%	90%					Y
	Elevation	Passing	Passing	Passing	Hazen	Delta Y	Delta X	Slope	intercept
Well No.	(ft. msl)	(mm)	(mm)	(mm)	(ft./day	(%)	(mm)	(DY/DX)	
LF-1	54	0.23	0.61		149.97	40.00	0.38	105.26	-14.21
WT-28	39	0.14	0.47		55.57	40.00	0.33	121.21	-6.97
	29	0.14	0.47		55.57	40.00	0.33	121.21	-6.97
	19	0.03	0.40		1.77	40.00	0.38	106.67	7.33
	9	0.16	0.50		72.58	40.00	0.34	117.65	-8.82
	4	0.24	0.70		163.30	40.00	0.46	86.96	-10.87
	-1	0.11	0.36		31.26	40.00	0.26	156.86	-6.47
	-3	0.09	0.36		22.96	40.00	0.27	148.15	-3.33
	-5	0.01	0.38		0.48	40.00	0.37	108.99	8.58
	-16	0.05	0.46		7.09	40.00	0.41	97.56	5.12
	-26	0.16	0.46		72.58	40.00	0.30	133.33	-11.33
	-36	0.12	0.42		40.82	40.00	0.30	133.33	-6.00
	-46	0.11	0.32		33.07	40.00	0.21	188.68	-10.38
	-66	0.31	0.70		272.44	40.00	0.39	102.56	-21.79
	-76	0.11	0.48		34.30	40.00	0.37	108.11	-1.89
LF-1	62	0.01	0.05		0.15	40.00	0.04	894.85	3.47
MW-38B	32	0.02	0.35		1.63	40.00	0.33	122.70	7.06
	22	0.01	0.11		0.14	40.00	0.10	388.35	7.28
	12	0.04	0.50		3.47	40.00	0.47	86.02	6.99
	-18	0.02	0.31		0.82	40.00	0.29	136.52	7.68
	-28	0.02	0.39		0.64	40.00	0.38	106.67	8.40
	-48	0.03	0.32		2.38	40.00	0.29	137.46	6.01
	-58	0.11	0.59		34.30	40.00	0.48	83.33	0.83
	-73	0.03	0.47		1.92	40.00	0.44	90.09	7.66
	-93	0.01	0.29		0.19	40.00	0.28	141.94	8.84
LF-1	-39.5	0.09	0.31		25.05	40.00	0.22	185.19	-7.41
MW-39B									
LF-1	1.1	0.02	0.27		1.37	40.00	0.25	161.29	6.45
MW-46A	-48.9	0.01	0.37		0.48	40.00	0.36	112.04	8.54
	-53.9	0.12	0.52		40.82	40.00	0.40	100.00	-2.00
	-63.9	0.00	0.20		0.00	40.00	0.20	201.11	9.78
	-78.9	0.00	0.00		0.00	40.00	0.00	23529.41	-4.12
	-88.9	0.20	0.77		113.40	40.00	0.57	70.18	-4.04
	-98.9	0.11	1.10		34.30	40.00	0.99	40.40	5.56
	-103.9	0.13	1.70		47.91	40.00	1.57	25.48	6.69
	-118.9	0.12	0.43		40.82	40.00	0.31	129.03	-5.48
	-126.9	0.00	1.50		0.05	40.00	1.50	26.74	9.89
LF-1	-56.6	0.00	0.00		0.00	40.00	0.00	13333.33	-6.00
MW-47									
LF-1	11.6	0.02	0.22		1.63	40.00	0.20	204.08	5.10

Appendix D. Hydraulic Conductivity Database

Appendix D. HYDRAULIC CONDUCTIVITY DATABASE									
		10%	50%	90%					Y
	Elevation	Passing	Passing	Passing	Hazen	Delta Y	Delta X	Slope	intercept
Well No.	(ft. msl)	(mm)	(mm)	(mm)	(ft./day	(%)	(mm)	(DY/DX)	
MW-50B	-8.4	0.23	0.54		149.97	40.00	0.31	129.03	-19.68
	-18.4	0.01	0.03		0.10	40.00	0.02	1666.67	0.00
	-38.4	0.01	0.16		0.34	40.00	0.15	268.46	7.05
	-48.4	0.01	0.20		0.48	40.00	0.19	213.90	7.22
	-88.4	0.02	0.26		0.64	40.00	0.25	163.27	7.55
	-98.4	0.00	0.03		0.01	40.00	0.03	1351.35	8.11
	-108.4	0.04	0.49		5.00	40.00	0.45	89.29	6.25
	-118.4	0.05	1.00		7.09	40.00	0.95	42.11	7.89
	-138.4	0.03	1.25		2.55	40.00	1.22	32.79	9.02
LF-1	-110.2	0.02	0.79		0.82	40.00	0.77	51.75	9.12
MW-53									
HG-2	12.5	0.01	0.82		0.41	40.00	0.81	49.50	9.41
MW-565	-17.5	0.36	0.62		367.42	40.00	0.26	153.85	-45.38
	-37.5	0.12	0.31		40.82	40.00	0.19	210.53	-15.26
	-57.5	0.09	0.25		22.96	40.00	0.16	250.00	-12.50
HG-1	0.3	0.11	0.30		34.30	40.00	0.19	210.53	-13.16
MW-567	-29.7	0.08	0.36		18.14	40.00	0.28	142.86	-1.43
	-39.7	0.01	0.30		0.48	40.00	0.29	139.37	8.19
HG-1	20.4	0.12	0.60		40.82	40.00	0.48	83.33	0.00
MW-567B									
HG-1	-49	0.00	19.00		0.03	40.00	19.00	2.11	9.99
MW-567	-51	0.22	1.00		137.21	40.00	0.78	51.28	-1.28
	-62	0.03	0.38		2.90	40.00	0.35	114.94	6.32
	-72	0.03	0.70		1.77	40.00	0.68	59.26	8.52
	-90	0.02	0.51		1.37	40.00	0.49	81.97	8.20
	-110	0.11	0.78		34.30	40.00	0.67	59.70	3.43
	-114	0.03	0.80		2.22	40.00	0.77	51.81	8.55
	-124	0.02	0.23		0.73	40.00	0.21	186.92	7.01
	-129	0.02	0.39		0.82	40.00	0.37	107.24	8.18
	-139	0.11	0.73		34.30	40.00	0.62	64.52	2.90
HG-1	10.6	0.08	0.20		18.14	40.00	0.12	333.33	-16.67
MW-568	-9.4	0.22	0.59		137.21	40.00	0.37	108.11	-13.78
HG-1	16.3	0.12	0.41		40.82	40.00	0.29	137.93	-6.55
MW-569	-23.7	0.09	0.43		22.96	40.00	0.34	117.65	-0.59
	-53.7	0.12	0.35		40.82	40.00	0.23	173.91	-10.87
	-83.7	0.08	0.27		18.14	40.00	0.19	210.53	-6.84

Appendix D. Hydraulic Conductivity Database

Appen						
	X	This report	CDM Fed			
	intercept	Sen (calc.)	Sen	Bedinger	Top	Slug
Well No.		(ft./day)	(ft./day)	(ft./day)	of Screen	(ft./day)
HG-1	0.00	0.00	0.00	6.00		
GB-7	0.05	16.93	16.93	131.02		
	0.00	0.61	0.61	96.26		
	-2.20	16317.97	253.93	26737.97		
	-0.85	2304.11	56.41	6419.79		
	0.13	86.00	86.00	142.49		
	0.08	29.21	29.21	30.91		
	0.06	18.30	18.30	89.95		
	0.05	15.48	15.48	51.76		
	0.20	173.17	173.17	72.30		
	0.08	29.21	29.21	30.91		
	0.09	34.36	34.36	10.70		
	0.13	85.10	85.10	86.87		
	0.09	41.80	41.80	77.97		
	0.02	1.31	1.31	5.24		
	0.07	24.80	24.80	18.07		
	0.08	29.38	29.38	14.14		
HG-1	-0.11	43.38	0.58	59.06		
GB-8	0.20	225.62	225.62	772.73		
W-64A,	0.23	230.55	230.55	96.26	-29.00	70.50
	0.02	4.10	4.10	86.87	-80.00	97.00
	0.00	0.01	0.01	0.14		
	0.06	17.88	17.88	47.17	-138.00	5.00
	-0.05	9.36	0.14	14.14		
LF-1	0.18	152.35	152.35	106.12		
GB-9	0.20	176.63	176.63	102.78		
MW-31	0.19	163.43	163.43	96.26		
	0.11	63.48	63.48	134.79	38.00	89.80
	0.17	136.66	136.66	102.78		
	0.14	90.29	90.29	116.47		
	0.20	173.17	173.17	72.30		
	0.21	194.87	194.87	72.30		
	0.09	40.96	40.96	64.20		
	0.06	18.58	18.58	34.65		
	-0.05	7.65	0.11	11.79		
	-0.05	7.59	0.10	10.70		
LF-1	0.04	12.55	12.55	106.12		
GB-16	0.08	29.74	29.74	66.84		
MW-25	0.00	0.30	0.30	24.06		
	-0.02	0.53	0.06	8.66	-84.00	5.10
	-0.02	1.38	0.04	4.52		
	-0.01	0.43	0.06	7.73		

Appendix D. Hydraulic Conductivity Database

Appen						
	X	This report	CDM Fed			
	intercept	Sen (calc.)	Sen	Bedinger	Top	Slug
Well No.		(ft./day)	(ft./day)	(ft./day)	of Screen	(ft./day)
LF-1	0.11	63.74	63.74	96.26		
GB-17	0.17	126.91	126.91	77.97		
WT-24	-0.09	30.00	0.42	42.78		
	0.07	21.80	21.80	40.67		
	0.07	19.43	19.43	9.65		
	-0.03	3.04	0.04	4.52		
LF-1	-0.01	0.47	0.01	1.71		
GB-20	0.00	0.62	0.62	47.17		
MW-41	-0.09	18.44	2.02	267.38		
	-0.02	1.03	0.04	5.24		
LF-1	0.06	16.79	16.79	27.38		
GB-21	0.05	10.12	10.12	14.14		
	0.07	21.96	21.96	20.96		
	0.08	31.00	31.00	12.94		
	-0.10	35.03	0.48	49.44		
	-0.13	51.51	0.97	106.12		
	-0.24	191.65	3.06	323.53		
	-0.04	4.10	0.35	44.95		
	0.08	35.32	35.32	106.12		
LF-1	-0.07	16.94	0.29	30.91		
GB-22	-0.02	1.06	0.04	4.52		
	0.00	0.00	0.00	0.08		
	-0.04	5.01	0.38	49.44		
	-0.03	2.47	0.30	40.67		
	0.04	9.12	9.12	14.14		
	-0.02	1.04	0.08	10.70		
	0.01	1.02	1.02	6.84		
	0.02	2.56	2.56	64.20	-109.00	0.20
	-0.40	546.63	7.52	772.73		
LF-1	-0.10	31.95	0.51	54.14		
MW-26B	-0.02	0.60	0.38	54.14		
	-0.01	0.22	0.93	142.49		
	-0.09	18.44	2.02	267.38		
	0.09	39.31	39.31	40.67		
	-0.06	11.71	0.15	15.40		
	-0.05	4.79	0.56	75.11		
	-0.06	11.89	0.22	24.06		
	-0.09	29.46	0.45	47.17		
	0.04	10.77	10.77	49.44	-98.00	6.50

Appendix D. Hydraulic Conductivity Database

Appen						
	X	This report	CDM Fed			
	intercept	Sen (calc.)	Sen	Bedinger	Top	Slug
Well No.		(ft./day)	(ft./day)	(ft./day)	of Screen	(ft./day)
LF-1	0.14	89.06	89.06	99.49		
WT-28	0.06	18.44	18.44	59.06		
	0.06	18.44	18.44	59.06		
	-0.07	15.04	0.37	42.78		
	0.08	29.74	29.74	66.84		
	0.13	79.47	79.47	131.02		
	0.04	9.67	9.67	34.65		
	0.02	3.65	3.65	34.65		
	-0.08	20.65	0.36	38.61		
	-0.05	7.61	0.45	56.58		
	0.09	36.49	36.49	56.58		
	0.05	11.76	11.76	47.17		
	0.06	15.51	15.51	27.38		
	0.21	210.67	210.67	131.02		
	0.02	3.05	3.05	61.60		
LF-1	0.00	0.03	0.01	0.72		
MW-38B	-0.06	10.39	0.28	32.75		
	-0.02	1.12	0.03	3.24		
	-0.08	20.68	0.58	66.84		
	-0.06	10.21	0.23	25.70		
	-0.08	20.53	0.37	40.67		
	-0.04	5.67	0.23	27.38		
	-0.01	0.02	0.61	93.07		
	-0.09	23.29	0.53	59.06		
	-0.06	13.00	0.21	22.49	-90.00	107.00
LF-1	0.04	8.79	8.79	25.70	-42.00	2.30
MW-39B						
LF-1	-0.04	4.87	0.16	19.49		
MW-46A	-0.08	19.33	0.34	36.60	-48.00	10.20
	0.02	3.84	3.84	72.30		
	-0.05	8.13	0.11	10.70		
	0.00	0.00	0.00	0.00		
	0.06	21.96	21.96	158.53		
	-0.14	54.22	2.61	323.53		
	-0.26	212.57	6.57	772.73	-103.00	4.30
	0.04	10.77	10.77	49.44		
	-0.37	471.82	5.97	601.60		
LF-1	0.00	0.00	0.00	0.00		
MW-47						
LF-1	-0.03	1.72	0.10	12.94		

Appendix D. Hydraulic Conductivity Database

Appen						
	X	This report	CDM Fed			
	intercept	Sen (calc.)	Sen	Bedinger	Top	Slug
Well No.		(ft./day)	(ft./day)	(ft./day)	of Screen	(ft./day)
MW-50B	0.15	109.53	109.53	77.97		
	0.00	0.00	0.00	0.24		
	-0.03	2.16	0.06	6.84		
	-0.03	3.61	0.09	10.70		
	-0.05	6.87	0.16	18.07		
	-0.01	0.12	0.00	0.26		
	-0.07	14.75	0.54	64.20		
	-0.19	114.36	2.41	267.38		
	-0.28	254.97	3.97	417.78	-138.00	2.60
LF-1	-0.18	105.03	1.59	166.87	-102.00	206.00
MW-53						
HG-2	-0.19	122.97	1.74	179.79		
MW-565	0.30	387.71	387.71	102.78		
	0.07	25.45	25.45	25.70	-32.00	101.00
	0.05	12.44	12.44	16.71		
HG-1	0.06	19.29	19.29	24.06	2.00	27.90
MW-567	0.01	1.23	1.23	34.65		
	-0.06	11.35	0.22	24.06	-39.00	4.20
HG-1	0.00	0.61	0.61	96.26	-19.00	122.70
MW-567B						
HG-1	-4.75	77813.26	NA	96524.06		
MW-567	0.02	8.45	8.45	267.38		
	-0.06	9.14	0.32	38.61		
	-0.14	68.66	1.21	131.02		
	-0.10	32.88	0.63	69.55		
	-0.06	7.08	1.20	162.67		
	-0.17	90.54	1.59	171.12		
	-0.04	4.41	0.12	14.14		
	-0.08	19.10	0.37	40.67		
	-0.05	3.71	1.02	142.49		
HG-1	0.05	11.98	11.98	10.70	12.00	25.10
MW-568	0.13	79.76	79.76	93.07	-8.00	249.00
HG-1	0.05	12.78	12.78	44.95	25.00	152.00
MW-569	0.01	0.78	0.78	49.44	-23.00	130.00
	0.06	19.87	19.87	32.75	-48.00	83.90
	0.03	5.92	5.92	19.49	-76.00	84.70

Appendix E. Alyamani/Sen Analysis for Formula Parameters

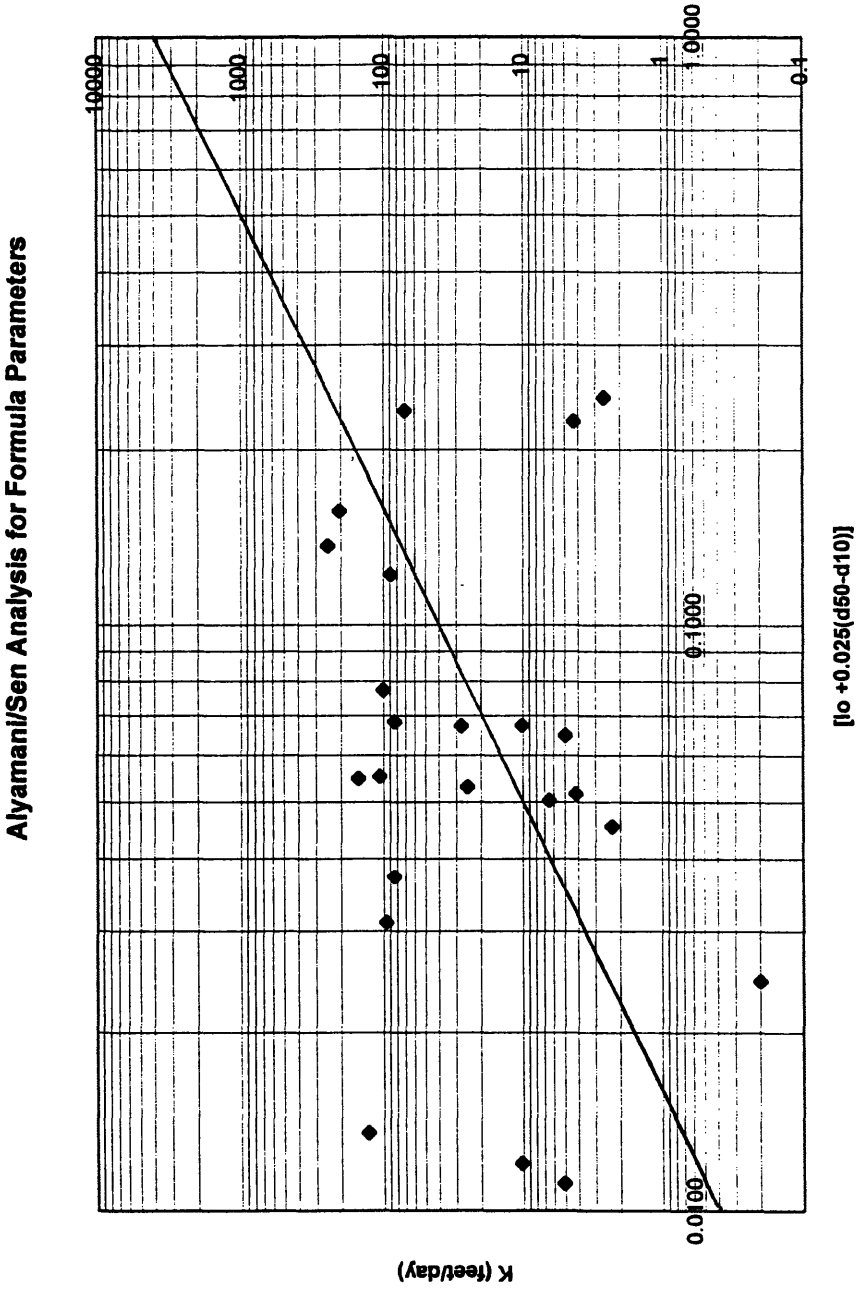

Appendix F. Team Report Results: An Investigation of Environmental Impacts of the Main Base Landfill Groundwater Plume, Massachusetts Military Reservation, Cape Cod, MA

Groundwater Modeling and Particle Tracking Simulation

This section of the report describes a three dimensional groundwater model and particle tracking simulation of the portion of the aquifer that is deemed to affect the spatial characteristics and migration pathlines of the LF-1 plume. The DYN System modeling package developed by CDM, Inc., is utilized for this purpose. The goals of the modeling effort are as follows,

I. Develop a steady state flow model for the study area.

II. Track particles released from a continuous source area and observe migration patterns.

III. Determine flushing time and plume migration with source removed.

IV. Determine sensitivity of model results (plume migration) to the Buzzards Bay Moraine and other geologic features and characteristics of the region.

V. Explore the possibility that the deep plume observed in advance of the main plume is caused by a pool of dense leachate from the landfill sinking below the source area.

DYNFLOW, DYNTRACK and DYNPLOT Systems

The groundwater flow system of the Western Cape is modeled with the DYNFLOW groundwater modeling package. DYNFLOW is a FORTRAN based program that simulates three-dimensional flow using a finite element formulation. A distinct advantage of the finite element based model over a finite difference model like MODFLOW is that the former allows

the user the flexibility to use variable sized grid elements. Thus, in regions of interest, the user can obtain higher resolution without having to implement the same degree of resolution throughout the model and obtain significant advantages in terms of computational time and complexity.

DYNTRACK simulates three-dimensional contaminant mass transport and uses the same finite element grid, flow field and aquifer properties that were used in and derived from DYNFLOW. DYNTRACK models either single particle tracking or 3-d transport of conservative or first-order decay contaminants with or without adsorption and dispersion.

DYNPLOT is a graphical pre- and post-processor that can create full color displays in plan view or cross-section of observed data, DYN system calculated data and simulated results. DYNPLOT is also capable of generating the finite element grid used by the flow and tracking models.

Study Area and Grid

The roughly triangular study area of the model was chosen to be large enough to ensure that boundary effects did not unduly influence the calculated flow and head values in the area of concern. The study area, approximately 58 square miles in extent, is depicted in Figure 3-4. The northern and eastern boundaries of the model are streamlines (no-flux boundaries). The western part of the grid area is bounded by the ocean. The ocean-aquifer interface is of particular interest because it determines how far out at sea the LF-1 plume will discharge if it is not completely contained.

The grid covering the LF-1 study area was generated in DYNPLOT, with smaller grid elements in the sources area and presently observed plume locations and progressively coarser grid elements moving away from these locations. The study grid is composed of 3156 triangular elements and 1652 nodes. The grid discretizes the vertical dimension of the study area in 8 layers (9 levels). The bottom (1st) level follows the bedrock contours, while the top (9th) level approximates the surface topography.

Model Formulation

Assigned Geologic Materials

The geologic structure of the LF-1 study area was represented as depicted in Figures 3-5, 3-6, 3-7 and 3-8. The geographic locations of the material were assigned according to USGS maps of the region. The Mashpee Pitted Plain (MPP) was represented vertically as two material types and two horizontal sections. This was done to accurately represent the upward coarsening and north-south fining that is observed (LeBlanc, 1986) The Buzzards Bay Moraine (BBM) was defined vertically as four different material of increasing permeability upwards and two horizontal divisions. The Buzzards Bay Outwash (BBO) was depicted by two vertical materials, coarsening upwards. All three deposit types were underlain by a layer of Glacio-Lacustrine deposits (GLS) of varying thickness and bedrock.

Source

The LF-1 source was represented by six distinct cells within the source area. In the particle tracking simulation, three cells were defined as being non-sources after 1994. This was done to simulate a successful capping of part of the landfill in 1994 by the IRP.

Ponds

Ponds were modeled as a layer of material that was almost infinitely permeable horizontally and with a high vertical conductivity of the order of 500 ft/day. The pond material layer was extended to the observed depth of the each pond. These pond nodes were then assigned a rising head boundary condition. With this method, the material defined as the pond displays a consistent horizontal head and acts as a sink for groundwater upgradient of the pond and a source of groundwater to sections of the grid downgradient. This formulation was considered to most closely approximate the behavior of ponds in the Cape Cod region.

Hydraulic Properties

Hydraulic Conductivity

Estimates of hydraulic conductivity for the LF-1 region have been made through field investigations. Many slug tests, and laboratory tests of soil samples have been carried out for the sediments found in the Cape Cod region. The previous section on site characterization carries a full discussion of these empirical findings. For the purposes of the groundwater model, hydraulic conductivities proved to be the parameter to which the flow model was most sensitive. Hydraulic conductivity values of each sediment type were considered a variable input, and were assigned values within an empirically determined range obtained from literature in calibrating the flow model. The final values of hydraulic conductivities assigned to each geologic material are included in Table 3-1.

Material	K_x, K_y ft.day	K_z ft/day	Long. Disp ft.	Trans. Disp ft	Disp Ratio vert./horiz
Lacustrine	15	5	90.0	3.3	0.03
Fine Sand West	80	27	90.0	3.3	0.03
Coarse Sand West	180	60	90.0	3.3	0.03
Fine Sand South	135	45	90.0	3.3	0.03
Coarse Sand South	210	70	90.0	3.3	0.03
BBM Low -North	30	10	90.0	3.3	0.03
BBM Med Low-North	110	33	90.0	3.3	0.03
BBM Med High-North	150	50	90.0	3.3	0.03
BBM High-North	170	57	90.0	3.3	0.03
BBM Low -South	15	5	90.0	3.3	0.03
BBM Med Low-South	60	20	90.0	3.3	0.03
BBM Med High-South	100	33	90.0	3.3	0.03
BBM High-South	135	45	90.0	3.3	0.03
Nant. Ice Deposits	190	63	90.0	3.3	0.03
Pond Material	10^{-5}	10	90.0	3.3	0.03
Fine Sand North	140	47	90.0	3.3	0.03
Coarse Sand North	270	90	90.0	3.3	0.03
Fine Lacustrine	10	3	90.0	3.3	0.03

Table 3-1 Hydraulic Conductivities and Dispersivities used in flow and mass transport models.

Dispersivity

Accurately characterizing the dispersivity at a field site is essential in predicting the transport and spreading of a contaminant plume. Due to natural heterogeneities in the field that cause irregular flow patterns, field-scale dispersivities are several orders of magnitude larger than laboratory scale values (Gelhar et al., 1992). In this model, a tabulation of field-scale dispersivity data is used to obtain suitable values of the dispersivity coefficients while taking into account the scale of the LF-1 source. These values are also included in Table 3-1.

Effective Porosity

Porosity estimates for the outwash in the LF-1 study area range from less than 1% to over 30% (CDM Federal, 1995). These values are somewhat lower than expected from tracer tests of Cape Cod, which range from 38-42% (Masterson and Barlow, 1994). It was decided to use an effective porosity value of 39% throughout the model.

Boundary Conditions

Saltwater-Freshwater Interface

The saltwater-freshwater interface determines where the landfill plume, if not fully contained, will discharge in to Megansett, Red Brook and Squeteague harbors. The steepness and the distance from shore of the interface depends on the aquifer discharge and geologic characteristics of the coastal region. Available geologic information does not indicate the existence of low permeability layers above the aquifer near the shore that will force the salt-fresh interface further into the ocean. Therefore, for the purposes of this report, it is assumed that the location and shape of the salt-fresh interface along the Western Cape Cod shore are determined entirely by the discharge and hydraulic conductivity of the aquifer. The distance from the shore to the salt-fresh interface was calculated to be approximately 500 ft.

No-Flux Boundaries

No-flux boundaries are modeled in DYNFLOW by assigning all nodes on streamlines at the edge of the study area a "free head" boundary condition. It is assumed that the no-flux

boundaries are far enough from the areas of the model we wish to observe that they do not influence the calculated values of head and velocity.

Recharge

Natural recharge is the largest source of replenishment of the West Cape aquifer system. This natural recharge is composed entirely of rainfall infiltrate through the surface layer. Cape Cod on average receives 46 inches of rainfall annually. Nearly half of this precipitation, or 46-50%, infiltrates to the groundwater system through the highly permeable top soil (LeBlanc et al., 1986). There is little or no surface runoff due to the permeable nature of the soils and the small topographic gradients present in this region. Artificial recharge and pumping is considered to be negligible in this region in comparison with the natural recharge.

Results

The calibrated flow model agreed with observed water table measurements at 106 wells within 0.044 ft mean difference and 2.159 ft standard deviation. Figure 3-9 shows the calibrated model results and calculated water table contours. The calculated contours are also consistent with observed water table contours in the region.

The flow model was found to be very sensitive to the difference in permeability between the moraine and surrounding deposits. This sensitivity is highlighted by the curvature of the model calculated head contours, which in turn significantly influence the migration pathlines of a contaminant released at the LF-1 site. The sensitivity of the particle paths to head

contours is enhanced by the fact that the LF-1 source area is located close to the point where north south head contours change to an east-west orientation.

The first particles released at the LF-1 site will migrate to the ocean in 50 years. Figure 3-10 shows a 51 year mass transport simulation in plan view, with particles reaching the ocean interface. Figure 3-11 is a cross section of the simulated plume. Thus, assuming that the volatile organic compounds of concern at this site were released in 1945, the predicted extent of the plume reaches the ocean discharge face by 1996. The initial discharge point is at Red Brook Harbor. This finding is in agreement with the Op-Tech Data Gap Report which concludes that the LF-1 plume has now reached Red Brook Harbor (Op-Tech, 1996).

If the entire landfill is successfully capped by the year 2000, and the contaminated groundwater is allowed to flush unmitigated into the ocean, the DYNTRACK simulation time of 110 additional years is required for all LF-1 derived contaminants in the aquifer to travel beyond the Buzzards Bay Moraine. A further 55 years is required for all the contaminant particles to be discharged from the aquifer.

The predicted plume exhibits the same differential North and South Lobe travel times observed in the field. In the model, the presence of a low-permeability layer in the moraine causes the southern part of the plume to be retarded. The northern section, by virtue of having to travel a shorter distance to the moraine, is at a higher elevation than the southern part of the plume and thus travels through a higher permeability layer of the moraine. These differential travel velocities through the moraine cause the distinct northern and southern lobes observed

in the simulated plume. Figure 3-12 is a north-south cross-section of the plume at the point of entry into the moraine, showing the differential elevations of the particles from north to south.

The previous finding that the portion of the plume at a lower elevation is retarded by the presence of a lower conductivity layer of moraine deposits indicates that the deep plume observed near the shoreline cannot be simulated by a sinking source of contaminant in this model formulation. A tenable explanation for the observed deep northern plume is that the down-sloping bedrock surface near the shoreline causes the faster moving simulated northern lobe to sink further due to infiltration as it traverses the Buzzards Bay Outwash towards the shoreline. Since the slower moving southern lobe is still in the moraine, the leading edges of the northern lobe near Red Brook Harbor now appear to be a northern plume lobe at a lower elevation.

If an extraction well system is constructed along Route 28, and it is assumed that the extraction pumping and infiltration are carried out so that the hydraulic system is relatively unchanged, the uncaptured section of the LF-1 plume will take a further 12 years to completely discharge into the ocean. This result was obtained assuming that the portion of the plume upgradient of the extraction well fence is fully captured.

In summary, the groundwater flow and particle transport model provides results that are similar to field observations. The Buzzards Bay Moraine exerts a great deal of influence on the regional hydrologic system. The geologic characteristics assigned in the flow model to the BBM defines the shape of the regional head contours and thus the travel path and velocity of the simulated plume. Therefore, it is essential that the geology of this moraine be properly

identified if a flow and particle tracking model that can accurately represent the region is to be formulated. In the absence of such data, any groundwater flow model of the LF-1 region will contain a significant degree of uncertainty and error. The models developed in this study can be used to determine the effects of an extraction system to contain or capture the LF-1 plume and also as a means of designing an efficient capture system for this contaminated site. The following section addresses the risks associated with the LF-1 plume and how these risks can be managed.

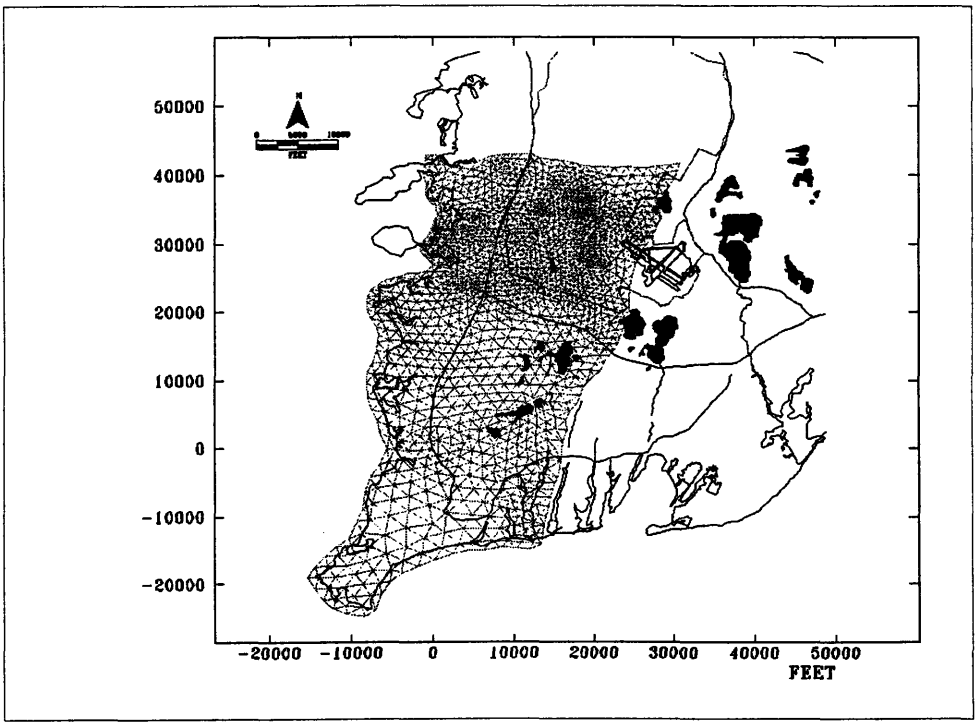

Figure 3-4 LF-1 study area and finite element grid.

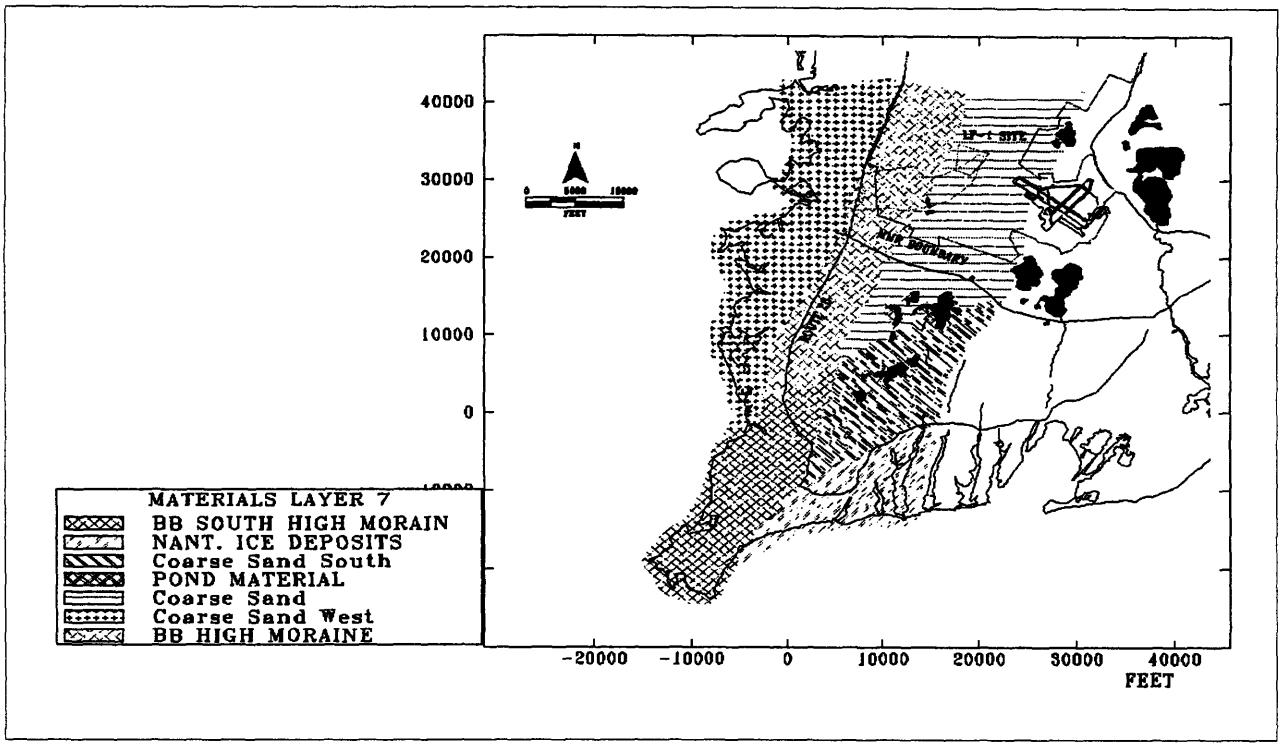

Figure 3-5 Plan view of LF-1 study area with assigned geologic materials.

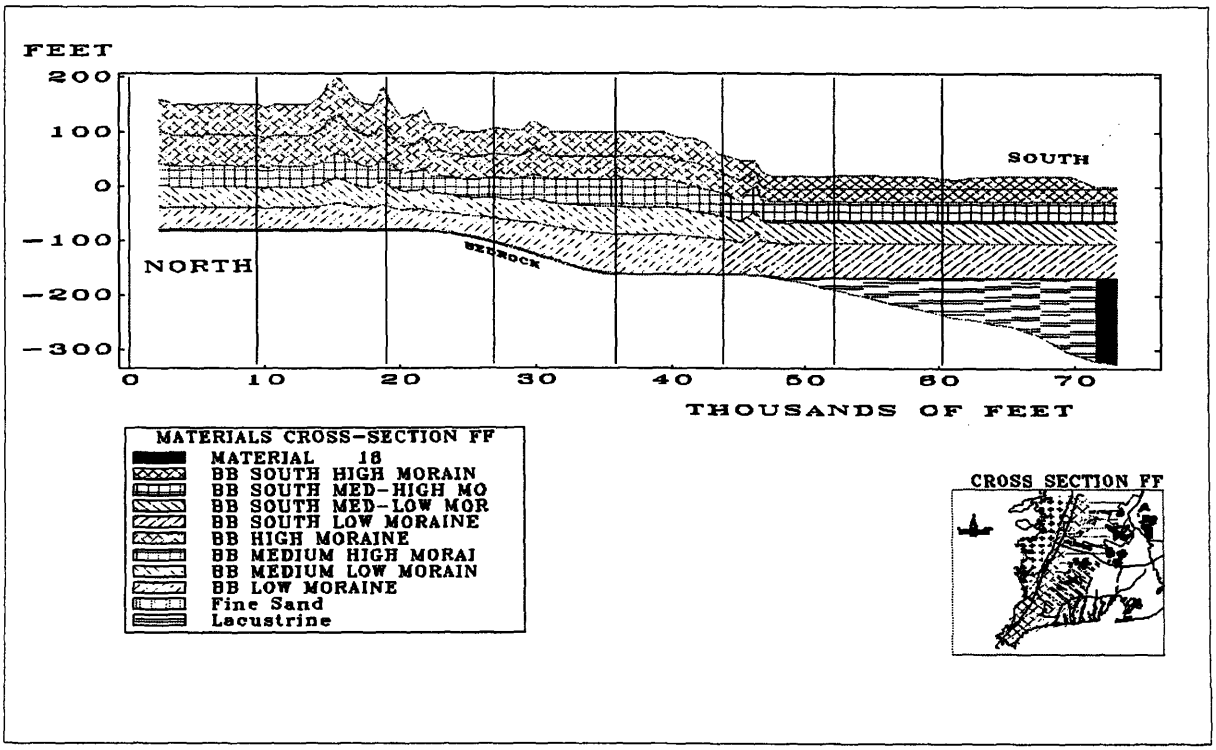

Figure 3-6 Cross-sectional view of Buzzards Bay Moraine deposits.

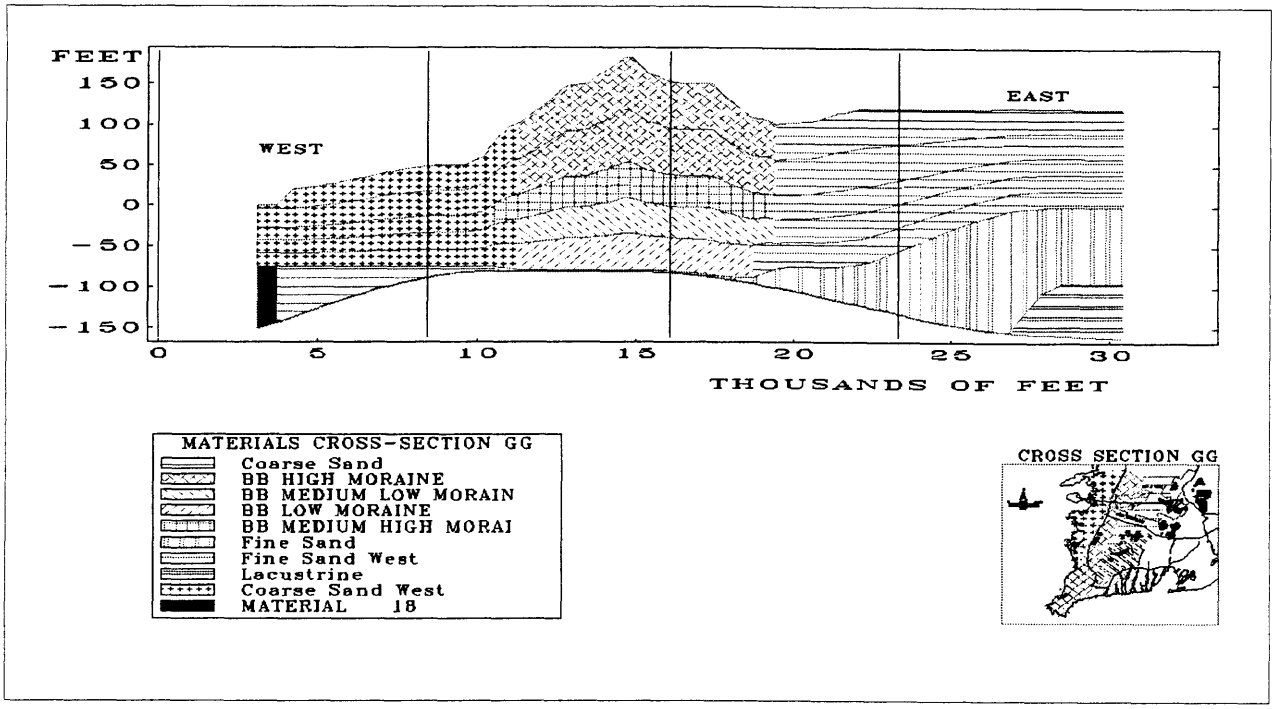

Figure 3-7 East-West cross-section of study area near Buzzards Bay.

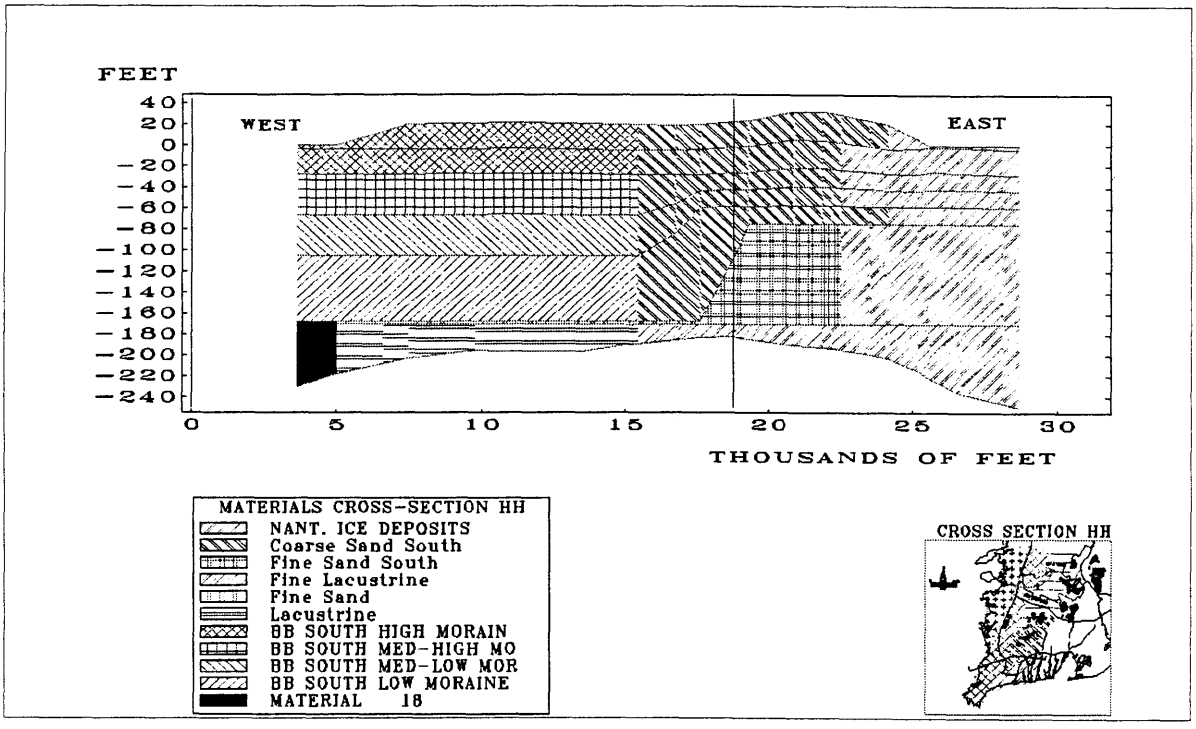

Figure 3-8 East-West cross-section of study area near Nantucket Sound.

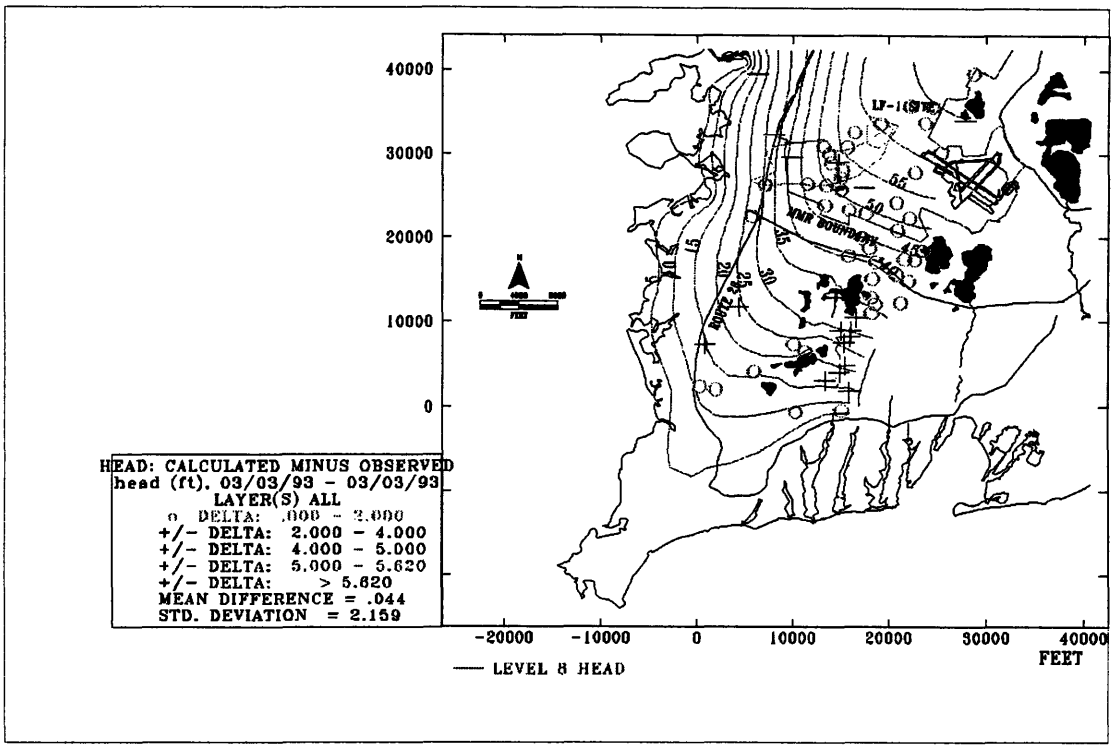

Figure 3-9 Calculated water table elevation contours and flow model calibration results.

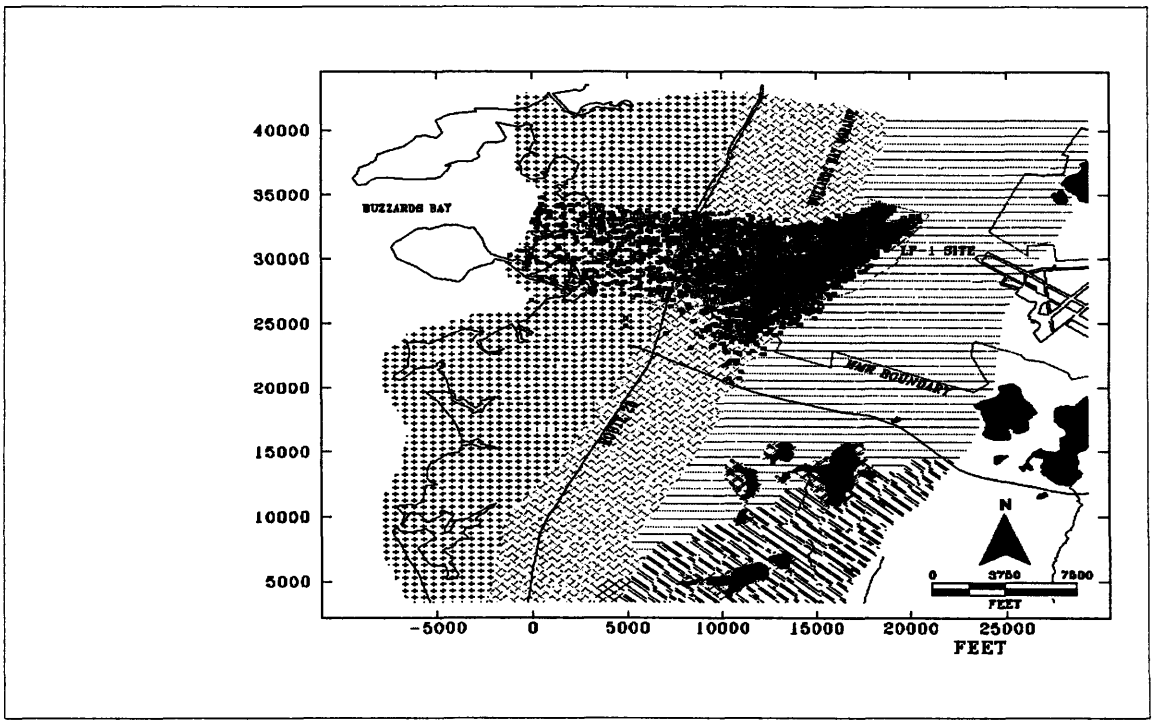

Figure 3-10 Plan view of simulated LF-1 plume. Buzzards Bay Moraine is also shown.

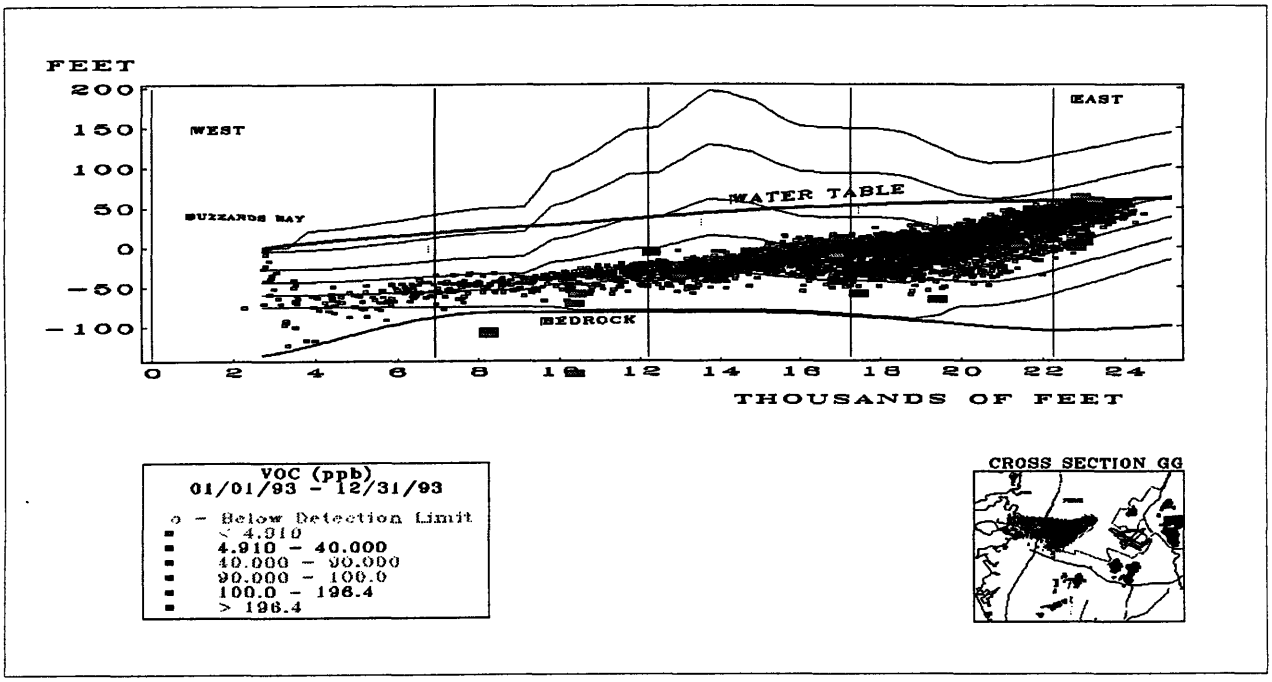

Figure 3-11 Cross-Section of simulated LF-1 plume and observed contamination locations.

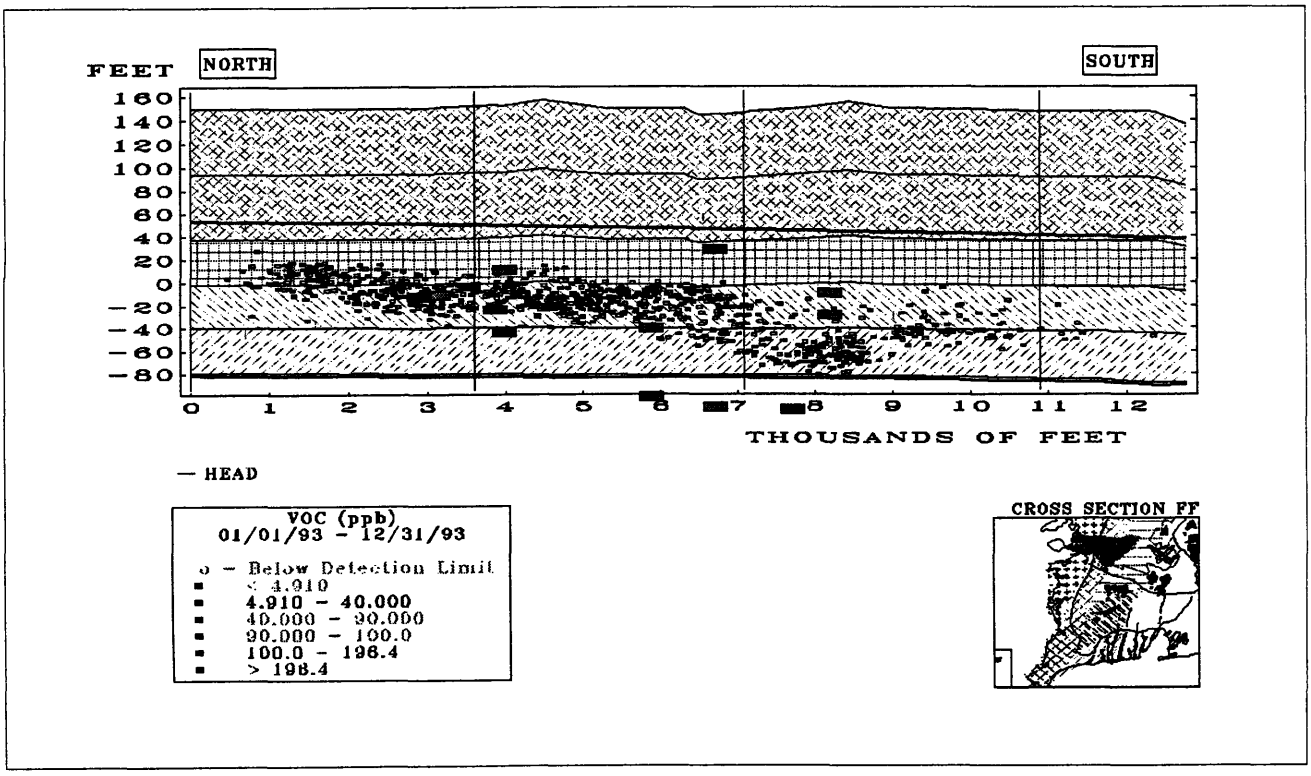

Figure 3-12 Cross sectional view of LF-1 plume as it enters the Buzzards Bay Moraine.

Risk Assessment & Management of Risks

The IRP's Remedial Investigation (RI) Report and their Final Risk Assessment Handbook (RAH) present an evaluation of potential adverse effects to human health from materials identified in the MMR LF-1. The MMR site has been classified using EPA guidelines which were not specifically developed for the MMR site. The accuracy of the health and environmental risk scores are limited by the constraints of the EPA's deterministic risk assessment model.

Cancer risk is the statistical increase in mortality rate for a member of the local community who has been exposed to carcinogenic materials identified in the MMR LF-1 as compared to the rate for a member of the local community if the MMR LF-1 did not exist. It is the probability of an event occurring and the magnitude of the effect which an event will likely produce. More simply, cancer risk is the product of the probability of dying from cancer because of exposure to carcinogens and the probability of exposure to carcinogens.

Toxicology

According to the EPA guidelines (cited in both the RAH, 1994 and LaGrega et. al., 1994), toxicology and dose are to be calculated by following specific protocols. In terms of toxicology, carcinogens are considered to vary greatly in their potency. "When considering lifetime cancer risk to humans, it is widely accepted that carcinogenesis works in a manner such that it is possible, however remote, that exposure to a single molecule of a genotoxic

carcinogen could result in one of the two mutations necessary to initiate cancer". (LaGrega et. al., 1994, p. 277). Therefore, the calculation of carcinogenic risk from toxicology involves the use of cancer potency factors which are basically the slopes of the dose-response curves for carcinogens which are extrapolated to zero for extremely small doses. These extrapolated slopes are commonly referred to as cancer slope factors (CSFs) and they are used for the toxicological component of the EPA's acceptable risk calculations. CSFs are maintained in the EPA's Integrated Risk Information System (IRIS) database.

Many papers have been published which comment upon the uncertainty of the EPA's CSFs. In addition, "the EPA is well aware of the problems associated with overly conservative risk estimates and has repeatedly stressed that the unit cancer risk estimate only provides a plausible upper limit for a risk that can very well be much lower. The problem is that, in reality, official EPA unit risk estimates are widely used , more or less, as absolute standards." (LaGrega et. al., 1994, p.280). Due to insufficient expertise in toxicology, this report will not offer an opinion concerning specific toxicological uncertainty of the EPA's CSFs.

Dose

In terms of dose calculations, it is important to understand the environmental pathway. Therefore, for this cancer risk evaluation it is important to identify the following:

- carcinogens
- source of carcinogens
- release mechanisms
- transport mechanisms
- transfer mechanisms
- transformation mechanisms
- exposure paths
- exposure point concentrations

- receptors

However, it is interesting to note that in performing an EPA risk assessment, only the carcinogens and the exposure point concentrations are used to calculate risk. Although the other seven above-referenced factors are essential for developing spatially distributed exposure point concentrations, EPA protocol requires maximum detect concentrations for maximum or upper bound risk calculations. In addition, EPA protocol requires arithmetic averaging of detect concentrations for mean risk calculations. That is to say, two sites with hazardous materials at similar concentrations with entirely different hydrogeologic conditions, would have the same risk according to EPA guidelines. However, at their discretion, EPA will review risk assessments which incorporate site-specific conditions into their calculations.

Identification of Hazardous Materials

Hazardous materials are broadly defined as non-carcinogens which are known to have harmful systemic effects upon humans, and carcinogens which have a propensity to initiate and promote cancer. Both terminal and "quality of life" health problems from exposure to hazardous materials are primary human health concerns. Because of these health concerns, human exposure to hazardous materials, especially carcinogens, is a source of risk and is of primary concern for risk assessment and management. However, for this report, only the carcinogenic materials identified in the MMR LF-1 are being evaluated for potential risk; they are identified in the risk spreadsheets presented in Tables H1-H5.

According to Boston University's School of Public Health Upper Cape Cancer Incidence Study which was prepared under contract to the Massachusetts Department of Public Health,

cancer incidence rates for the MMR regional area have increased at a relative rate of approximately fifty six (56) percent overall (BUSPH, 1992). In addition, according to the Journal of the American Medical Association cancer incident rates are increasing steadily for the United States at a relative rate of approximately forty four (44) percent overall (JAMA, Vol. 271, No. 6, 1994). Furthermore, it is generally accepted that approximately twenty five (25) percent of all annual deaths in the US are caused by cancer. When the uncertainties presented in the above-referenced reports are taken into account, both the MMR cancer rate and the US cancer rate are very similar. Since these cancer rates are so similar, it is difficult to discern if the cancer rate increase at the MMR region is caused on account of reasons which are linked to the background national cancer rate increase, or if cancer rate increase near the MMR is tied to the release of carcinogenic materials at the MMR site.

Review Existing Reports

Part of this investigation was a comprehensive review of the RI, and the RAH which are relevant to risk assessment for the MMR LF-1. An examination of the methodology used, the consistency of the reports with respect to the EPA's regulatory guidelines, and independent spreadsheet calculations using the equations and numerical values which are cited in the above-referenced reports supplied similar results. This three part process confirmed the consistency of the reporting which has been provided to MIT to calculate risk and formulate risk opinions. Independent spreadsheet calculations are included in Tables H1-H5. As the MMR LF-1 is part of an on-going clean-up, new and updated data from the above-referenced

reports has been included, as required, to present the most current EPA approved health risk connected with the MMR LF-1.

Uncertainty

In all statistically intensive calculations there are uncertainties specific to the numerical model which is being used. Since the EPA's model is the requisite regulatory guideline for Superfund sites, their model is the one which is being scrutinized. The EPA's deterministic model does not distribute uncertainty uniformly. When combined, concentration uncertainty and cancer slope factor (CSF) uncertainty account for approximately 97% of total risk uncertainty. Approximately 80% - 95% of the total risk uncertainty is CSF uncertainty. (Hines, J.J. 1996) The EPA understands that their methods are statistically conservative and consequently will tend to overestimate risk, because the EPA incorporates policy constructs into risk quantification calculations. Basically, the EPA uses regulated risk assessment as opposed to probabilistic risk assessment coupled with regulations for risk management. Ultimately, risk regulated by the EPA is as uncertain as the EPA's CSFs. Recently, according to several major journals including the April 17, 1996 issue of the Wall Street Journal, the EPA has proposed policy changes for their assignment of CSFs. This should decrease the statistically localized risk uncertainty inherent within EPA regulated risk assessment calculations.

Assessment of Risk from Ingestion of Contaminated Shellfish

From the current data of the LF-1 plume, the contaminants are projected to discharge into Red Brook, Squeteague, and Megansett harbors of Buzzards Bay (OpTech, 1996, CDM Federal,

1995). The shallow tidal flats of these harbors support a rich population of local shellfish species. Soft shell clams, quahogs (hard clams), oysters, bay scallops, surf clams, mussels, and conch which are harvested by local commercial and recreational fishermen. Since metals are part of the LF-1 plume contaminants and shellfish have been shown to bioaccumulate metals in their body tissue, the potential discharge of the plume into the harbors along the shoreline pose a risk to the coastal marine shellfish population as well as to human health from the consumption of tainted shellfish.

	Max. C@,1 (ug/l)	Max. C@,2 (ug/l)	Oral SF	Oral RfD	Cancer Risk[1]	Cancer Risk[2]	Hazard Index[1]	Hazard Index[2]
Aluminum	20900	10200	NA	1	NA	NA	3.18217	1.55302
Antimony		2.6	NA	0.0004	NA	NA	0	0.98967
Arsenic	3.5	8.4	1.75	0.0003	0.00093	0.00224	1.77633	4.2632
Barium	400	107	NA	0.07	NA	NA	0.87004	0.23274
Beryllium	3.6	1.1	4.3	0.005	0.00236	0.00072	0.10963	0.0335
Cadmium	2	2	NA	0.001	NA	NA	0.30451	0.30451
Chromium#	54.2	66.3	NA	0.005	NA	NA	1.65047	2.01893
Copper	48.7	28.2	NA	NA	NA	NA	NA	NA
Cyanide	16.4		NA	0.02	NA	NA	0.12485	0
Iron	134,000	24000	NA	0.5	NA	NA	40.8049	7.30834
Lead	27.8	9.8	NA	NA	NA	NA	NA	NA
Manganese	5040	824	NA	0.14	NA	NA	5.48126	0.89614
Mercury	0.3*	0.3*	NA	0.0003	NA	NA	0.15226	0.15226
Nickel	24.4	184	NA	0.02	NA	NA	0.18575	1.40077
Vanadium	33	41	NA	0.007	NA	NA	0.71778	0.89179
Zinc	262	184	NA	0.3	NA	NA	0.13297	0.09338

Notes:

1 Derived from CDM Federal (1995)
2 Derived from OpTech (1996)
@ Maximum total concentration
# Chromium (VI) values are used
* Maximum dissolved concentration

SF = Cancer slope factor
RfD = Non-cancer reference dose
NA = Not available

Table 1 Maximum cancer and non-cancer risk for each metal

The results of maximum cancer and non-cancer risk assessment of consuming contaminated quahogs over a life time are calculated for each metal in Table 1. The maximum concentration of metals detected in well samples from the LF-1 plume are derived from the reports of CDM Federal (1995) and OpTech (1996). The oral cancer slope factors (SF) and non-cancer reference doses (RfD) of the metals are obtained from the Risk Assessment Handbook for MMR published by Automated Sciences Group (1994). Using the CDM Federal (1995) data, the maximum cancer risk from consumption of tainted quahogs is 3.3E-03. This risk is interpreted as the incremental increase in probability of developing cancer above background level for each exposed resident. The United States Environmental Protection Agency (USEPA) acceptable risk standard ranges from 1.0E-06 to 1.0E-04. The standard is set independently for each site and case. The increased risk of 3.3E-03 for each exposed resident is above the highest acceptable USEPA standard. A maximum cancer risk of 3.0E-03 is calculated when maximum concentration of metals from OpTech (1996) data is used in the assessment. The cancer risk for humans from consumption of tainted quahogs are derived from only two metals - arsenic and beryllium - since these are the only metals with published cancer slope factors.

The overall maximum hazard index (HI) for non-cancer risk from potential exposure to the contaminated quahogs are 55.5 and 20.1, when CDM Federal (1995) and OpTech (1996) data, respectively, are used in the assessment. The USEPA's acceptable HI standard for non-cancer risk is 1.0. Calculated HI that are above the USEPA standard pose possible non-cancer

deleterious health effects to the exposed population. The maximum cancer and non-cancer risks from contaminated quahogs are summarized in Table 2.

	Maximum Cancer Risk	Maximum Hazard Index
CDM Federal Data	3.3E-03	55.5
OpTech Data	3.0E-03	20.1

Table 2 Total maximum cancer and non-cancer risks from consumption of tainted quahogs

The risk assessment results show that both cancer and non-cancer risks are above the USEPA standards. The USEPA risk standards are set at levels that adequately protect human health and the natural environment. The calculated risk results indicate that tainted quahogs from the coastal harbors where LF-1 plume is predicted to discharge pose significant risk to consumers of shellfish from these harbors. The calculated risk estimations are based on worst case assumptions. Thus, the risk is a conservative estimate and indicates the maximum risk posed to human health. The methodology and assumptions used in the current risk calculations are detailed in Appendix A4 (Lee, 1996). From these results, it is recommended that a monitoring program for shellfish harvested from Red Brook, Squeteague, and Megansett harbors be implemented.

Qualitative Assessment of Potential Ecological Risk

Since quahog clams are predicted to bioaccumulate metals, the discharge of the LF-1 groundwater plume into Red Brook and Megansett harbors is likely have detrimental effects

to the coastal ecological system. Quahogs are a food source for certain marine species that reside in the coastal harbors of Buzzards Bay. The contamination of the quahog clams can potentially reduce the population thus triggering a decline in the population of marine species that depend on quahogs as their sole food source. The decline of key species in the ecosystem can lead to an overall decline of the whole ecosystem.

The bioaccumulation of metals by the quahog clams can also have detrimental effects on the ecosystem in a separate way. Since quahog clams are not at the top of the shoreline ecosystem food web, they are consumed by higher order food chain species. In this process of nutrient transfer up the food chain, contaminants accumulated within lower food chain organisms are also transferred up the food web. Thus, tainted quahogs clams can potentially transfer toxic metals to higher food chain species. The bioaccumulation of metals in the higher order organisms can also lead to the decline of particular population of species and the ecosystem as a whole.

Public Perception: Management of Public Interaction at the MMR

An analysis of the approaches used to manage public interaction at the Massachusetts Military Reservation was undertaken to characterize the evolution of public perception of risk posed by past activities at the MMR. Public meetings at the MMR between January 15 and March 31, 1996, were attended. In addition, a comparison of management approaches at other bases was carried out. This included interviewing personnel at military bases in California and Arizona. As part of the analysis, suggestions future approaches at IRPs were explored. This included

the design of public opinion surveys to be carried out early in the IRP process. Other suggestions for future approaches are also presented.

Public Perception in Superfund Cleanup

In any scenario where pollution is an issue, there is frequently a gap between the perceived risk to human health and the actual risk posed by contamination. Because of scientific uncertainty in risk assessment, often times, the actual risks are not known, and so the perceived level of risk results from speculation by many parties. In the siting of hazardous waste facilities, the potential threat to human health results in the NIMBY ("Not in my backyard") syndrome. Often times this "potential threat" is a perceived one. Public interest groups have fought many a facility siting and won, not due to actual risk, but because of a perceived one. In Superfund cases, unlike potential hazardous waste facility sitings, contamination has already occurred, but there is still a question of whether the contamination poses a real threat to public health. The gap between actual and perceived risks in this case results in the answer to the question of "how clean is clean?" becoming a policy, rather than a scientific, one. Groundwater contamination at the Massachusetts Military Reservation Superfund site is perceived to be a problem, and steps are being taken to remediate this problem to the greatest extent feasible. Public opinion has defined "the greatest extent feasible" as the level to which groundwater is treated to "non-detect" levels for contaminants that pose threats to human health. In private sector cases, economics would figure into the calculation of feasibility of cleanup, but in the case of the MMR, where an entity as large as

the federal government is funding the cleanup, the public believes that "anything is affordable" and therefore feasible.

History of Public Involvement at the MMR

The initial approach to management of public interaction surrounding the Installation Restoration at the MMR was similar to the "compliance-based" approach many companies take towards environmental regulation--the National Guard Bureau met only the minimum requirements necessary. Actions taken by the NGB were reactive rather than proactive. The NGB promulgated press releases and sent reports to local libraries, as well as holding news conferences after technical meetings, but any actions beyond that were minimal. Technical meetings concerning IRP activities were closed to the public and media, and virtually no public information meetings were held.

During 1990 and 1991, there was a modest effort to increase public involvement in the cleanup at Otis, as the IRP office at the MMR was created to manage the program locally rather than from far away. The "Joint Public Involvement Community Relations Plan" was presented, bi-monthly public information meetings were initiated, site tours/briefings were made possible, a site mailing list was created, and the IRP office began to print quarterly fact sheets that described the IRP activities. Although these fact sheets were limited in scope, they, along with the public information meetings, represented the first real effort to inform the public about specific activities associated with the IRP.

Late-1991 marked a major change in the way public interaction was managed at the MMR. The IRP office began updating technical reports much more frequently, and progress reports

were made available to all interested parties. The local IRP office began educating the public by participating on local radio/cable TV programs as well as taking part in neighborhood association meetings. An educational display was created for to be used at these meetings and at libraries, and detailed bi-monthly fact sheets were developed. In addition, all technical meetings were opened to the public and media.

The post-1991 period also has included the creation of many committees that assist the cleanup activities at the MMR. These committees, called "process action teams", are made up of personnel from the MMR, the relevant regulatory agencies, and the public. These process action teams (or "PATs") report to the senior management board, which was created to oversee the restoration. Presently, a total of 8 community working groups hold regular meetings (Karson, 1995). Although the public is highly involved in the IRP process at this point, how much influence the public actually has in the decisionmaking process is still a question.

Design Of Future Approaches At The MMR And Elsewhere

There are several things that should be considered before an Installation Restoration Program is initiated at a particular base or military reservation. Not the least of these is the management of public interaction surrounding the restoration. Public and public interest group opinion are very likely to polarize as soon as contamination and threat to public health are made known. Public distrust of government, especially on the federal level, compounds the fear that public health is in danger and contributes to the belief that any cleanup activities will be inadequate to alleviate the problem of contamination.

There are steps that can be taken to minimize the potential for adversarial relationships developing between all interested parties in base cleanup. Since the public has been involved in the restoration process at the MMR, the relationships between all interested parties have become less of a barrier to cleanup as all parties are seen to have input into the process. However, analysis of the approach used to manage public interaction at the MMR shows that, even though outwardly it appears that all the "right" approaches were taken, public concern is still an issue. This is due to the fact that early on in the MMR IRP process, the public was not included and was seen more as a "problem" than a potential source of solutions.

B. Remedial Approaches

Source Containment

Introduction

As part of remediation operations at MMR, several of the cells at the Main Base Landfill have recently been secured with a final cover system. These cells include the 1970 cell, the post-1970 cell, and the kettle hole. The remaining cells (1947, 1951, and 1957) have collectively been termed the Northwest Operable Unit (NOU). Remedial investigation as to the necessity of a final closure system for these cells is ongoing. This proposal is focused on the design of a final closure system for the 1951 cell. The landfill final closure requirements of the Resource Conservation and Recovery Act (RCRA) and Massachusetts Solid Waste Management Regulations will be examined and adapted to site specific conditions. Material and design options for the components of the cover system will be examined and choices made according

to performance, availability, and relative cost, as applicable to site-specific conditions. A cross-section of the proposed cover system is provided in Figure 3-1.

Regulatory Review

Massachusetts Solid Waste Management regulations specify the following as minimum design requirements for a landfill final closure system (MA DEP, 1993):

- Subgrade layer
- Venting layer with minimum hydraulic conductivity of $1X10^{-3}$ cm/sec
- Low conductivity layer with minimum thickness of 18 inches and maximum hydraulic conductivity of $1x10^{-7}$ cm/sec, or an approved flexible membrane liner (geomembrane)
- Drainage layer with minimum thickness of 6 inches and minimum hydraulic conductivity of $1x10^{-3}$ cm/sec, or a synthetic drainage net (geonet)
- Combined vegetative support / protection layer of minimum thickness 18 inches, with at least 12 inches of soil capable of supporting vegetation.

Subparts G, K, and N of the Resource Conservation and Recovery Act (RCRA) Subtitle C (Hazardous Waste Management) regulations dictate the requirements for hazardous and mixed waste landfill cover systems (US EPA, 1991). The EPA recommends that a final cover system consist of the following (US EPA, 1991):

- A low hydraulic conductivity geomembrane / soil layer consisting of a 24 inch layer of compacted natural or amended soil with a hydraulic conductivity of $1x10^{-7}$ cm/sec in intimate contact with a geomembrane liner of minimum thickness 0.5 mm (20 mil).
- A drainage layer of 12 inch minimum thickness having a minimum hydraulic conductivity of $1x10^{-2}$ cm/sec, or a geosynthetic material of equal transmissivity.

- A top vegetative support / soil layer consisting of a top layer with vegetation or an armored surface, and a minimum of 24 inches of soil graded at a slope between 3 and 5 %.

The EPA does encourage design innovation, and will accept an alternative design upon a showing of equivalency.

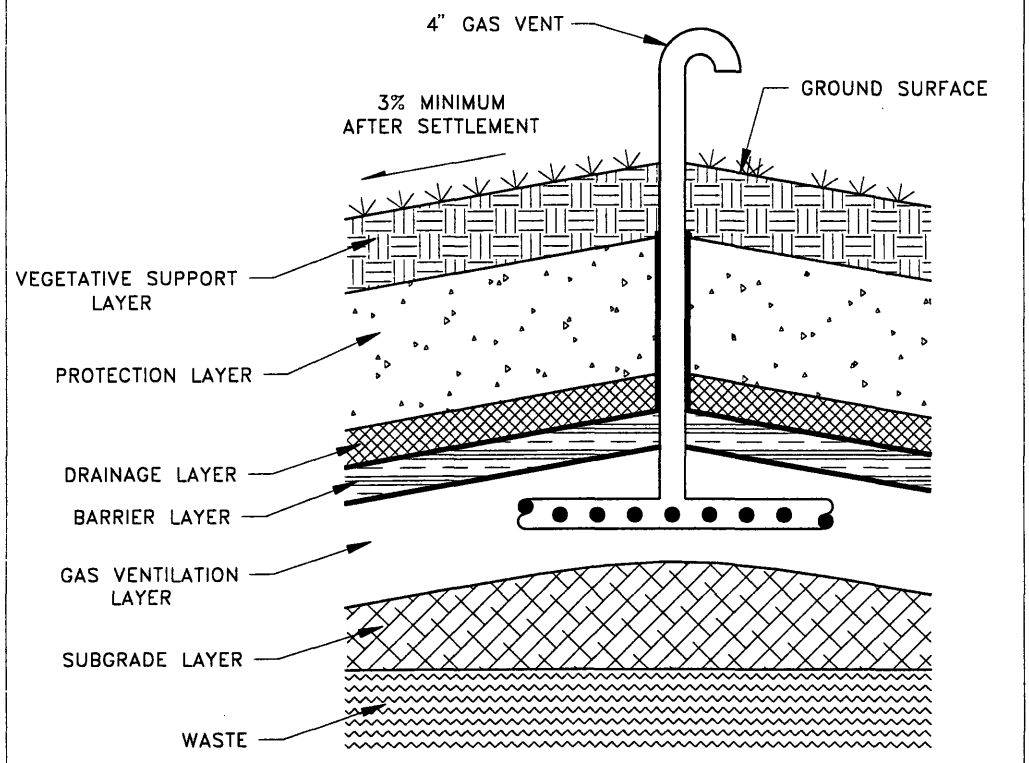

LAYER	MATERIAL	SPECIFICATIONS
Vegetative Support	Loam	6" thickness
Protection	Borrow Soil	18" thickness
Drainage	Geonet	Transmissivity> 3×10^{-5} m^2/sec
Barrier	Geomembrane over Geosynthetic Clay Liner	Geomembrane: 60mil VLDPE Geosynthetic Clay Liner: Gundseal with 40mil VLDPE Substrate
Gas Ventilation	Screened Borrow Soil	12" thickness Hydraulic conductivity> 1×10^{-3} cm/sec

NOT TO SCALE

Figure 4.1: Cross-Section of Proposed Cover Design

Subgrade Layer

The subgrade layer acts as a foundation for the overlying layers of the cap, and it is also used as a contouring layer to create the appropriate final slope of the cover system. It is recommended that the foundation layer be placed to provide a final grade (after settlement) no greater than 5% and no less than 3%. This slope range provides sufficient grade to promote some surface water runoff while not being so steep as to produce erosion of the surficial soils. Allowance must be made for waste settlement that will occur as a result of the vertical stresses imposed by the weight of the cover materials.

Materials typically utilized for foundation layers include a variety of soils, and some acceptable wastes. At sites such as MMR where soil borrow volumes are relatively plentiful, soil is the obvious choice for the foundation layer. Results of on-site borrow characterization tests (ABB, 1993) have revealed that this material is acceptable for use in the foundation layer. The material is classified as a fine-to-medium sand with trace-to-some fine-to coarse gravel (ABB, 1993). This material has a relatively low fines content and has acceptable compressibility characteristics, therefore it is recommended for use in this layer. The subgrade should be placed in lifts of approximately 8 inches and compacted by 4 to 6 passes of a typical sheepsfoot roller. This placement procedure should result in compaction to approximately 90% of the maximum dry density.

Gas Ventilation Layer

The gas venting layer is a permeable layer containing piping for the collection and venting or recovery of gases produced from waste degradation. Based on the cell composition

(predominantly burn-fill), the moist, aerobic conditions provided by the intermediate cover, and the time since placement (over 40 years) it is concluded that gas generation rates at the 1951 cell will be low. Consequently, a passive gas venting system is recommended. It is recommended that material from the "lower layer" of the borrow area be utilized for the ventilation layer. The soil must be screened on a 3/8 inch sieve prior to placement, and then placed with a light machine in a single lift with no further compaction efforts. To collect the gas, PVC collector pipe is bedded in the sand and run laterally along the slope. To vent the gas to atmosphere, it is recommended that a total of ten ventilation risers be installed and spaced equidistantly. Flexible (to accommodate loading and settlement) 4 inch perforated PVC is recommended for the collector pipe, and 4 inch non-perforated rigid PVC is recommended for the risers.

Hydraulic Barrier Layer

The barrier layer is designed to minimize the percolation of water through the cover system directly by impeding infiltration and indirectly by promoting storage and drainage of water in the overlying layers and eventual removal of water by runoff, evapotranspiration, and internal storage (Geosyntec, 1994). This design proposal recommends a composite geomembrane over geonsynthetic clay liner (GCL) as the hydraulic barrier layer. The specified geomembrane is a 60 mil (1.5 mm) textured very low density polyethylene (VLDPE), and the specified GCL is a Gundseal® GCL with a 40 mil (1.0 mm) textured VLDPE substrate placed bentonite-side up.

Drainage Layer

The drainage layer functions to remove water which infiltrates the vegetative support/protection layer. It should be designed to minimize the standing head and residence time of water on the barrier layer in order to minimize leachate production (US EPA, 1989). The recommended drainage layer for this design is an extruded solid rib geonet with factory bonded nonwoven, heat-bonded geotextile on both faces. The composite drainage layer must have a minimum transmissivity of $3x10^{-5}$ m^2/sec.

Surface Layer

The top layer of the cover system is actually comprised of two separate layers; the lower layer termed the protection layer and the upper layer termed the surface layer. On-site or local soil is the most commonly used and typically the most suitable material for the protection layer. Suitable on-site materials are available for use in the protection layer. The on-site borrow materials have been classified as a fine-to-medium sand with trace-to-some fine-to coarse gravel (ABB, 1993). This material has a relatively low fines content and a low organic content, therefore it is acceptable for use in the protection layer. The borrow material should be placed to a thickness of 18 inches using a small dozer with low ground-pressure to protect the underlying cover components. Compaction beyond that which occurs during placement is not necessary.

Vegetation is specified as the surface layer cover, consequently the surface layer will be designed for vegetative support. The on-site borrow material is not well suited to supporting vegetation, therefore it is recommended that loam be imported from an off-base supplier and

placed to a thickness of 6 inches. A warm season grass mix is specified as the vegetative cover. Periodic mowing and inspection of the vegetative cover are recommended as part of the Postclosure Program.

Conclusions

It is concluded that this cover system, if constructed with appropriate construction quality assurance / quality control, will satisfy the primary objective of containing the source of pollution, thus minimizing further contamination of groundwater by the waste fill. The composite geomembrane / geosynthetic clay liner barrier layer is theoretically nearly impermeable. Estimates of the hydraulic conductivity of VLDPE geomembranes are on the order of $1x10^{-10}$ cm/sec (Koerner, 1994), and estimates of the hydraulic conductivity of Gundseal® GCLs are on the order of $1x10^{-12}$ cm/sec (Eith et al., 1991). Essentially all infiltration that does occur through such a composite barrier is the result of defects from manufacturing and / or construction processes. Theoretical performance of the cover was evaluated using the Hydrologic Performance of Landfill Performance (HELP) computer model (Schroeder et al., 1994). HELP is a quasi-two-dimensional, deterministic, water-routing model for determining water balances (Schroeder et al., 1994). HELP predicted 0.000000 inches of annual percolation through the barrier layer. Clearly, this prediction is unrealistic as no cover is absolutely impermeable. Because the performance of the cover system is so closely linked to construction QA/QC, it is very difficult to make an accurate estimate of anticipated infiltration through the barrier layer. It is accurate to state, however, that if this proposed cover system is constructed with appropriate QA/QC, it will meet and

exceed the regulatory performance specifications. To accurately monitor the performance of the cover system, it is recommended that the downgradient groundwater quality be closely monitored before and after cover construction to reveal contaminant concentration trends indicative of cover system effectiveness.

While the primary objective of the cover system is to minimize infiltration into the waste fill, there are several other significant performance criteria which must be satisfied. Given the site-specific conditions, the cover system must also:

* isolate the waste from humans, vectors and other animals, and other components of the surrounding ecosystem
* control gases generated within the waste fill
* be resistant to erosion by wind and water
* be resistant to static and seismic slope failures
* be durable, maintaining its design performance level for 30 years (regulatory) or the life of the waste fill (prudent)
* control surface water runoff and lateral drainage flow in a manner which does not promote erosion and does not adversely impact the surrounding environment

As presented in Appendix A-6, these criteria are satisfied by the proposed cover design. The waste is well isolated from the surrounding ecosystem by a total of over 5 feet of soil. Any gases produced by the waste will be vented to atmosphere to prevent explosive conditions from occurring within the waste layer. Additionally, atmospheric monitoring is included as part of the post-closure program to ensure that vented gases do not violate Clean Air Act

standards and to ensure that no gas migrates off-site. The cover is designed to be erosion-resistant. The surface is graded to a moderate slope, seeded with an appropriate grass mixture, and covered with straw mulch. Surface water runoff and lateral drainage flow are handled by a network of open channels and culverts which divert flow to specified recharge areas in a controlled manner which also assists in erosion control. The cover system is also resistant to static and seismic slope failure. The minimum static factor of safety of the proposed cover system is 3.1, the minimum seismic factor of safety is 1.0. The recommended minimum factors of safety are 1.5 and 1.0 respectively. It should be noted that it is relatively rare to have a cover design satisfy the seismic stability safety factor in a seismically active area such as Cape Cod. The issue of durability is not so clearly satisfied, in the author's opinion. Relatively little research on the long-term durability of geosynthetics in landfill covers has been performed, and since the history of geosynthetics in cover systems is fairly short, there are few, if any, case studies of sufficient length (e.g., over 30 years) to fill the data gap. However, the research that has been performed indicates that a cover system is an environment which is relatively conducive to geosynthetic survivability (Koerner et al., 1991). In a cover, the geosynthetics are not exposed to toxic chemicals, they are isolated from ultraviolet radiation, and they are fairly well protected from the effects of freeze/thaw cycles. Thus, it seems likely that the cover system will maintain its integrity well into the future.

In summary, it is contended that the proposed cover system will adequately contain the source of the LF-1 plume. If constructed with appropriate construction QA/QC, the proposed cover system design will provide a nearly impermeable barrier while also controlling lateral

drainage flow, surface runoff, and decomposition gases with a stable, durable design that should maintain its integrity for decades.

Bioremediation

Bioremediation of the LF-1 plume has been considered as a potential remedial action for the site, but a comprehensive plan has yet to be proposed (ABB Environmental, 1992). Conventional enhanced bioremediation systems stimulate microbial degradation by amending groundwater from the aquifer with oxygen and nutrients and recirculating it through the contaminated area (O'Brien & Gere Engineers Inc., 1995). The immense size of the LF-1 plume would necessitate the pumping and recirculation of hundreds of millions of gallons of water in order to ensure the removal of all of the chlorinated solvents. This plan would not only be prohibitively costly, it would also be ineffective because the plume contains PCE which cannot be aerobically degraded (Pavlostathis and Zhuang, 1993).

In order to solve the technical problems associated with a traditional enhanced bioremediation action, a passive anaerobic/aerobic system can be used. This system would consist of two groups of horizontal injection wells which are driven into the aquifer at a depth just below that of the plume (see Figure 6-1). The wells would be driven across the width of the plume and have thousands of small injection ports along the top of each one. The ports are used to inject gases into the aquifer in order to stimulate the microbes which will degrade the plume contaminants. Each set of wells will form a distinct biozone above it. The first biozone will be anaerobic and will treat the PCE in the plume, while the second biozone will be an aerobic

treatment phase which will remove the remaining chlorinated solvents. This system has a significant advantage over traditional systems because it is a flow-through system; the gas is injected below the plume where it can rise up into the contaminated water and stimulate microbial activity as the plume flows over the gas injection wells. This significantly reduces the pumping costs associated with a more traditional bioremediation system.

The LF-1 plume contains significant quantities of PCE which can only be degraded anaerobically because methanotrophic bacteria possess a monooxygenase enzyme which cannot oxidize a fully chlorinated ethene molecule (Semprini, 1995). Therefore, the first stage of the system must be designed to turn the system anaerobic so that anaerobic bacteria can utilize the PCE in the plume in the process of reductive dechlorination. PCE is an oxidized chemical species while organic matter is relatively reduced. Reductive dechlorinating bacteria use the PCE as a chemical oxidant in a redox reaction with organic matter in order to obtain energy to function and grow (Hollinger et al, 1993). In the process, one or more chlorines are removed from the PCE and replaced with hydrogen. This renders the PCE susceptible to aerobic attack.

In order to turn the aquifer anaerobic, methane and air are injected at the first biozone. This injection serves a threefold purpose. Methanotrophs utilize the methane for growth and deplete the oxygen in the plume as it flows past the well. In addition, the methanotrophs will also degrade some of the TCE and DCE in the plume since their monooxygenase enzymes can degrade the solvents as well as methane (Semprini, 1995). Finally, as methane is utilized by

the methanotrophs for growth, biomass will be accumulated in the region above the treatment well. This biomass will then be used by methanogenic bacteria to fuel the process of reductive dechlorination of PCE within the plume.

Once the oxygen is depleted from the plume, the first biozone will be anaerobic. It will remain anaerobic since there will be little or no vertical mixing with oxygenated recharge water (Domenico and Schwartz, 1990). Furthermore, oxygen will be depleted from the plume as it flows into the biozone by periodic injections of methane. Bacteria in this anaerobic zone will utilize the dead biomass and reductively dechlorinate the solvents in the plume. This is a slow biological process; based on laboratory batch studies and the temperature and pH of the aquifer the biozone needs to produce at least five milligrams per liter of biomass and it should take about 540 days to achieve extensive removal (greater than 99 percent) of the PCE in the plume (see appendix A7). Given a PCE migration rate within the plume of .9 ft per day and a treatment zone of two hundred feet associated with each horizontal well, three six-thousand foot horizontal wells will need to be installed to create the first biozone. Some of the TCE and DCE in the plume will also be dechlorinated within this area, rendering all of the chlorinated solvents in the LF-1 plume more susceptible to treatment by aerobic degradation.

The second biozone will be an aerobic zone that will be used to degrade the bulk of the chlorinated solvents in the plume. Gaseous methane, air, nitrous oxide, and triethyl phosphate will be injected into the aquifer (Skiadas, 1996). Methanotrophs will feed on this and will also degrade the solvents in a process termed cometabolic oxidation. One horizontal well

must be used to produce the aerobic biozone which will achieve a ninety-five percent reduction in the concentration of TCE and ensure total remediation of DCE and VC (See Appendix A7). This level of remediation is more than sufficient to ensure that federal MCLs for the pollutants in the LF-1 plume are not exceeded in private drinking wells in the path of the plume.

It is apparent that the enhanced bioremediation system proposed above has the potential to effectively remediate the chlorinated solvent plume emanating from the main base landfill at the MMR on Cape Cod. The system would be difficult to manage and expensive to emplace, but it does offer many cost advantages over other remediation or containment schemes because it does not involve pumping large volumes of water or treating contaminated groundwater with granular activated carbon to remove the chlorinated organics. However, this type of system has never been used in the field so a pilot-scale study should be conducted at a smaller site to ensure that the concept works and is cost-effective. If this test produces positive results, then a sequential anaerobic/aerobic enhanced bioremediation system of this nature could be used to clean up the LF-1 plume.

Project Report References

ABB Environmental Services, Inc., "Installation Restoration Program, Massachusetts Military Reservation, Interim Remedial Investigation, Main Base Landfill (AOC LF-1)", Portland, Maine, March 1992.

Alyamani, M.S., and Z. Sen, "Determination of Hydraulic Conductivity from Complete Grain-Size Distribution Curves", *Ground Water*, v. 31, no. 4, p. 551-555, 1993.

Alden, D.S., "Subsurface Characterization of the Massachusetts Military Reservation Main Base Landfill Superfund Site," M.Eng. Thesis, Massachusetts Institute of Technology, Cambridge, Massachusetts, 1996.

Amarasekera, K.N., "A Groundwater Model Of The Landfill Site At The Massachusetts Military Reservation", M.Eng. Thesis, Massachusetts Institute of Technology, Cambridge, Massachusetts, 1996.

Aschengrau, A. And Ozonoff, D., *Upper Cape Cancer Incidence Study Final Report*, Massachusetts Department of Public Health, Boston, January 9, 1992.

Automated Sciences Group, Inc., Hazardous Waste Remedial Actions Program, and Oak Ridge National Laboratory, *Risk Assessment Handbook*, Oak Ridge, Tennessee, 1994.

Bouwer, Herman and R.C. Rice. "A Slug Test for Determining Hydraulic Conductivity of Unconfined Aquifers With Completely or Partially Penetrating Wells", *Water Resources Research*, v. 12, no. 3, p. 423-428, 1976.

Bradbury and Muldoon, "Hydraulic Conductivity Determinations in Unlithified Glacial and Fluvial Materials," ASTM STP 1053, *Ground Water and Vadose Zone Monitoring*, 1990.

Camp Dresser & McKee Inc., *DYNFLOW, DYNTRACK and DYNPLOT, 3-Dimensional Modeling Systems For Groundwater Studies*, Camp Dresser & McKee Inc., Boston, Massachusetts, 1984.

Cape Cod Commission, "Cape Trends, Demographic and Economic Characteristics and Trends, Barnstable County - Cape Cod", Barnstable, Massachusetts, 1996.

CDM Federal Programs Corporation, "Remedial Investigation Report Main Base Landfill (AOC LF-1) and Hydrogeological Region I Study", Boston, Massachusetts, April 1995.

Collins, M., "Design of a Sequential In-Situ Anaerobic/Aerobic Enhanced Bioremediation System for a Chlorinated Solvent Contaminated Plume", M.Eng. Thesis, Massachusetts Institute of Technology, Cambridge, Massachusetts, 1996.

Davis, D.L. et al., "Decreasing Cardiovascular Disease and Increasing Cancer Among Whites in the United States From 1973 Through 1987", Journal of the American Medical Association, Vol. 271, No. 6, February 9, 1994.

Domenico, Patrick A., and Franklin W. Schwartz. *Physical and Chemical Hydrogeology*, John Wiley & Sons, New York, NY, 1990.

E.C. Jordan Company, "Hydrogeologic Summary, Task 1-8, Installation Restoration Program, Massachusetts Military Reservation", Portland, Maine, April 1989.

Eith, A. W., Boschuk, J., and Koerner, R. M., "Prefabricated Bentonite Clay Liners", in *Proceedings of the 4th GRI Seminar on the Topic of Landfill Closures - Geosynthetics, Interface Friction and New Developments*, Geosynthetic Research Institute, Philadelphia, 1991.

Elias, K.G., "Source Containment at the Massachusetts Military Reservation Main Base Landfill: Design of a Hazardous Waste Landfill Cover System," M.Eng. Thesis, Massachusetts Institute of Technology, Cambridge, Massachusetts, 1996.

Freeze, R.A., and J.A. Cherry, *Groundwater*, Prentice-Hall, Inc., Englewood Cliffs, NJ, 1979.

Gelhar, L. W., C. Welty and K. R. Rehfeldt, A critical review of data on field-scale dispersion in aquifers, *Water Resources Research*, 28(7), 1958-1974, 1992.

Hines, J.J., "Uncertainty of Risk to Human Health from Groundwater Impacted by the Massachusetts Military Reservation Superfund Site Landfill", M.Eng. Thesis, Massachusetts Institute of Technology, Cambridge, Massachusetts, 1996.

Hollinger, Christof, Gosse Schraa, Alfons J. M. Stams, and Alexander J. B. Zehnder. *A Highly Purified Enrichment Culture Couples the Reductive Dechlorination of Tetrachloroethene to Growth.* Applied and Environmental Microbiology, Vol. 59, No. 9, pp. 2991-2997, 1993.

Jordan, B.R., " ", M.Eng. Thesis, Massachusetts Institute of Technology, Cambridge, Massachusetts, 1996.

Koerner, R. M., "*Designing with Geosynthetics*", Third Edition, Prentice Hall, Englewood Cliffs, New Jersey, 1994.

LaGrega, D.M., P.L. Buckingham, and J.C. Evans, *Hazardous Waste Management*, McGraw-Hill, New York, 1994.

LeBlanc, D.R., J.H. Guswa, M.H. Frimpter, and C.J. Londquist, "Groundwater Resources of Cape Cod, Massachusetts", U.S. Dept. of the Interior, U.S. Geological Survey, Hydrologic Investigations Atlas HA-692, 1986.

Lee, R.F., "Human Health and Coastal Ecosystem Risk Assessment of the Massachusetts Military Reservation Main Base Landfill Groundwater Plume", M.Eng. Thesis, Massachusetts Institute of Technology, Cambridge, Massachusetts, 1996.

Masterson, J. P. and P. M. Barlow, *Effects of Simulated Ground-Water Pumping and Recharge on Ground-Water Flow in Cape Cod, Martha's Vineyard, and Nantucket Island Basins, Massachusetts*.. U.S. Geological Survey Open-File Report 94-316, 1994.

O'Brien & Gere Engineers Inc. *Innovative Engineering Technologies For Hazardous Waste Remediation*, Van Nostrand Reinhold, New York, NY, 1995.

Oldale, R.N., "Glaciotectonic Origin of the Massachusetts Coastal End Moraines and a Fluctuating Late Wisconsinian Ice Margin", Geological Society of America Bulletin, v. 95, 1984.

Operational Technologies Corporation, "Plume Containment Design Data Gap Field Work Technical Memorandum", San Antonio, Texas, February 1996.

Operational Technologies Corporation, "Technical Memorandum Containment of Landfill-1 Plume", San Antonio, Texas, January 1996.

Pavlostathis, Spyros G., and Zhuang, P., "Reductive Dechlorination of Chloroalkenes in Microcosms Developed with a Field Contaminated Soil", *Chemosphere*, Vol. 27, No. 4, pp. 585-595, 1993.

Schroeder, P. R., Dozier, T. S., Zappi, P. A., McEnroe, B. M., Sjostrom, J. W., and Peyton, R. L., "The Hydrologic Evaluation of Landfill Performance (HELP) Model: Engineering Documentation for Version 3", EPA/600/9-94/xxx, U.S. Environmental Protection Agency Risk Reduction Engineering Laboratory, Cincinnati, Ohio, 1994.

Semprini, L., "In-Situ Bioremediation of Chlorinated Solvents", *Environmental Health Perspectives*, Volume 103 (Suppl 5), pp. 101-105, 1995.

Skiadas, P., "Design of an In-Situ Bioremediation Scheme of Chlorinated Solvents by Reductive Dehalogenation Sequenced by Cometabolic Oxidation", M.Eng. Thesis, Massachusetts Institute of Technology, Cambridge, Massachusetts, 1996.

Springer, R.K., "Application Of An Improved Slug Test Analysis To The Large-Scale Characterization Of Heterogeneity in a Cape Cod Aquifer", M.S. Thesis, Massachusetts Institute of Technology, Cambridge, Massachusetts, 1991.

Thompson, K.D., "The Stochastic Characterization of Glacial Aquifers Using Geologic Information", Ph.D. Thesis Massachusetts Institute of Technology, Cambridge, Massachusetts, 1994.

U.S. Environmental Protection Agency (US EPA), "Guidance for Conducting Remedial Investigations and Feasibility Studies under CERCLA", Office of Solid Waste and Emergency Response, OSWER Directive 9335.3-01, March 1988.

Van Der Kamp, G., "Determining Aquifer Transmissivity by Means of Well Response Tests: The Underdamped Case", *Water Resources Research*, v. 12, no. 1, p. 71-77, 1976.